

UNIVERZA V LJUBLJANI
BIOTEHNIŠKA FAKULTETA

Mitja FERLAN

**THE USE OF MICRO-METEOROLOGICAL
METHODS FOR THE MONITORING OF THE
CARBON FLUXES IN KARST ECOSYSTEMS**

DOCTORAL DISSERTATION

Ljubljana, 2013

UNIVERZA V LJUBLJANI
BIOTEHNIŠKA FAKULTETA

Mitja FERLAN

**THE USE OF MICRO-METEOROLOGICAL METHODS FOR THE
MONITORING OF THE CARBON FLUXES IN KARST
ECOSYSTEMS**

DOCTORAL DISSERTATION

**SPREMLJANJE TOKA OGLJIKA V KRAŠKIH EKOSISTEMIH Z
MIKROMETEOROLOŠKIMI METODAMI**

DOKTORSKA DISERTACIJA

Ljubljana, 2013

Doktorsko delo je bilo opravljeno na Biotehniški fakulteti Univerze v Ljubljani v okviru podiplomskega študija bioloških in biotehniških znanosti (znanstveno področje: gozdarstvo). Eksperimentalni del naloge je potekal na območju Podgorskega krasa med Črnotičami, Petrinjem in Prešnico. Pri delu smo uporabljali raziskovalno opremo, katera večji del je v lasti Gozdarskega Inštituta Slovenije, del v lasti Oddelka za agronomijo Biotehniške fakultete Univerze v Ljubljani in del v lasti Univerze v Vidmu (Italija).

Senat Biotehniške fakultete in Senat Univerze v Ljubljani sta za mentorja doktorske disertacije imenovala prof. dr. Franca Batiča in za somentorja dr. Primoža Simončiča.

Komisija za oceno in zagovor:

Predsednik: prof.dr. Jurij Diaci

Mentor in član: prof.dr. Franc Batič

Somentor in član: prof.dr. Primož Simončič

Član: prof.dr. Alessandro Peressotti

Datum zagovora: 29.3.2013

Doktorsko delo je rezultat lastnega raziskovalnega dela. Podpisani se strinjam z objavo svoje naloge v polnem tekstu na spletni strani Digitalne knjižnice Biotehniške fakultete. Izjavljam, da je naloga, ki sem jo oddal v elektronski obliki, identična tiskani verziji.

Mitja FERLAN

KLJUČNA DOKUMENATCIJSKA INFORMACIJA

ŠD Dd
 DK GDK 114.12(497.4Kras)--015(043.3)=111
 KG sekundarna sukcesija/kroženje ogljika/Eddy covariance/neto izmenjava CO₂/dihanje tal/padavinski pulzi/toplotna korekcija/kraški ekosistemi
 KK
 AV FERLAN, Mitja, univ. dipl. inž. gozd.
 SA BATIČ, Franc (mentor) / SIMONČIČ, Primož (somentor)
 KZ SI-1000 Ljubljana, Jamnikarjeva 101
 ZA Univerza v Ljubljani, Biotehniška fakulteta, Podiplomski študij bioloških in biotehniških znanosti, področje gozdarstvo
 LI 2013
 IN SPREMLJANJE TOKA OGLJIKA V KRAŠKIH EKOSISTEMIH Z MIKROMETEOROLOŠKIMI METODAMI
 TD Doktorska disertacija
 OP XII, 102 str., 8 pregl., 31 sl., 111 vir.
 IJ en
 JI en/sl
 AI Kljub intenzivnim raziskavam o kroženju ogljika so nekateri ekosistemi na tem področju še vedno slabo raziskani. Eni takšnih so tudi kraški ekosistemi. Raziskave predstavljene v tem delu so bile narejene na ravnini Podgorskega Krasa (400 - 430 m.n.v.) v sub-mediteranski regiji Slovenije. Na zaraščajočem območju sta bili izbrani dve ploskvi: pašnik in površina v zaraščanju. Na obeh ploskvah so bile v juliju 2008 vzpostavljene mikrometeorološke meritve po metodi Eddy covariance (EC) na višini 15 m (zaraščanje) in 2 m (pašnik). Prav tako so bile v okviru ploskev izvajane meritve dihanja tal z mikrometeorološko metodo zaprtih in odprtih komor ter vse potrebne spremljajoče meteorološke meritve. V preučevanem obdobju od 1. 7. 2008 do 30. 11. 2012 ni bilo med obema ploskvama zaznati večjih razlik v zračni temperaturi in količini padavin. Kar se tiče kvalitete podatkov pridobljenih po metodi EC, smo uporabili 59,7 % podatkov na ploskvi zaraščanje in 33,7 % podatkov na ploskvi pašnik. Ploskev zaraščanje je v preučevanem obdobju delovala kot ponor ogljika ($NEE = -184 \pm 19 \text{ gCm}^{-2}\text{leto}^{-1}$), medtem ko je bila ploskev pašnik vir ($NEE = 293 \pm 34 \text{ gCm}^{-2}\text{leto}^{-1}$) ogljika. Na podlagi mikrometeoroloških meritev po metodi EC lahko zaključimo, da zaraščanje pašnikov vpliva na povečano ponorno aktivnost ekosistema za ogljik. Ko smo na podatke NEE aplicirali B4 korekcijo, ki je potrebna zaradi samogretja merilne opreme, je ploskev zaraščanje delovala kot šibak ponor ogljika ($NEE = -28 \text{ gCm}^{-2}\text{leto}^{-1}$), medtem ko je pašnik deloval kot vir ($NEE = 456 \text{ gCm}^{-2}\text{leto}^{-1}$) ogljika. Ob aplikaciji korekcije NEE zaradi samogretja merilne opreme, ki je bila razvita na podlagi lastnih meritev (SISC), je ploskev zaraščanje delovala kot ponor ogljika ($NEE = -127 \text{ gCm}^{-2}\text{leto}^{-1}$), medtem ko je pašnik deloval kot vir ($NEE = 362 \text{ gCm}^{-2}\text{leto}^{-1}$) ogljika. Meritve so pokazale, da je potrebna tovrstna korekcija tudi v naših razmerah in ne le v hladnejših (Burba et al., 2008), vendar mora biti uporabljena korekcija razvita na podlagi lastnih meritev. Kar zadeva meritve dihanja tal smo v študiji pokazali, da lahko avtomatski sistem za tovrstne meritve močno prispeva k večji časovni gotovosti meritev. Kombinacija meritev temperature in vlage tal skupaj z ročnimi meritvami dihanja tal pa močno prispeva k prostorki gotovosti meritev.

KEY WORDS DOCUMENTATION

DN Dd
 DC FDC 114.12(497.4Kras)--015(043.3)=111
 CX secondary succession/carbon cycle/Eddy covariance/net ecosystem CO₂ exchange/soil respiration/precipitation pulse/self-heating correction/Karst ecosystem
 CC
 AU FERLAN, Mitja
 AA BATIČ, Franc (supervisor) / SIMONČIČ, Primož (co- supervisor)
 PP SI-1000 Ljubljana, Jamnikarjeva 101
 PB University of Ljubljana, Biotechnical Faculty, Postgraduate Study of Biological and Biotechnical Sciences, field Forestry
 PY 2013
 TI THE USE OF MICRO-METEOROLOGICAL METHODS FOR THE MONITORING OF THE CARBON FLUXES IN KARST ECOSYSTEMS
 DT Doctoral dissertation
 NO XII, 102 p., 8 tab., 31 fig., 111 ref.
 LA en
 AL en/sl
 AB Despite intensive research, carbon cycle is still under-investigated and not fully understood for many ecosystems, especially the ones which are of minor direct importance in terms of food and wood production. Karst ecosystems can be included in this group of ecosystems. The study was conducted at the Podgorski Kras plateau (400 - 430 m.a.s.l.), which was in the past subjected to agriculture land abandonment, in the sub-mediterranean region of Slovenia (SW Slovenia). Within the study area two study sites were chosen: grassland and forest succession. At both sites, in July 2008, an open-path Eddy covariance (EC) was installed at 15 m and 2 m height for Succession site and Grassland site, respectively. Also Rs and other auxiliary measurements were performed. For the observed period (July 1st 2008 – November 30th 2012) no major differences were measured between Grassland site and Succession site concerning air temperature and precipitation. Concerning the EC data quality for the observed period, 59.7% and 33.7% of expected data have not been discarded for Succession site and Grassland site, respectively. On the average annual basis Succession site was net sink of carbon ($NEE = -184 \pm 19 \text{ gCm}^{-2}\text{y}^{-1}$) while Grassland site was a source of carbon ($NEE = 293 \pm 34 \text{ gCm}^{-2}\text{y}^{-1}$). Based on the eddy covariance measurements it can be concluded that overgrown area increased sink activity compared to the extensive grassland in observed period. After B4 correction was applied on our datasets cumulative NEE fluxes changed. For observation period Succession site shifted to weak sink ($-28 \text{ gCm}^{-2}\text{y}^{-1}$) of carbon, while the Grassland site remained a source ($456 \text{ gCm}^{-2}\text{y}^{-1}$). Applying SISC correction NEE changed to $-127 \text{ gCm}^{-2}\text{y}^{-1}$ and $362 \text{ gCm}^{-2}\text{y}^{-1}$ for Succession site and Grassland site, respectively. Our measurements showed the need for self-heating correction also for our ecosystems. It is more appropriate to use site specific self-heating correction based and developed on own measurements than those suggested by Burba et al. (2008). Concerning the Rs measurements it can be concluded that knowledge of temporal variability can be greatly improved with an automatic system. Corresponding measurements of soil temperature and moisture together with manual Rs measurements, improved the knowledge about spatial variability of Rs.

TABLE OF CONTENTS

Ključna dokumenatcijska informacija	III
Key words documentation	IV
Table of contents	V
List of tables	VII
List of figures	VIII
Abbreviations and symbols	XII
1 INTRODUCTION	1
2 STATE OF THE ART	4
2.1 MICROMETEOROLOGICAL METHODS IN ECOLOGY	4
2.2 EDDY COVARIANCE METHOD	5
2.2.1 Instrumentation	6
2.2.2 Location of flux tower, data processing software and footprint	7
2.2.3 Data processing and corrections	9
2.2.4 Instrument self-heating correction	10
2.3 CHAMBER METHOD	13
2.4 SINK ACTIVITY OF TERRESTRIAL ECOSYSTEMS	16
2.4.1 Grassland	16
2.4.2 Abandoned grassland or agriculture land	17
2.4.3 Karst ecosystem	18
3 MATERIALS AND METHODS	20
3.1 STUDY AREA	20
3.2 EDDY COVARIANCE MEASUREMENTS	24
3.2.1 Instrument self-heating correction	25
3.2.2 Gap-filling and flux-partitioning	28
3.2.3 Uncertainty analysis	29
3.3 CHAMBER MEASUREMENTS	30
3.3.1 Automatic soil respiration system	31
3.4 AUXILARY MEASUREMENTS	37

3.4.1	System for measuring Ts and SWC soil profiles	38
4	RESULTS	44
4.1	SINK ACTIVITY OF INVESTIGATED ECOSYSTEMS	44
4.2	DATA QUALITY AND EDDY COVARIANCE MEASUREMENTS	51
4.3	INSTRUMENT SELF-HEATING CORRECTION	53
4.4	SOIL RESPIRATION	59
5	DISCUSSION AND CONCLUSIONS	69
6	SUMMARY	78
6.1	SUMMARY	78
6.2	POVZETEK	84
7	REFERENCES	90
ZAHVALA		

LIST OF TABLES

Table 1:	List of micrometeorological methods	4
Table 2:	Land use change in 52 years for the study area.	22
Table 3:	Detailed characteristics of the sites.	23
Table 4:	Some environmental parameters and NEE averaged or summed by the vegetation and non-vegetation season (from April to beginning of October).	47
Table 5:	Percentage of missing, hard and soft flagged eddy covariance data presented as data gaps. Hard flags: rainy or foggy conditions, or when condensation occurs on the instrument optical lens. Soft flags: stationarity test and friction velocity filtering. Gap-filled data with quality indicators present how data gaps were filled (A - Rg, Ta and VPD data are available in temporal window smaller than 14 days or Rg is available in temporal window smaller than 7 days, B - Rg, Ta and VPD data are available in temporal window greater than 14 days and smaller than 28 days. C - only flux is available at different temporal window sizes start at 7 days (for details see chapter 3.2.2)).	51
Table 6:	Linear models derived from measurements of OP-IRGA body temperatures, mock temperatures and Ta between 22 nd of January 2011 and 3 rd of April 2012.	53
Table 7:	Models for Rs based on Ts and SWC derived for each Ukulele chamber.	67
Table 8:	Parameters of models (similar to Bahn et al., 2008) for soil respiration derived from manual measurements using LI-6400. Models are separated for Grassland site, forest patches and gaps at Succession site.	68

LIST OF FIGURES

Figure 1:	Schematic representation of general principle of EC (Burba and Anderson, 2010: 17).	5
Figure 2:	Typical application of OP IRGA sensor LI-7500 and sonic anemometer (3D CSAT) installed on our research plot.	7
Figure 3:	CNF dependency on the measuring height at fixed wind speed and friction velocity.	8
Figure 4:	Orto-photograph of the studied site (2009); rectangle (850 by 1700 m) indicates an area that was subjected to land use analysis, triangles indicate position of the Eddy towers .	22
Figure 5:	Automatic soil respiration system. Left: Schematic view of automatic chamber design. Middle: Automatic chamber installed on the field. Right: Central data storage electronic with multiplexer containing 2x16 electromagnetic valves.	32
Figure 6:	Electrical schematic of chamber electronic circuit board.	33
Figure 7:	(a) Circuit board with sensors DS18B20 and finished measurement stick. (b) Microcontroller circuit board with battery pack. (c) Waterproofed housing with system for measuring and logging soil temperature profile and soil water content. (d) Female DB9 connector for serial communication with the system built outside.	41
Figure 8:	Electrical schematic of circuit board.	42
Figure 9:	Footprint analyses (using model after Schuepp et al., 1990) and wind roses for Succession site (green color) and for Grassland site (brown color) site according to azimuth.	44
Figure 10:	Mean daily Ta, Ts, SWC and precipitation measured at two study sites (Succession site: green line; Grassland site: brown line)	45
Figure 11:	Phenology was observed on both sites. Up: On the Succession site ocular observation of phenology for main tree species every week or biweekly were performed. Down: On the Grassland site continuous measurements of incoming and reflected PPFD were performed (7-days moving window average is presented).	46
Figure 12:	Monthly NEE with estimated standard deviation. Succession site: green bars, Grassland site: brown bars.	48

Figure 13:	Monthly values of GPP and Reco based on Lasslop et al. (2010) and Rs using model similar to Bahn et al. (2008) based on manual Rs measurements (LI-6400). Succession site: green bars, Grassland site: brown bars.	49
Figure 14:	Relationship between modeled monthly Rs (Bahn et al., 2008), modeled monthly Reco (Lasslop et al., 2010) and Ta. Larger points present higher Ta which varies from 0.5°C to 28°C. Green points: Succession site, brown points: Grassland site.	50
Figure 15:	Percent of valid data during measuring campaign (January 1 st 2009 – November 30 th 2012) averaged by months (Succession site: green line; Grassland site: brown line)	51
Figure 16:	Energy balance closure for Succession site (green points) and Grassland site (brown points) site. The relation between consumed (LE + H) and available (Rn - G) energy. LE and H determined from eddy covariance, Rn and G measured half-hourly on meteorological station with net radiometer (NR-LITE, Campbell Scientific, Logan, UT USA) and soil heat flux plates at 10 cm depth (HFP01SC, Campbell Scientific, Logan, UT USA).	52
Figure 17:	Temperature difference between T _{mock} , T _{licor} and Ta. Values are averaged by Ta classes with step of 1°C. Gray zone represents values where R _g might influence the surface temperature (T _{surface}).	54
Figure 18:	Flux corrected by B4 and SISC plotted vs. air temperature for daytime (up panel) and night-time (down panel). Air temperature and corrected fluxes were averaged by temperature classes with step of 1°C.	54
Figure 19:	Flux corrected by B4 and SISC plotted vs. wind speed for daytime (up panel) and night-time (down panel). Wind speed and corrected fluxes were averaged by wind speed classes with step of 0.5 ms ⁻¹ .	55
Figure 20:	Flux corrected by B4 and SISC plotted vs. global radiation. Global radiation and corrected fluxes were averaged by global radiation classes with step of 10 Wm ⁻² .	55
Figure 21:	Cumulative fluxes of NEE: B4 correction applied (dashed line), SISC correction applied (dotted line) and NEE without self-heating correction (solid line) with uncertainty band. Brown lines: Grassland site; green lines: Succession site.	56

Figure 22:	Half-hourly Ta and Ws data. Flux data are presented without self-heating correction, with B4 correction and SISC correction. Data are presented for six warm days in July 2012.	57
Figure 23:	Half-hourly Ta and Ws data. Flux data are presented without self-heating correction, with B4 correction and SISC correction. Data are presented for six cold days in February 2012.	58
Figure 24:	Half-hourly Rs fluxes measured with new designed closed dynamic automatic chamber system (Ukulele) plotted vs. open dynamic automatic chamber system (Kukulo).	59
Figure 25:	Hourly Rs fluxes measured with new designed closed dynamic automatic chamber system (Ukulele) plotted vs. closed dynamic manual chamber system (LI-6400 with chamber LI-6400-9).	60
Figure 26:	Modeled monthly sums of half-hourly Rs fluxes based on measurements with new designed closed dynamic automatic chamber system (Ukulele) plotted vs. Rs fluxes based on measurements with closed dynamic manual chamber system (LI-6400 with chamber LI-6400-9). For model (similar to Bahn et al., 2008) data measured from 1 st of September 2012 till 30 th of November 2012 and biweekly from July 2008 to November 2010 for automatic and manual system, respectively.	61
Figure 27:	Half-hourly Rs fluxes (night-time) measured with new designed closed dynamic automatic chamber system (Ukulele) plotted vs. night-time ecosystem fluxes measured by Eddy covariance method. Data measured from 1 st of September 2012 till 30 th of November 2012.	62
Figure 28:	Soil respiration with standard deviation estimation for period from 1 st of September 2012 till 30 th of November 2012 measured with Ukulele system plotted vs. number of measuring points. Standard deviation was calculated from 100 datasets generated randomly choosing between 2 to 14 measuring points.	63
Figure 29:	Standard deviation of soil respiration for 2 and 15 measurements points plotted vs. soil temperature. Standard deviation of soil respiration was averaged by temperature classes with step of 1°C. Solid lines are trend lines of presented points.	64

Figure 30:	Ts at 10 cm depth measured with new system for measuring soil profiles plotted vs. thermocouples (TCAV, Campbell Scientific, Logan, UT USA) connected to CR3000 data logger.	65
Figure 31:	SWC at 10 cm depth measured with new system for measuring soil profiles plotted vs. time domain reflectometer (CS616, Campbell Scientific, Logan, UT USA) connected to CR3000 data logger.	66

ABBREVIATIONS AND SYMBOLS

APAR	Absorbed photosynthetic active radiation
B4	Self-heating correction according to method 4 in Burba et al. (2008)
CP	Close path analyzer
CV	Coefficient of variation
E	Water vapour flux
EC	Eddy covariance method
F _c	Carbon flux
GPP	gross primary production
IRGA	Infrared gas analyser
NEE	net ecosystem exchange of CO ₂
NEP	net ecosystem productivity
OP	Open path analyzer
P	Precipitation
PPFD	Photosynthetic flux density
PRT	Fine-wire self-heating correction technique where temperature is measured directly in OP (Grelle and Burba, 2007).
Reco	respiration of the ecosystem
R _g	Global radiation
RI	Rewetting index
R _s	Total soil CO ₂ efflux
s.d.	Standard deviation
SISC	Site specific self-heating correction
SWC	Soil water content
T _a	Air temperature
T _s	Soil temperature
VPD	Vapour pressure deficit
W _s	Wind speed

1 INTRODUCTION

Micrometeorology is a part of meteorology dealing with atmospheric phenomena and processes limited to atmospheric boundary layer, which is defined as the layer of a fluid in which heat, momentum and mass exchanges take place between the surface and the fluid (Arya, 1988). The height of atmospheric boundary layer varies from 20 m to 5 km and is mainly dependent on the heating or cooling of the surface, winds and roughness of the surface. The typical height of atmospheric boundary layer is between 20 m and 500 m. The lowest one-tenth of atmospheric boundary layer is called the surface layer (Arya, 1988). In this layer a significant part of heat, momentum and mass exchange occurs; therefore it receives greater attention from micrometeorologist than other parts of atmospheric boundary layer. With the extensive development of electronic equipment and instruments micrometeorological methods have become more widely used and are also available for ecological studies. Suspicions regarding global climate changes have encouraged ecologists to use them for more in-depth research on greenhouse gases.

The constant rise of atmospheric concentrations of carbon dioxide (CO₂) in last 400 years is the consequence of anthropogenic emissions. The CO₂ concentration had risen from 280 ppm in the 18th century to 375 ppm in the year 2011 (Wu et al., 2012). About 75% of these emissions are due to fossil fuel burning and the rest are from land use change (Climate change, 2001). These facts led to an intensive research of the carbon balance for different land use changes and ecosystems. According to their characteristics and the state, ecosystems can over extended periods of time have a carbon gain, i.e. they act as carbon sink, or have a carbon loss, i.e. they release carbon or act as carbon source. Monitoring of the carbon cycle and determining whether a given ecosystem is a sink or a source of carbon (sink activity) is important in terms of knowledge of the sink capacity of a single ecosystem and consequently the issue of mitigating the climate change effects. This balance can be studied by applying different approaches. For direct estimate of net ecosystem carbon exchange (NEE) between an ecosystem and the atmosphere Eddy correlation also known as Eddy covariance(EC) method (Desjardins, 1974) has been commonly used. Later, it was successfully applied for various types of ecosystems.

The EC gives an insight into net exchange of carbon for an entire ecosystem, but not into the individual segments of the carbon cycle which are defined as (Schulze et al., 2002):

$$NEP = GPP - (R_{aut} + R_{het} + T_{leac} + T_{dist} + T_{oth}) \pm T_{lat} \quad \dots(1)$$

Where NEP is net ecosystem production, GPP is gross primary production, R_{aut} is autotrophic respiration, R_{het} is heterotrophic respiration, T_{leac} is leaching of carbon, T_{dist} is removal of carbon due to disturbances, T_{oth} presents other removal of carbon from ecosystem and T_{lat} presents lateral efflux or influx of carbon from or to the ecosystem.

Assuming that there are no specific interventions in terms of biomass removal or other major disturbances, the equation (1) can be simplified:

$$NEP = GPP - Reco = -NEE \quad \dots(2)$$

In an ecosystem decomposition and respiratory activity of the heterotrophic and autotrophic organisms could be combined under a common component of ecosystem respiration (Reco). Soil respiration (Rs) represents, especially in the winter, a major part of Reco. Rs is an important component of the carbon cycle, which is driven by photo-assimilate supply (Bahn et al., 2009) and strongly influenced by soil temperature and soil water content (Almagro et al., 2009). Main contributors to total Rs, also called soil the CO₂ efflux are (Kuzyakov, 2006): microbial decomposition of soil organic matter in root-free soil without undecomposed plant remains, microbial decomposition of soil organic matter in root-affected or plant residue-affected soil, microbial decomposition of dead plant remains, microbial decomposition of rhizodeposits from living roots, and root respiration.

Despite intensive research, carbon cycle is still underinvestigated and not fully understood for many ecosystems, especially the ones which are of minor direct importance in terms of food and wood production. These are normally low productivity ecosystems that are not of major interest in economic terms. Carbon research is also less intensive in ecosystems with a high heterogeneity of environmental factors (vegetation, soil, water and nutrient supply...) which limits application of conventional methods and makes research more difficult. Due to both reasons, karst ecosystems are among the less studied ecosystems. A terrain with sinkholes may present difficulties for micro-meteorological measurements. A high spatial variability can be found in soils, where soil depth varies from a few centimetres to several meters in soil pockets. This fact can restrict the use of certain conventional measurements methods.

In this study we used Eddy covariance method in the karst ecosystem. Furthermore we used portable and automatic soil respiration systems for measuring Rs and as supporting measurements soil temperature and soil water content profiles were installed.

In the framework of this study we want to answer on the following objectives:

Sink activity of investigated ecosystems. (H1) Based on micro-meteorological measurements we expect an increased sink activity in the current overgrown area compared to the extensively used grasslands. Carbon balance should change, and ecosystem is larger sink if the succession with woody species began in abandoned pastures and meadows.

Data quality and eddy covariance measurements. (H2) We expect that some features of karst ecosystems, such as relief, the heterogeneity of the terrain, wind conditions, could affect the use of Eddy covariance method and can significantly affect the quality of measurements. Since also vegetation influences the measurements, we anticipate that different approaches should be used for NEE measurements on the extensive pasture in comparison to the overgrown area.

Instrument self-heating correction. (H3) The data processing of eddy covariance measurements has to be corrected for the heat loss of measurement electronics (Burba et al., 2008) when the ambient temperatures are low. We assume that in our case this correction will not be necessary, because of ecosystem temperature range.

Soil respiration. (H4) We expect that soil respiration measurements, with an improved automatic system and corresponding measurements of soil temperature and moisture, could be improved by a larger number of cuvettes that would improve the information about the temporal and spatial variability of Rs. Automatic system for measuring Rs with more cuvettes and associated soil temperature and moisture measurements greatly improves knowledge of temporal and spatial variability of Rs.

2 STATE OF THE ART

2.1 MICROMETEOROLOGICAL METHODS IN ECOLOGY

The use of micrometeorological methods and principles for vegetation surfaces, such as crops, grasslands and forests requires special attention. In this case the researchers are interested in the atmospheric environment within and above plant canopies and also in the interaction between the ecosystem and the atmosphere. Each method requires certain measurements which are performed over different temporal scales from milliseconds to hours, depending on what time resolution is needed for measuring campaign. Usually measurements are performed with automatic measuring systems continually left on the site and data from these systems usually have a high temporal resolution. Some measurements are performed with portable systems, usually with high spatial resolution. Micrometeorological measurements are performed on measuring plots of different sizes ranging from millimetres up to kilometre. The spatial scale and resolution depend on the needs of the measuring campaign, the size of measuring plot and usually on the budget of measuring campaign. Several micrometeorological methods are being used in the field of ecology and some of these are listed below.

Table 1: List of micrometeorological methods appropriate for measuring flux (after Burba and Anderson, 2010 and Arya, 1988)

Method	Short description
Eddy covariance	Simultaneously and fast measurements of gas and 3D wind speed.
Eddy accumulation	Fast measuring of vertical wind speed and proportional sampling of updraft and downdraft of gas.
Relaxed eddy accumulation	Fast measuring of vertical wind speed and not proportional sampling of updraft and downdraft of gas.
Aerodynamic method	Measurements of wind and gas profiles.
Chamber methods	Measurements of changing or increased gas in the chamber with known volume and area.
Profile method	Measurements of gas on at least two levels.
Resistance method	Measurements of gas and their resistance to transport.
Mass balance for small areas	Measuring the differences in mass for certain part of ecosystem.

It is not in the scope of this work to go into details of each listed method, they are merely listed and it is explained how they can be used during certain measuring campaigns. In our work the Eddy covariance and Chamber methods are described.

2.2 EDDY COVARIANCE METHOD

Measurements of the net exchange of gases between the ecosystem and the atmosphere using the Eddy covariance method (EC) are made above the ecosystem, in the surface layer in which turbulence is more or less constant. This method was used for the first time in the 1970s (Desjardins, 1974, Baldocchi et al., 1988). Thereafter the number of studies using this method was growing every year. The use of the phrase "eddy covariance" when searching for the scientific articles in the ISI Web of Knowledge for the period between 1982 and 1996 returns only 64 contributions, while for the period between 1996 and 2011 it returns more than 2300 contributions. The advantage of Eddy covariance method is that with appropriate position of sensors above the canopy gas (e.g. CO_2 , O_3 , NO_x , CH_4 ...), heat and water exchange can be measured for any ecosystem regardless of its heterogeneity. The method requires input of data for wind speeds from all three directions (x, y, z), the concentration of a gas being monitored (for example CO_2) and air temperature recorded at a frequency of at least 10 Hz. Data is processed using established and recognized methodologies that are proposed by many researchers (Aubinet et al., 2000; Webb et al., 1980; Foken and Wichura, 1996; Reichstein et al., 2005; Papale et al., 2006; Richardson and Hollinger, 2007; Lasslop et al., 2010), and after a successful processing of data a half-hourly NEE values are obtained.

The principle for measure flux according to EC is to measure how many particles of component of interest are moving up and down over time and how fast they are. Imagine the air flow over the investigated area as a horizontal flow of numerous rotating eddies as presented in Figure 1. At a certain time 1 eddy 1 moves air parcel c_1 downward with the speed w_1 and at the same point in the time 2 eddy 2 moves parcel of air c_2 upward with speed w_2 . Air parcels c_1 and c_2 have their gas concentrations, temperatures and humidities. If we can measure this movement and characteristics of air, vertical flux can be represented as a covariance of vertical velocity and concentration or temperature of the entity of interest.

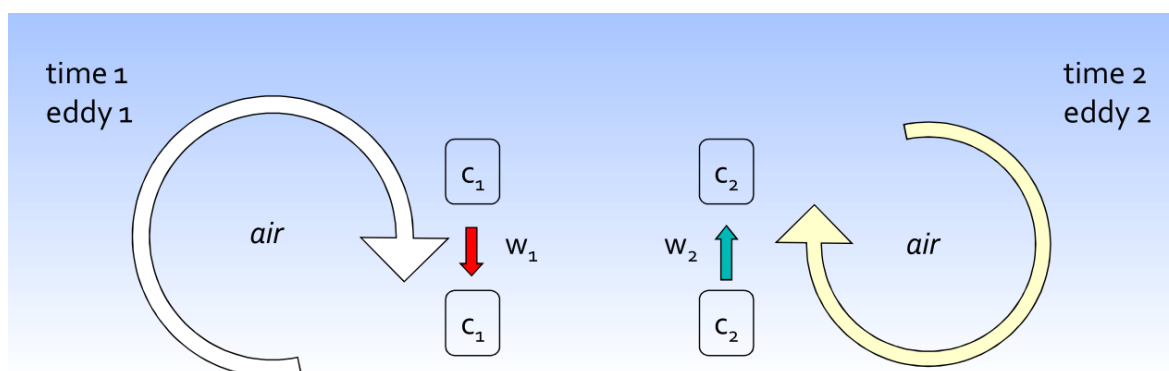


Figure 1: Schematic representation of general principle of EC (Burba and Anderson, 2010: 17).

In turbulent flow, vertical flux is equal to a mean product of air density, vertical wind speed and the mixing ratio of the entity of interest (Burba and Anderson, 2010):

$$F = \overline{\rho_d} \overline{ws} \quad \dots(3)$$

After the application of Reynolds decomposition [$F = (\overline{\rho_d} + \rho'_d)(\overline{w} + w')(\overline{s} + s')$] and assumptions that air density fluctuations and mean vertical flow are assumed to be negligible for horizontal homogeneous terrain, equation for flux calculation is simplified to the product of the mean air density and the mean covariance between instantaneous deviations in vertical wind speed and mixing ratio.

$$F_m \approx \overline{\rho_d} \overline{w's'} \quad \dots(4)$$

Where F_m is final flux calculated using mixing ratio; ρ_d is dry air density; w is vertical wind speed component; s is mixing ratio.

EC method is a well defined method, but is based on mentioned assumptions and therefore there have been some proposals not to use it for some terrains. Is not very useful on slopes, but some researchers have shown that its use is possible (McMillen, 1988). Some features of karst ecosystems, such as relief, heterogeneity of the terrain and wind conditions, could affect the use of the EC method. Non homogeneous vegetation, typical for woody plant encroachment areas, can increase the roughness of the measured surface and consequently limits the use of EC method. One of the objectives of this study (H2) is to show that for grasslands and abandoned overgrown grasslands different approaches of EC measurements are needed.

2.2.1 Instrumentation

Near the surface several eddies could be found transferring most of the flux. Closer to the ground eddies are smaller and rotate quickly and higher above the ground eddies are bigger and rotate slowly. The sensors must therefore sample fast enough to cover the whole frequency range and need to be sensitive to small changes in quantities.

To perform EC measurement, for example to estimate NEE, vertical wind speed, temperature, and CO_2 and H_2O concentrations, measurements must be performed at least 10 times per second (10 Hz). For wind speed measurements a sonic anemometer should be used. It measures the speed of sound using ultrasonic transducers and receivers. Sonic temperature can also be calculated from the speed of sound. There are several companies that offer appropriate sonic anemometers, e.g. Gill Instruments, ATI, Young, Metek, etc. For measuring CO_2 and H_2O concentrations a non-dispersive infrared gas analyzer (IRGA) should be used. It works on the principle of absorption of radiation in the infrared region of the electromagnetic spectrum by carbon dioxide or water. There are several companies producing appropriate sensors, like PPsystem, ADC, etc., but most widely used are the instruments produced by Li-Cor Biosciences Inc., Lincoln, NE. Each instrument requires

careful installation and proper maintenance. For sonic anemometer it is important to maintain constant orientation to minimize the angle-of-attack errors and to keep the transducers clean to minimize the errors during sonic measurements. In general, sonic anemometers will not work during heavy precipitation events, however different models react differently to light precipitation, snow and ice. For measuring the CO₂ and H₂O concentration there are two different types of instruments; the open path (OP) and the closed path (CP) IRGAs. In 2010 Li-Cor developed an enclosed IRGA (LI-7200) which combines advantages of OP and CP designs. Most researchers still use older IRGAs, i.e. OP or CP designs, and therefore more attention will be paid to these two types here. The choice between different designs is dependent on power availability and the frequency of precipitation at the site. CP designs require an air pump to transport the air from measuring point near the sonic anemometer to the measuring cell and for that more power is needed on the site. The main advantage of a CP system is that precipitation has no impact on measurements, which is not the case when OP system is used, where even light precipitation will strongly influence measurements. OP instruments must not break large eddies because of their structure and must therefore be aerodynamic to prevent the creation of small eddies around them. The sensing volume of OP must be small enough and must not average small eddies. The main advantage of an OP system is its lower power consumption.



Figure 2: Typical application of OP IRGA sensor LI-7500 and sonic anemometer (3D CSAT) installed on our research plot.

2.2.2 Location of flux tower, data processing software and footprint

Before placing the flux tower in the field, the main objectives of the experiment must be established, taking into account the restriction of using EC method primarily on flat terrain. In the tower, fluxes from the wind direction will be recorded and it is therefore useful to know the predominant wind direction for the site. The general rule of thumb is that the measurement height must be 100 times lower than the desired fetch of the flux tower;

however, the height of the tower according to another rule of thumb should ideally be twice the canopy height.

According to the objective of the experiment, at the site of recording fluxes a tower must be erected and appropriate instrumentation and power requirements must be installed on it. After the first data recording, first data processing must be performed. For this purpose freely available micrometeorological software could be used, but the researchers usually write their own software for processing their specific datasets.

The next step of processing is to calculate the real footprint for a certain time period (day, month, year, etc.). For this purpose several models could be used and one of especially useful ones is the model of Schuepp et al. (1990) which evaluates the contributions of fluxes from a given distance from the tower. The model based on the equation (5) estimates cumulative normalized contribution to flux measurements (CNF) for near neutral conditions.

$$CNF = e^{-\frac{u \cdot (z-d)}{u^* \cdot k \cdot x}} \quad \dots(5)$$

Where u is wind speed, z is measuring height, d zero plane displacement, u^* is friction velocity, k is von Karman constant (0.40) and x is upwind distance from flux tower.

In order to demonstrate how CNF is affected by measuring height (figure 2), d was calculated according to Arya, (1988). In some studies (Barr et al., 2006) d was estimated as 63% of the canopy height.

$$\log(d) = 0.98 * \log(h_0) - 0.15 \quad \dots(6)$$

Where h_0 is vegetation height and in example on figure 2 $h_0 = 1$ m was chosen.

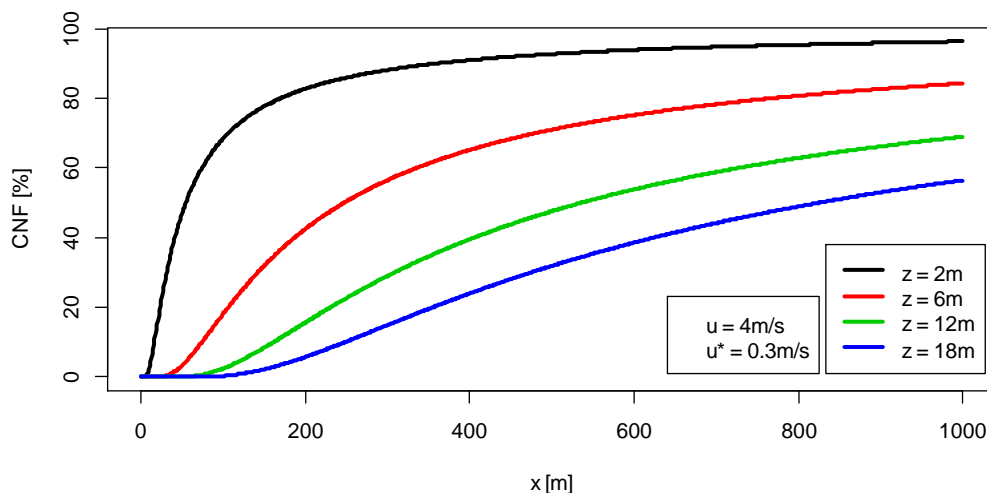


Figure 3: CNF dependency on the measuring height at fixed wind speed and friction velocity.

2.2.3 Data processing and corrections

Raw datasets collected from the EC tower require special steps in data processing in order to obtain correct fluxes (Burba and Anderson, 2010). Data processing could be broken down into the following steps:

- Unit conversion is a process where raw data are converted from millivolt or speed of sound readings to appropriate units of instantaneous values.
- De-spiking remove occasional spikes of high frequency instantaneous data due to electronic or physical noise.
- Coordinate rotation needs to be applied to assure that the axes of sonic anemometer, are perpendicular to the mean wind streamlines. Researchers usually use planar fit method to apply this correction. It works on the real data, collected for example over one month, and calculate the hypothetic plane of mean wind streamlines in order to find out true vertical stream direction which is perpendicular to hypothetic plane.
- Time delay compensates the difference between time acquisition from sonic anemometer and time acquisition from gas analyser. It is much more important for CP system where air sampled by sonic anemometer comes to IRGA several seconds later.
- De-trending is process where mean values from instantaneous values are subtracted to compute flux. Many of researchers uses block averaging method, since linear de-trending and non-linear filtering are less recommended.

A major group of corrections deals with flux losses at different frequencies of turbulent transport; they are called frequency response corrections. Frequency response corrections are based on cospectra. Cospectra are a distribution of the raw flux by frequency and describe how much of the flux is transported at each frequency. In the group of frequency response corrections, the following are the most important:

- time response correction,
- sensor separation correction,
- path and volume averaging correction,
- high and low pas filtering correction,
- digital sampling correction.

On some occasions sensor responses can also mismatch corrections and if closed-path sensor tube is used, attenuation correction must be applied. However, frequency response

corrections can increase fluxes by up to 30% or even more at night. Another correction which can decrease or increase fluxes by more than 40% is Webb-Pearman-Leuning correction, usually called WPL or density correction (Webb et al., 1980). The equation (7) could be used when the mixing ratio of gas is measured at high frequencies. Flux calculations are usually performed using gas density and therefore WPL correction must be applied to compensate for the fluctuations of temperature and water vapour content that affect the measurement:

$$F_d \approx \overline{w'\rho'} + \mu \cdot \frac{E}{\rho_a} \cdot \frac{\bar{\rho}}{\left(1 + \mu \cdot \left(\frac{\rho_w}{\rho_a}\right)\right)} + \frac{S \cdot \bar{\rho}}{C_p \cdot \bar{\rho}_a \cdot \bar{T}} \quad \dots(7)$$

Where F_d is final WPL corrected flux; ρ is gas density; μ is constant ratio of molar masses of air to water; E is evapotranspiration; ρ_w is the water vapour density; ρ_a is the total air mass density; C_p is specific heat of air; S is sensible heat flux; T is air temperature in open path measuring cell.

To calculate E , the following equation is used:

$$E = \left(1 + \mu \cdot \left(\frac{\rho_w}{\rho_a}\right)\right) \cdot \left(\overline{w'\rho_w'} + \frac{S \cdot \bar{\rho}_w}{C_p \cdot \bar{\rho}_a \cdot \bar{T}}\right) \quad \dots(8)$$

and for sensible heat flux:

$$S = C_p \cdot \bar{\rho}_a \cdot \overline{w'T'} \quad \dots(9)$$

As we have presented above, there are two corrections that can significantly affect the measured fluxes. The third that can be significant is the instrument self-heating correction which was proposed for the first time in 2006 by Georg Burba and is therefore also called the Burba correction (Burba et al., 2008). Since we paid a lot of attention to this correction in our study, it is presented in greater detail on the following pages.

Datasets with applied corrections listed above usually have a lot of gaps due to various reasons already mentioned. The dataset must therefore be gap-filled (Reichstein et al., 2005; Serrano-Ortiz et al., 2009). Furthermore, uncertainty analysis (Richardson and Hollinger, 2007; Wohlfahrt et al., 2008; Haslwanter et al., 2009) must be done to reach a valuable NEE estimation and flux partitioning (Lasslop et al., 2010; Gilmanov et al., 2010; Unger et al., 2009; Reichstein et al., 2005) must be performed to divide NEE into components of interest for the investigated ecosystem.

2.2.4 Instrument self-heating correction

Data processing is different for OP and CP measured data, in particular with regard to corrections which need to be applied to the raw covariances between the vertical wind speed and the mixing ratio or gas density of the CO_2 or H_2O . Some comparisons between

carbon (F_c) and water vapour fluxes (E) derived from OP and CP instruments show similar results (e.g. Ocheltree and Loescher, 2007; Wohlfahrt et al., 2008; Haslwanter et al., 2009), but other, especially in cold environments, show substantial differences (e.g. Hirata et al., 2007; Clement et al., 2009). Further investigations show that these differences between OP and CP instruments are caused by OP instrument surface heating due to electronics and that such heat should be accounted for in the density correction (Grelle and Burba, 2007). Burba et al. (2008) suggested a self-heating correction technique which can be applied to previously calculated fluxes based on data from OP instruments. The so-called Burba correction is based on traditional Webb Pearman Leuning (WPL) (Webb et al., 1980) correction (equation (7)) by adding estimated or measured sensible heat fluxes from OP instrument surfaces heated by its electronics or solar irradiance. It is not possible to correct raw gas densities measurements at high frequencies, because fast air pressure and temperature measurements are usually not performed in OP measuring cell and because Burba and also WPL correction correct half-hourly fluxes. Some recent studies use Burba correction for correcting fluxes (Alberti et al., 2010; Reverter et al., 2011) but some studies report that applying suggested self-heating correction to fluxes produces unreasonable results (Wohlfahrt et al., 2008).

At present Burba correction is generally used only at cold sites, but without objective criteria as to where and when it must be applied. Applying Burba correction to annual net ecosystem exchange (NEE) data measured with OP systems for several ecosystems has pushed annual NEE values towards carbon loss everywhere, with greater magnitude at colder sites (Reverter et al., 2011). However, Burba et al. 2008 have suggested 4 methods for correcting F_c and E fluxes and have declared measuring with CP system as best solution. Another two possibilities are to perform fast temperature measurements inside the optical path of OP and use them in standard WPL correction or estimate surface temperature of OP from air temperature via empirical equations. The most inappropriate method is to assume that the effect of surface heating is negligible.

All present studies deal with changes in sensible heat flux in the optical path of OP analyzer based on temperature measurements. The first step to measure F_c and E by EC is to make precise and reliable fast mixing ratio or gas density measurements for CO_2 and H_2O . This is only possible when an instrument with no effect on heat exchange around measuring point is used or if CP system is used. OP systems will always have an effect on heat exchange because the temperature of chopper housing needs to be regulated at 30°C . Temperature regulation is involved in measurements of CO_2 , H_2O and reference to perform measurements without the effect of dust on the lens. Analyzer LI-7500A that was developed and produced by Li-Cor allows the user to choose between two regulating temperatures for the chopper housing (between 5 and 30°C). This should solve the problems of self-heating correction with possible limitations when air temperatures are below 5 or over 30°C . Enclosed open-path IRGA LI-7200 with a short intake tube was tested and produced by Li-Cor. Depending on tube length it can operate similarly as OP

analyzer with short tubes or as CP analyzer with long tubes. The enclosed analyzer outputs are instantaneous gas density and also instantaneous mixing ratio measurements, so there is no need to implement WPL correction during the data processing. Some corrections and some assumptions could be avoided with using enclosed system LI-7200 (Burba et al., 2012).

Many studies were and still are performed using OP IRGA LI-7500 with no direct possibilities to minimize impact of instrument self-heating effect. When the surface of the instrument warms up the air, the air will expand and as a result CO₂ and H₂O density measurement will not be correct. At this point the need for OP instrument self-heating correction starts. We assume that in our case this correction will not be necessary, because of the temperature range of ecosystem (H3). One part of our investigation on OP IRGA self-heating correction will be to check if the Burba correction method 4 gives reasonable results for our ecosystem.

Furthermore, we will try to find out if it is possible to perform reliable, robust and continuous measurements of OP IRGA body to assess the difference in temperature caused by the heating of electronic components. Finally we will propose a site specific instrument self-heating correction (SISC) which will be appropriate for use with fluxes measured in our ecosystem.

2.3 CHAMBER METHOD

There are numerous studies on NEE, gross primary production (GPP) and respiration (Reco) of different natural ecosystems based on EC, but in some conditions (e.g., low canopy vegetation) the use of chamber method is also possible. The chamber method is most commonly used for measuring R_s , which represents the second largest carbon flux between ecosystems and the atmosphere (Raich and Schlesinger, 1992). On the basis of R_s measurement results reported in the scientific literature worldwide, the amount of CO_2 emitted by soil has been estimated at $68\text{--}80 \text{ PgCy}^{-1}$ (Raich et al., 2002); for comparison: only 10% of this amount is emitted by fossil fuel combustion (Climate change, 2001). Thus, even very slight change in intensification or mitigation of soil respiration process can affect the amount of CO_2 emitted from soil. Researchers have several different chamber techniques for flux measurements available, however according to Pumpanen et al. (2004) three major chamber techniques can be highlighted:

- closed static chamber (non-steady-state non-through-flow chamber),
- closed dynamic chamber (non-steady-state through-flow chamber),
- open dynamic chamber (steady-state through-flow chamber).

Despite the widespread use of chambers for R_s measurements, no standard is established with regard to the dimensions and type of chamber to perform these measurements. Pumpanen et al. (2004) tested 20 different types of chambers for the R_s measurement and compared them with well-defined values from CO_2 flux calibrating tank, which ranged from 0.32 to $10.01 \mu\text{molCO}_2\text{m}^{-2}\text{s}^{-1}$. They found out that on average all chambers performed well and that the results did not deviate by more than 4% from the calibrating values. Pumpanen et al. (2004) also reported that the main source of error in chamber measurement is the mixing of air within the chamber. The chambers always influence the object being measured. When a non-steady-state chamber is placed on the ground, the concentration in the chamber starts to change. Rising concentration within the chamber may influence the CO_2 efflux from the soil by altering the natural soil concentration gradient. Pressure anomalies caused by placing the chamber on the soil surface may also disturb the CO_2 concentration gradient. With steady-state chambers, pressure differences between the inside and outside of the chamber can generate mass flow of CO_2 from the soil into the chamber. Described problems, especially the mixing of air in chamber, are strongly connected with chamber volume and with their shape.

Majority of researchers measure R_s using non-steady-state chambers and due to this we will deal with this chamber technique. A simple but time consuming technique is using a chamber and a portable infrared gas analyser with an appropriate data logger and a system for pumping air. The weakness of a portable system for measuring soil respiration is that they enable only instantaneous non-continuous measurements. There are some manufactures producing such systems like PP-system and ADC, but one of the most

widely used is portable system for measuring soil respiration with a closed dynamic chamber LI-6400 (Li-Cor Biosciences Inc., Lincoln, NE). More complicated and more expensive but less time consuming is the use of automated systems for measuring soil respiration (e.g.: LI-8100, Li-Cor Biosciences Inc., Lincoln, NE). The most important feature of these systems is continuous measurement of soil respiration, due to the fact that daily variability, especially in vegetation season, can be very high and is strongly connected to daily T_s variations. In natural environments, high spatial variability, especially in soils, is not rare and therefore several repetitions of soil respiration measurement are needed. The problem with non-steady state chambers is how to mark and prepare the measuring point for a campaign or continuous measurements. Very often different types of collars are used. Collars can be placed very carefully less than 1 cm deep in the soil with extreme care, so that the roots are not cut. In this case, the collar is about 5 cm above ground. Over longer term, the soil inside the collar is exposed to different conditions: the collar can affect the wind speed above the ground and also the soil water content and temperature on the very first layer of the soil. Alternatively, the collars can be placed deeper into soil to cut the roots and to prevent the measuring point to be overgrown with roots from aside. This changes the environment in the soil very much and affects the R_s flux (Kutsch et al., 2010). Measuring R_s with non-steady chamber technique has many sources of errors, such as using collars and preparing measuring point by removing live plants. The basic problem of measurements in natural ecosystems is heterogeneity and this may be particularly well expressed in soil with the processes of R_s . For a better measurement of specific soil parameters it is not sufficient to perform multiple measurements at one point, the parameters should rather be measured simultaneously at several points. These requirements make measurements more expensive, but they provide a better insight into the temporal and spatial dynamics of monitored parameters.

Measurements made in closed dynamic chambers allow us to get the R_s value for shorter periods, e.g. hours. Some researchers made their own automatic systems for R_s measurements, tested them, and used them in their research. In all these systems, the chambers have to be installed on the measuring area and should allow the closing of chamber before measurement and its re-opening after it. They must be designed in a way that minimizes a long-term impact on the measuring point. The majority of researchers use a system, on which only the lid of the chamber is opened, and its perimeter stays at the measurement point (for example, McGinn et al., 1998; Edwards and Riggs, 2003; Delle Vedove et al., 2007).

To perform R_s measurement, all photosynthetically active biomass above ground must be removed at the measuring point. Between 8% and 52% of total fixed CO_2 in assimilates during photosynthesis is respired by roots (Lambers et al., 1996; Atkin et al., 2000). Part of assimilates allocated in roots is used by organisms associated with plant roots in the rhizosphere. The release of exudates, secretions and root residues results in a much higher concentration of micro-organisms in the rhizosphere around the roots in comparison to the

soil not directly influenced by the roots (Grayston et al., 1997). Therefore, removing live photosynthetic plants drastically changes the measuring point that is set for use for soil respiration measurements. If we cut the green part of the plant and leave the roots in the soil, we change the ratio of dead and live roots and therefore give more food to decomposers, the consequence of which is overestimation of R_s . If we cut the green part of the plant and wait several months for roots to be decomposed, and measure R_s after that, there is a possibility that we will underestimate the R_s . If the measuring point must be large because of big chamber diameter, the roots from side will not overgrow the volume. Furthermore, when aboveground biomass is removed on a larger area, the microclimatic conditions above ground change too. The measurement of the realistic R_s is not easy and we must take into account possible sources of errors due to the choice and management of measuring points.

In addition, besides R_s measurements, it is necessary, especially in the more heterogeneous ecosystem, to perform measurements of soil moisture and soil temperature. These two parameters can, in some cases, explain 80% of the time variability cases of R_s (Tang et al., 2006). To carry out the measurements of soil moisture there are different implementations of sensors available, while for soil temperature measurements most commonly thermocouples are used. Measurements of soil processes in karst ecosystems are more important, since the influx of carbon from the karst ecosystem to the atmosphere could be significantly contributed to by geogenic CO_2 (suggested in studies by: Emmerich, 2003; Kowalski et al., 2008, Inglima et al., 2009; Serrano-Ortiz et al., 2009; Serrano-Ortiz et al., 2010). This makes CO_2 research in karst ecosystems even more complex and demanding.

To eliminate or minimize described errors, a solution with a special chamber design must be found which will not seriously affect and change the environmental conditions around the measuring point and which will allow the measurement of R_s with minimum removal of living plants required. A system with the new chamber design must have the possibility to measure R_s with different chambers in case of soil heterogeneity. One of the objectives (H4) of this study is to design and construct a special chamber, to connect several of them onto an automatic soil respiration measurement system, and to verify if multiple repetitions are needed to improve the knowledge of temporal and spatial variability of R_s .

2.4 SINK ACTIVITY OF TERRESTRIAL ECOSYSTEMS

Steady-state ecosystem over a long-time period with absence of human activities or other disturbances would achieve a balance between GPP and Reco to reach the state when NEP is zero. In reality, human activities, natural terrestrial disturbances and climate variability impact GPP and Reco and cause non-zero NEP for short time periods. The time lag required for Reco to catch up with a change in GPP has been estimated to be on the order of 10 to 30 years (Raich and Schlesinger, 1992). The terrestrial ecosystems globally act as a sink for carbon despite large releases of carbon due to deforestation and agricultural activities in some regions (Climate change, 2001).

Deforestation has been responsible for almost 90% of the estimated emissions due to land-use change since 1850 (Houghton, 1999). However, managed or regenerated forest usually presents a sink of carbon, but the harvested wood must be turned into long-lasting products and actions for forest regeneration must be taken. Valentini et al. (2000) report annual NEP in range of 0.7 to 5.9 $\text{MgCha}^{-1}\text{y}^{-1}$ for tropical forests and 0.8 to 7.0 $\text{MgCha}^{-1}\text{y}^{-1}$ for temperate forests, while boreal forest sink activity was estimated to 2.5 $\text{MgCha}^{-1}\text{y}^{-1}$. Sink activity of 80-year-old beech stand in Denmark measured by the EC was on average 1.8 $\text{MgCha}^{-1}\text{y}^{-1}$ (Pilegaard et al., 2001). Teklemariam et al. (2009) report for 100-year-old mixed forest of pine, maple and aspen to have sink activity of 1.4 $\text{MgCha}^{-1}\text{y}^{-1}$.

Conversion of natural vegetation to agricultural land is also a major source of carbon, usually in connection with deforestation activities. Carbon losses occur also due to increased decomposition of soil organic matter caused by disturbance and energy cost of various agricultural practices (Schlesinger, 2000). Croplands can either act as a carbon sink or carbon source, depending on the agricultural practice, within range from -2.1 $\text{MgCha}^{-1}\text{y}^{-1}$ up to 6.4 $\text{MgCha}^{-1}\text{y}^{-1}$ (Gilmanov et al., 2010). For example: Beziat et al. (2009) reported wheat crop acts as a carbon sink of -3.7 $\text{MgCha}^{-1}\text{y}^{-1}$, while sunflower crop acts as a carbon source of 0.28 $\text{MgCha}^{-1}\text{y}^{-1}$.

2.4.1 Grassland

Grasslands contribute to the biosphere-atmosphere exchange of greenhouse gases mainly with fluxes of carbon dioxide (CO_2) and methane (CH_4) that are intimately linked to management (Soussana et al., 2007). Cutting regime, grazing, fertilization and other disturbances can severely alter different components of carbon cycle and can strongly influence the rates of carbon gain or loss. Gilmanov et al. (2010) reported about sink activities, measured by EC above the extensive and intensive grasslands. Analyses of 316 plots from all around the world show that 80% of all plots act as a carbon sink. Extensive and intensive grasslands were on average a net carbon sink: 0.7 $\text{MgCha}^{-1}\text{y}^{-1}$ and 1.8 $\text{MgCha}^{-1}\text{y}^{-1}$, respectively. Generally, majority of the variation in grassland net ecosystem exchange (NEE) is influenced by the amount of precipitation (Flanagan et al., 2002). In this respect, arid and semi-arid grasslands are especially sensitive to inter-annual variability in precipitation (Huxman et al., 2004). For example, Nagy et al. (2007) who

were studying NEE dynamics and carbon balance of a dry, extensively managed sandy grassland on the Great Hungarian Plain in the years 2003 and 2004 found that it was a weak source of carbon in 2003 ($0.22 \text{ MgCha}^{-1}\text{y}^{-1}$), owing to the exceptionally hot and dry conditions, while it was a moderate sink in 2004 ($0.51 \text{ MgCha}^{-1}\text{y}^{-1}$), when the amount of precipitation was considerably above the 10-year average. Carbon dioxide exchange of dry annual C_3 grassland and a proximate oak-grass savanna was also studied by Ma et al. (2007). This 5-year study focused on inter-annual variation in NEE, which was found to be significantly related to length of growing season for the savanna, grassland, and tree canopies: annual net carbon exchange (NEE) ranged from -0.42 to $-0.15 \text{ MgCha}^{-1}\text{y}^{-1}$ and from -0.24 to $0.38 \text{ MgCha}^{-1}\text{y}^{-1}$ at the savannah and nearby grassland, respectively. Gross primary productivity (GPP) and ecosystem respiration (Reco) depended primarily on the amount of seasonal precipitation. Inglima et al. (2009) reported that Reco is stimulated after first autumn rains following summer drought thus resulting in positive NEE in different Mediterranean ecosystems.

2.4.2 Abandoned grassland or agriculture land

In relation to land use, the spontaneous transition of grasslands to forests, which is especially widespread in regions where the agriculture is limited due to unfavourable geomorphological, pedological and climatic conditions, has been one of the most evident environmental changes in recent decades in Europe and beyond (McLauchlan et al., 2006; Mottet et al., 2006; MacDonald et al., 2000). At global level it has been estimated that this abandoned area amounts to $385 - 472 \cdot 10^6 \text{ ha}$ (Campbell et al., 2008). Hurtt et al. (2006), using HYDE (Historical Database of the Global Environment, by Goldewijk, 2001), estimated that $269 \cdot 10^6 \text{ ha}$ of crop lands were permanently converted to other land uses between the years 1700 and 2000. It has been estimated that about 13% of agricultural areas were abandoned in Europe in four decades since 1961 (Rounsevell et al., 2003; Rounsevell et al., 2006) with the Mediterranean (Pinto-Correia, 1993) and mountain regions (MacDonald et al., 2000) being subjected to the most intensive marginalization and abandonment. For Italy, Falcucci et al. (2007) report on forest share increase from 18.7% of national territory in 1960 to 32.5% in 2000; the share of agricultural (especially pasture) areas dipped simultaneously from 56.6% down to 38.5%. Similar pattern was also observed for SW part of Slovenia (Kaligaric et al., 2006).

When grasslands or agriculture land are abandoned, becoming overgrown by woody plants, their carbon balance drastically changes. With our investigation the change in carbon sink activity for grassland and abandoned land will be determined (H1). This issue has been addressed in several studies (Post and Kwon, 2000; Jackson et al., 2002; McKinley and Blair, 2008) but, despite of the rapid growth of regional and global networks for the measurement of biosphere and atmosphere gas exchanges (Valentini et al., 2000; Baldocchi, 2003; Papale et al., 2006), including the Mediterranean region (Unger et al., 2009; Reichstein et al., 2002b; Rambal et al., 2003, Xu and Baldocchi, 2004; Rambal et al., 2004; Ciais et al., 2005; Ma et al., 2007; Pereira et al., 2007; Serrano-Ortiz et al., 2007),

the consequences of regional land use changes for the carbon cycle remain poorly understood. Measurements above overgrown areas indicate that these areas have stronger carbon sink activity in comparison to abandoned areas. Vaccari et al. (2012) measured sink activity of $2.6 \text{ MgCha}^{-1} \text{ y}^{-1}$ on the island of Pianosa above overgrown farmland.

Shifting dominance among herbaceous and woody vegetation alters net primary production (NPP), plant allocation, rooting depth and soil processes which affects nutrient cycling and carbon storage. The invasion of woody vegetation into grasslands is generally thought to lead to an increase in amount of carbon in those ecosystems, changing two major carbon pools, woody plant biomass and soil organic matter (e.g. Alberti et al., 2008). While increase in aboveground biomass represents a dominant sink of carbon, soil carbon pools show an inconsistent response under woody plants encroachment. In fact, this response has been found to be extremely dynamic and dependent on vegetation, litter recalcitrance properties and on environmental conditions that influence decomposition. Jackson et al. (2002), studying carbon budgets of woody plants invading grasslands with different precipitation regimes, found a clear negative relationship between precipitation and changes in soil organic carbon and nitrogen, with drier sites gaining and wetter sites losing carbon. In some cases the rate of the loss overrode the sink strength gained by aboveground biomass increment. Water relations also proved to be of significant importance for carbon budget of invaded grasslands in other studies (Scott et al., 2006; Kurc and Small, 2007).

2.4.3 Karst ecosystem

A large portion of arid ecosystems in Mediterranean countries is characterized by carbonate rocks, the bedrock material in Karst systems. Carbonate rocks outcrop on ca. 12% of dry land on Earth (Ford and Williams, 1989) and may play a direct role in the global carbon cycle. Dissolution of limestone or dolomite, weathering, and carbonate precipitation are key reactions of geological cycling of CO_2 and are mostly governed by the physical-chemical conditions of soil environment.

Several studies suggest that cycling through the inorganic pool is an important contribution to the ecosystem CO_2 fluxes in Mediterranean ecosystems and should not be neglected when partitioning the fluxes (Emmerich, 2003; Kowalski et al., 2008; Inglima et al., 2009; Serrano-Ortiz et al., 2009; Serrano-Ortiz et al., 2010; Were et al., 2010).

Thus, the research of carbon cycling in karst grasslands that are exposed to invasion of woody plants is challenging in many respects. There are also, however, difficulties that are inherent to experimentation in these karst ecosystems. To start with, relief with depressions, sinkholes and subterranean cavities might affect, together with wind conditions, the quality of eddy flux measurements. This necessitates a careful selection of the measuring site, for which the history of use has to be well-known, especially when C cycling is studied in relation to natural forest succession. Secondly, the high degree of

heterogeneity of the ecosystems has to be taken into account. This heterogeneity is to a large extent related to spatial heterogeneity of soil, which can be for example extremely shallow but can also develop deeper organic patches. Stony soil with rocks limits the application of some conventional methods (e.g. root exclusion for partitioning of R_s) and makes other methods difficult to be applied.

3 MATERIALS AND METHODS

3.1 STUDY AREA

The study was conducted at the Podgorski Kras plateau (400-430 m.a.s.l.) in the sub-mediterranean region of Slovenia (SW Slovenia). Due to its position at the transition between the Mediterranean and central Europe, the karstic landscape of this area is subjected to major human influences. Overgrazing effects in the past centuries almost completely destroyed vegetation cover and caused severe soil erosion which resulted in stony, bare landscape. Later, the economic development lead to abandonment of agriculture which caused a slow but extensive spontaneous afforestation. During the Eighteenth century, some Austrian pine (*Pinus nigra* Arnold) plantations were also established. Historic human activities and natural conditions resulted in today's diverse landscape with co-occurring successional stages ranging from grasslands to the secondary oak forests.

Woody plant encroachment is characterized by shrubs of early successional stages (*Juniperus communis* L., *Prunus mahaleb* (L.) Mill., *Cornus sanguinea* L., *Cotinus coggygria* Scop.) and also tree species of mid- and late forest succession (*Quercus pubescens* Willd., *Ostrya carpinifolia* Scop., *Fraxinus ornus* L.). Species-rich calcareous grasslands of the *Scorzoneretalia* order still cover around 20% of the area, but more than 60% of former grasslands were transformed to the forest and shrub vegetation types (Kaligarić et al., 2006). The most abundant grassland species are *Bromopsis erecta* (Huds.) Fourr., *Carex humilis* Leyss., *Stipa eriocaulis* Borb., *Centaurea rupestris* L., *Potentilla tommasiniana* F.W. Schultz, *Anthyllis vulneraria* L., *Galium corrudifolium* Vill. and *Teucrium montanum* L. Vegetation surveys were made by dr. Klemen Eler, Biotechnical faculty Ljubljana.

The bedrock is composed of Paleocene and Eocene limestone. In the upper Pliocene epoch, karst phenomena (chemical weathering) caused the formation of Leptosols and Cambisols, which represent insoluble fractions of carbonate (Pleničar et al., 1973). Soil depth is very uneven ranging from 0 cm (rocky outcrops) to several decimetres in soil pockets between rocks. Rocks occupy on average 50% soil volume of the upper 40 cm of the soil profile. Soils have clay texture and are low in plant nutrients, especially phosphorus. Percent of soil organic matter of the topsoil is 12-15%. Soil reaction is slightly basic to slightly acidic. In small depressions and sinkholes (small dolines) eutric cambisols of much larger soil depth are developed.

The climate is transient between the mediterranean and continental. It is generally considerably more humid than true mediterranean climate, has less pronounced dry period in summer and colder winter. This type of climate is often designated as submediterranean. The mean annual temperature is 10.5°C, the mean daily temperature in January is 1.8°C and in July 19.9°C. Average annual precipitation reaches 1370 mm (data from 30 year average [1971-2000] of four meteorological stations in submediterranean region

[Environmental Agency of the Republic of Slovenia]). There are two precipitation peaks; primary one occurs in autumn and secondary in late spring. Winters are rather windy (Bora wind up to 35 ms^{-1} ; look at figure 9 for more details); snow cover is only periodic. The growing season ranges from April to October.

Within the study area two study sites were chosen on the basis of current and historic land use. The spatial distance of the sites is 1 km. The Grassland site has been used more or less permanently as a low intensity pasture (donkey, horse or sheep grazing at stocking rates below 0.25 livestock unit per hectare) in the last few decades and nowadays. Tree coverage on the Grassland site is below 5%, concentrated around sinkholes, which is a traditional way of wind erosion protection. On the Succession site small trees and shrubs cover 40% of the area. The average height of tree layer, which is mostly represented by *Quercus pubescens*, is 7 m and aboveground woody biomass is $96 \text{ m}^3 \text{ ha}^{-1}$. The coverage of woody species is uneven. With the continuing forest succession woody species spread from nests of shrubs, which are presumably located on the deeper soil, leaving larger or smaller gaps covered by herbaceous species. The composition of herbaceous layer is similar as for the Grassland site, with *Bromopsis erecta*, *Carex humilis* and *Stipa eriocalis* being the most abundant species. Vegetation surveys were made by dr. Klemen Eler, Biotechnical faculty Ljubljana. The slope of neither site exceeds 3 degrees. On the figure 4 is aero photograph taken in 2009 where the research area with locations of two research sites is marked with red rectangles. One site is on the extensive pasture (thereafter Grassland site) and another is on the abandoned area with forest succession (thereafter Succession site).

Since we are interested only in changes in type of aboveground biomass cover, we take into account only two land uses: forest (or forest patches) and other land use (mainly grasslands). For this purpose we chose aero-photographs from years 1957, 1975 and orto-photograph from year 2009 (Surveying and Mapping Authority of the Republic of Slovenia). Geo-referencing for years 1957 and 1975 was done in ESRI ArcMap with reference to the geo-referencing orto-photograph from year 2009. The area of interest was clipped within 1700 km x 850 km rectangle (figure 4) and forest and other land uses were separated. Polygons with area smaller than 9 m^2 were chosen and eliminate to the nearest land use. At the end calculation of area for each polygon were performed and summarized within land use. This analysis showed that forest has overgrown 21% of the analysed area (144.5 ha) in the last 52 years.

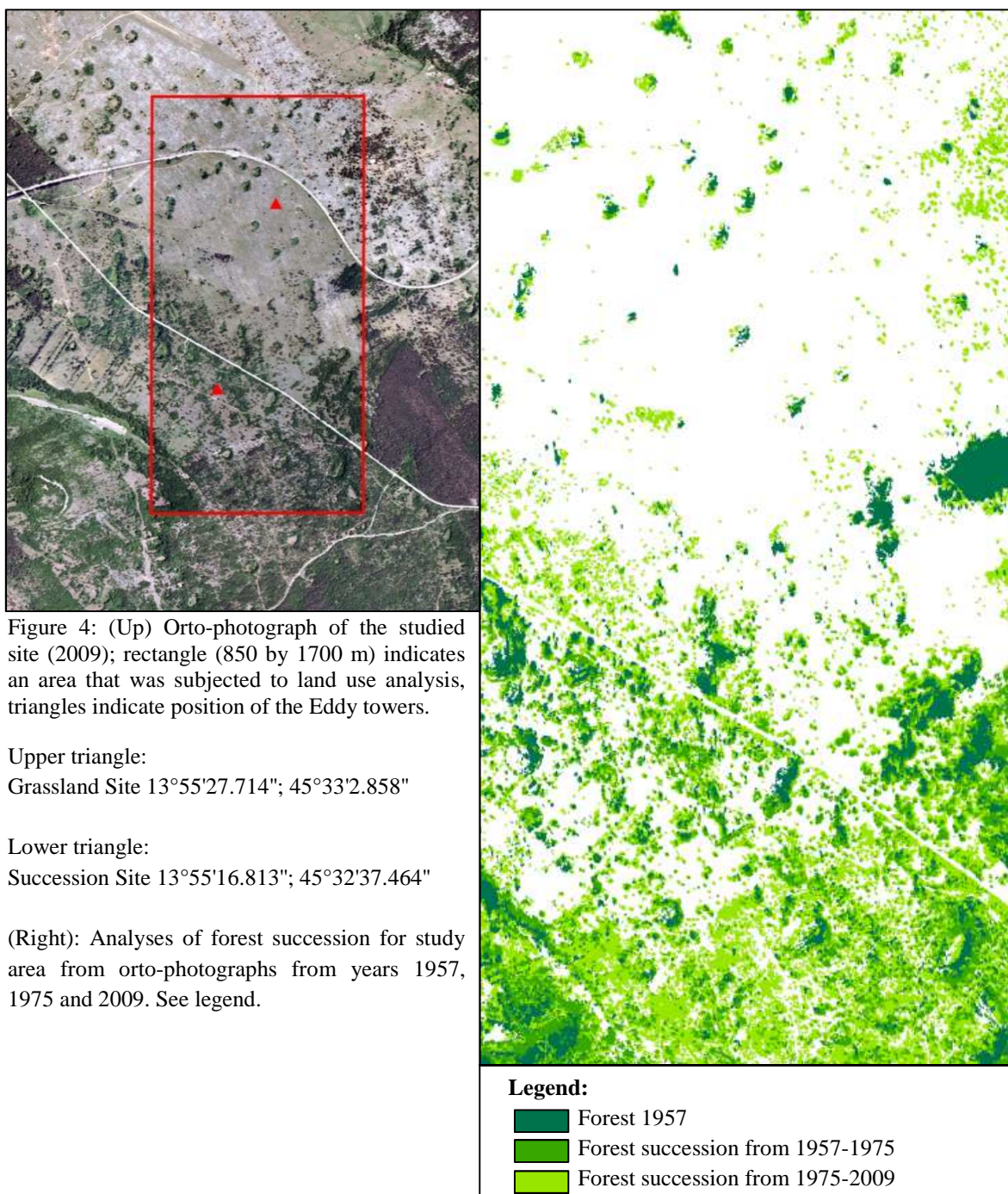


Table 2: Land use change in 52 years for the study area.

Year	Other land use	Forest land use
1957	94%	6%
1975	90%	10%
2009	73%	27%

Table 3: Detailed characteristics of the sites.

	Grassland site	Succession site
<i>Meteorology</i>		
Mean annual temperature (1971-2000 data)	10.5 °C	10.5°C
Mean annual precipitation (1971-2000 data)	1370 mm	1370 mm
<i>Soil</i>		
Soil type	rendzic leptosol + eutric cambisols	rendzic leptosol + eutric cambisols
Soil rockiness (40 cm depth)	53 ± 14%	46 ± 30%
Average SOC (40 cm depth)	9.1 ± 1.2%	7.0 ± 2.4%
Soil carbon stock (40 cm depth)	167 ± 46 t ha ⁻¹	172 ± 52 t ha ⁻¹
C _{org} :N ratio	11.0 ± 0.6	12.2 ± 1.1
pH	7.2 ± 0.6	6.9 ± 0.8
<i>Vegetation</i>		
Vegetation type (alliance/association)	<i>Scorzoneretalia villosae</i> (Carici humilis-Centaureetum rupestris)	Forest succession stage towards <i>Quercetalia pubescentis</i> (Ostryo-Quercetum pubescentis)
Tree cover	< 5%	40%
Aboveground tree biomass	< 5 m ³ ha ⁻¹	96 m ³ ha ⁻¹
Peak aboveground herbaceous biomass (2009 data)	2.45 ± 0.60 t ha ⁻¹	2.35 ± 0.80 t ha ⁻¹
<i>Scorzonera austriaca</i> peak flowering (2009 data)	26 th April	29 th April
<i>Centaurea rupestris</i> peak flowering (2009 data)	17 th June	22 nd June
<i>Euphorbia nicaeensis</i> peak flowering (2009 data)	1 st July	13 th July
Mean / max vegetation height	0.4 / 0.6 m	3.4 / 7.0 m

3.2 EDDY COVARIANCE MEASUREMENTS

Eddy covariance systems were installed on both research sites (locations are marked with triangles on figure 4) in July 2008.

When choosing the location of the eddy tower on the grassland site, special attention was paid to avoiding the sinkholes in the vicinity, since these might substantially affect horizontal and vertical wind direction. The eddy tower was located at least 140 m away from the deeper sinkholes with a depth of 2 m. On the succession site, the sinkholes are densely covered or surrounded by woody species and presumably have no major influence on wind direction and speed. At both sites, an open-path eddy covariance system consisting of an open path infrared gas (CO_2 and H_2O) analyzer (LI-7500, Li-Cor, Lincoln, NE USA) and sonic anemometer (Succession site: CSAT3, Campbell Scientific, Logan, UT USA. Grassland: USA-1, Metek GmbH, Elmshorn, Germany) was installed at 15 m height for the succession site and 2 m height for the grassland site. The LI-7500 was pointed towards the north at an angle of 20° to minimise solar radiation influence and to facilitate the shedding of water droplets from sensor lenses after rain events. Data from the sonic anemometer and the open path infrared gas analyzer (IRGA) were recorded at a frequency of 20 Hz using a CR3000 (Campbell Scientific) and at 10Hz using a Compact Eddy (Matese et al., 2008) for the Succession site and Grassland site, respectively.

The data for EC were downloaded bi-weekly to a notebook. The processing of NEE values was made in several steps. The first step was to prepare the data, where the binary data were transformed into a file containing one-hourly data sets. Since the EC is a well-recognized method, programs to process one-hour processing files are available. One of the freely available programs is EdiRe Data Software (University of Edinburgh, 1999). EdiRe program was set up with basic information about the measured ecosystem before starting. In the program it was also necessary to include all the corrections that must be applied to data. After successful processing, half-hourly eddy covariance data were merged with meteorological data. As it is well known, open path IRGA provide inadequate and erroneous data during rainy or foggy conditions, or when condensation occurs on the optical lens of the instrument, especially in autumn. Typically, the malfunctioning of IRGA in such conditions causes the occurrence of spikes, and in this case a spike analysis algorithm (called hard flags) was applied to accept or discard data. Quality assessment (stationarity test) was conducted according to Foken and Wichura, (1996) and friction velocity (u^*) filtering was performed (called soft flags) according to calculated u^* threshold. If the results of stationarity test for CO_2 and H_2O flux exceeded the ratio of 60% (similar to Haslwanter et al., 2009), the stationarity test set the soft flag. The u^* threshold was derived for each site using 95% threshold criteria similar to Reichstein et al. (2002a): the data sets were split into six temperature classes and for each temperature class, the set is split into 20 u^* classes. The threshold is defined as the u^* class where the night-time flux reaches more than 95% of the average flux at the higher u^* classes. The final threshold is defined as the median of the thresholds of at least six temperature classes. Thresholds were

0.21m s^{-1} and 0.1m s^{-1} respectively for succession site and grassland site, and the soft flag was set if the u^* was below calculated u^* threshold. The task of the second step in process was to fill the missing values (gap-filling). A gap-filling procedure was applied to obtain half-hourly fluxes (Reichstein et al., 2005) when the hard or soft flag was set. The third step in the processing was the execution of uncertainty analyses (Papale et al., 2006; Richardson and Hollinger, 2007). The fourth step was partitioning of NEE between gross primary productivity (GPP) and total ecosystem respiration (Reco) and was performed according to Lasslop et al. (2010) using daytime data-based estimates including temperature sensitivity of respiration and vapour pressure deficit (VPD) limitation of GPP.

3.2.1 Instrument self-heating correction

From the equations in chapter 2.2.3 it is evident that beside other parameters high-frequency measurements of temperature are necessary in order to support the calculations of sensible heat flux, evapotranspiration and CO_2 flux. Beside high frequency values, average temperature is also needed for calculations. These temperature values should be obtained by measuring air temperature in the measuring cell of open path IRGA. In most experimental designs, however, this temperature is assumed to be the same as the temperature measured with sonic anemometer or fine-wire thermocouple near instruments. Some recent studies, however, have found that this is not true (e.g.: Grelle and Burba, 2007; Burba et al., 2012).

Self-heating correction was applied to our data sets according to method 4 in Burba et al. (2008) (B4). In addition, we investigated more about site-specific instrument self-heating correction (SISC).

Following Burba et al. (2008), we measured the air temperature and the temperature of IRGA body in December 2009. Only night-time measurements were taken into account in order to avoid any influence of solar radiation on temperature probes (air temperature range: -10 to 15°C). A strong linear relationship between the air temperature (T_a) and the temperature at the bottom of the IRGA (T_s) was found for both ecosystems. Difference between T_s and T_a was within the probe precision ($\pm 0.5^\circ\text{C}$) and could not be considered significant. Furthermore, Burba et al. (2008) reported much higher difference between T_s and T_a during nights (slope = 0.88, intercept = 2.17°C). Those preliminary results showed that OP IRGA self-heating can be assumed negligible for our ecosystem. The temperature sensors that were used in this preliminary experiment had a very slow response time and were imprecise and therefore we decided to perform a more detailed study on this topic.

A more detailed research into OP IRGA self-heating was performed only at the succession site and was run between 22nd of January 2011 and 3rd of April 2012. For detailed monitoring of self-heating the mock OP IRGA, i.e. non-powered analyzer with similar albedo, and OP IRGA were equipped with 3 digital temperature sensors DS18B20. OP IRGA was mounted at the angle of 15° and temperature sensors were taped with

aluminium tape at three locations: (bottom) 4 mm from the lower window, (spar) on the spar 70 mm from the lower end and (top) on the detector housing 4 mm from the upper window. The execution of temperature measurements was done as suggested for method 4 in Burba et al. (2008). The mock OP IRGA was mounted at the same angle and sensors were taped in the same way as on OP IRGA. For better thermal conductivity between the material and the temperature sensors thermal paste was used. All sensors were connected to a home-made data logger unit, which was programmed to read digital signals using 1-wire protocol every 30 minutes. All other meteorological parameters (wind speed and air temperature) were recorded by a weather station installed in the flux measurement tower.

B4 suggests the linear models to generate temperature of bottom, top and spar of OP IRGA body based on the air temperature, but they are different for night- and daytime data. Surface sensible heat fluxes are then calculated using heat conduction/convection equations (Nobel, 2009), taking into account the model OP IRGA body temperatures and air temperatures and wind speed. Heat conduction/convection for one-dimensional case could be expressed as:

$$S_{surface} = K_{air} \frac{(T_{surface} - T_a)}{\delta^{bl}} \quad \dots(10)$$

Where $S_{surface}$ is the rate of heat conduction per unit area (Wm^{-2}), K_{air} is the thermal conductivity of air ($0.0259 Wm^{-1}C^{-1}$ for temperatures from $20-25^{\circ}C$), T_a is the temperature of air outside an air boundary layer of thickness δ^{bl} and $T_{surface}$ is the surface temperature. Equations for cylindrical and spherical objects are formulated different as follows.

Since different linear models were found in our detailed investigation between T_a and OP-IRGA body temperatures, we used our measured and modelled temperatures to calculate surface sensible heat fluxes according to equation suggested by Burba et al. (2008) .

$$S_{bot} = K_{air} \frac{(T_{bot} - T_a)}{\delta^{bot}} \quad \dots(11)$$

$$S_{top} = K_{air} \frac{(r_{top} + \delta^{top}) \cdot (T_{top} - T_a)}{r_{top} \cdot \delta^{top}} \quad \dots(12)$$

$$S_{spar} = K_{air} \frac{(T_{spar} - T_a)}{r_{spar} \cdot \ln\left(\frac{r_{spar} + \delta^{spar}}{r_{spar}}\right)} \quad \dots(13)$$

$$\delta^{bot} = 0.004 \sqrt{\frac{d_{bot}}{w_s}} + 0.004 \quad \dots(14)$$

$$\delta^{top} = 0.0028 \sqrt{\frac{d_{top}}{w_s}} + \frac{0.00025}{w_s} + 0.0045 \quad \dots(15)$$

$$\delta^{spar} = 0.0058 \sqrt{\frac{d_{spar}}{W_s}} \quad \dots(16)$$

$$S = C_p \cdot \overline{\rho_a} \cdot \overline{w'T'} + S_{bot} + S_{top} + 0.15 \cdot S_{spar} \quad \dots(17)$$

Where T_a is the ambient air temperature ($^{\circ}\text{C}$); S_{bot} , S_{top} , and S_{spar} represent sensible heat fluxes from key instrument surfaces of bottom window, top window, and spar, respectively (Wm^{-2}); T_{bot} is the surface temperature near the bottom window ($^{\circ}\text{C}$); T_{top} is the surface temperature near the top window ($^{\circ}\text{C}$); T_{spar} is the surface temperature of the spars ($^{\circ}\text{C}$); r_{top} is the radius of the sphere (0.0225 m); r_{spar} is the radius of the cylinder (0.0025 m); d_{bot} is the diameter of the source housing treated as a plane (0.065 m), (0.004 m is added to compensate for the angle of the shoulders in relation to the horizontal bottom window); d_{top} is the diameter of the detector housing treated as a sphere (0.045 m), (0.0045 m is added to compensate for the nonspherical surface of the top window); d_{spar} is the diameter of the spars treated as cylinders (0.005 m); W_s is horizontal wind speed (ms^{-1}).

Final corrected flux with SISC correction, after sensible heat fluxes had been calculated, was then calculated using equations (17) and (7).

3.2.2 Gap-filling and flux-partitioning

Various methods are available for gap-filling meteorological and eddy covariance data. Most of researchers used their own procedures to gap-fill datasets, but there are some procedures that are used more often. One of such is a procedure by Falge et al. (2001), which was upgraded with covariation of fluxes with meteorological variables and with the temporal auto-correlation of the fluxes by Reichstein et al. (2005). The procedure is based on the comparison of similar meteorological conditions. For the fluxes, the most important meteorological data are global radiation (R_g), air temperature (T_a) and vapour pressure deficit (VPD). Similar conditions for these three variables are present when they do not deviate by more than 50 W m^{-2} , 2.5°C and 5 hPa for R_g , T_a and VPD, respectively. The algorithm of gap-filling procedure identifies three different conditions/methods: (1) Only flux data are missing, but R_g , T_a and VPD data are available; (2) T_a or VPD is missing, but R_g is available; (3) Also R_g data is missing. The gap-filling procedure also assigns quality marks for filled-in data which are based on the temporal window size for comparison of similar meteorological conditions. In case of method (1) and temporal window being smaller than 14 days or in case of method (2) and temporal window being smaller than 7 days the quality mark is A. The quality mark A is also reached if the flux is available within 1 hour before or after the missing value. Quality mark B is reached in case of method (1) and temporal window being greater than 14 days and smaller than 28 days. In case of method (2) and temporal window being smaller than 7 days the quality mark is B and with temporal window being greater than 7 days the quality mark is C. The quality mark for filled-in data is C where only flux is available at different temporal window sizes greater than 7 days. However, flux measurement datasets have numerous data gaps due to weather conditions. For good quality filling-in of this missing data very good meteorological data are needed and therefore their measurements deserve a lot of attention.

There are several techniques available to divide NEE of CO_2 between the ecosystem and atmosphere to GPP and Reco. Nighttime data-based estimate is calculated according to Reichstein et al. (2005) and assumes GPP to be zero during night-time periods. Measured NEE during night (Reco) is then used to fit the model after Lloyd and Taylor (1994), to find the relation between Reco and T_a .

$$\text{Reco} = a \cdot e^{\left(\frac{b}{T_{\text{ref}} - T_0} - \frac{b}{T_a - T_0}\right)} \quad \dots(18)$$

T_{ref} is set to 15°C and T_0 to -46.02 . The difference between the modelled Reco and the measured NEE represents the estimated GPP. More complex models use light-response curve for daytime data including temperature sensitivity of respiration like suggested by Lasslop et al. (2010) and use of VPD limitation of GPP is strongly recommended.

$$\text{NEE} = \frac{\alpha \cdot \beta \cdot e^{-k(\text{VPD} - \text{VPD}_0)} \cdot R_g}{\alpha \cdot R_g + \beta \cdot e^{-k(\text{VPD} - \text{VPD}_0)}} + a \cdot e^{\left(\frac{b}{T_{\text{ref}} - T_0} - \frac{b}{T_s - T_0}\right)} \quad \dots(19)$$

Where α and β are parameters of light response curve, R_g is global radiation, VPD is vapour pressure deficit and VPD_0 is vapour pressure deficit threshold, in our case set to 14 hPa. Parameter k is estimated only for cases where VPD is larger than VPD_0 ; in other cases is set to 0. Respiration component in equation (19) must be added to model respiration according to equation (18) during daytime, since during night-time NEE represents Reco. This procedure was also applied to our datasets to divide NEE to Reco and GPP. The threshold for the definition of night-time data was set to R_g lower than 4 Wm^{-2} .

3.2.3 Uncertainty analysis

To estimate the uncertainty of carbon balance for each site two different sources of random errors were investigated. First, we followed the Richardson and Hollinger, (2007) methodology to calculate the uncertainty introduced in NEE by the random errors in measurements (σ_{MEAS}). Pairs of half-hourly fluxes in similar climatic conditions on two successive days (criteria after Richardson et al., 2006), were used to determine random errors (δ) which were defined as differences between corresponding half hourly NEEs of a pair of successive days. To consider higher errors at higher NEE values the relation between $\sigma(\delta)$ and NEE was established as described in Beziat et al. (2009). Random noise was then added 100 times to the filtered half hourly NEE values following a Laplace distribution with 0 mean and $\sigma(\delta)$ standard deviation dependent on half hourly NEE value. For each repetition dataset was gap-filled according to Reichstein et al. (2005) and half-hourly cumulative NEE was calculated. Daily, monthly or annual sums, different due to random noise, were used to obtain (σ_{MEAS}). Second, uncertainty and errors introduced by the gap-filling procedure (σ_{GAP}) were calculated following Beziat et al. (2009). Gaps (same number, same size and with similar distribution between night and day) were randomly created in continuous annual dataset. Then gap-fill procedure according to Reichstein et al. (2005) was performed. Gap generation and gap-fill were repeated 100 times. Daily, monthly or annual sums, different due to errors introduced by the gap-filling, were used to obtain (σ_{GAP}). Finally, daily, monthly or annual cumulative NEE uncertainty (σ_{NEE}) was estimated by taking the square root of the sum of variances σ_{MEAS}^2 and σ_{GAP}^2 .

3.3 CHAMBER MEASUREMENTS

Since CO₂ fluxes from soils (heterotrophic and autotrophic) could present around 50% of Reco, it is important to monitor Rs together with NEE. In this study, manual and automatic closed dynamic chamber techniques were used. Furthermore, a comparison between automatic closed dynamic chamber system and automatic open dynamic chamber system was performed. Manual Rs measurements were conducted periodically through 14 days with a portable meter LI-6400 and the closed dynamic chamber LI-6400-09 (Li-Cor Inc., Lincoln, NE) between July 2008 and November 2010. This Rs data was used only to support flux-partitioning and discussion. Measurements were carried out with cooperation of staff from the Department of Agronomy, Biotechnical Faculty in the frame of project J4-1009 funded by Slovenian Research Agency and Slovenian Ministry of Agriculture, Forestry and Food. At the grassland site, three plots with approximately 15 m² of area and about 10 m apart from each other were set up. Seven permanent locations for Rs measurements were randomly selected on each and circular collars (diameter 11.4 cm, height 4.4 cm) were placed on them, so that they were halfway inserted into the soil. At the succession site, six plots of 15 m² were selected and distances between these plots were 20 m or less. Seven collars were installed on each plot as described for grassland site. Due to very stony soil, some problems occurred during collar insertion and later on during the measurements. Soil temperature at 10 cm depth (Ts) was measured adjacent to the soil collars at the same time as flux measurements. On the measuring plots soil temperature and soil moisture were continuously measured using the system for measuring Ts and SWC soil profiles described in chapter 3.4.1.

After measurements data were downloaded from the portable meter LI-6400 and reprocessed in R 2.13.2 statistical environment (R Development Core Team, 2011) using packages for linear and nonlinear regressions. To find the relationship between Rs and driving parameters for it model after Lloyd and Taylor, (1994) was used:

$$R_{soil} = a \cdot e^{\left(\frac{b}{T_{ref}-T_0} - \frac{b}{T_s-T_0}\right)} \quad \dots(20)$$

where Ts is measured soil temperature at 10 cm depth (in °C), a and b are fitting parameters. Tref is reference temperature and is set to 10°C and therefore parameter a also indicates the Rs at 10° C. To is kept constant at -46.02°C. Another possibility to model Rs data is the model with adding SWC parameter (like in Bahn et al., 2008),

$$R_{soil} = a \cdot e^{\left(\frac{b}{T_{ref}-T_0} - \frac{b}{T_s-T_0}\right)} \cdot e^{-e^{(c-d \cdot SWC)}} \quad \dots(21)$$

where SWC is the measured volumetric soil water content (in %) and c and d are the additional fitting parameters.

3.3.1 Automatic soil respiration system

Portable soil respiration systems such as LI-6400-09 do not allow a deeper insight into the temporal variability of R_s . For this, automated systems for measuring soil respiration are needed. Drawback of existing systems is their very high price of approximately EUR 80,000. Another drawback could be the impact of mechanical parts of the automatic chamber into the measuring point. Collars that are inserted around the location and assist in the stability of the chamber can affect the measurement point and could have the effect on increasing temperature and/or soil moisture. In the Laboratory for Electronic Devices, which was established in 2009 at the Slovenian Forestry Institute, an automatic chamber with an improved mechanism for opening and closing was developed. The automatic soil respiration system includes automatic chamber(s) with electronics, central data storage electronic devices and infrared gas analyzer LI-840.

The first step in the development of automatic soil respiration system was to construct the automatic chamber with electronics. As for all micrometeorological measurements also this instrument should not be too bulky. All known automatic chambers have a big body with collar and the body has installed an electronic system with a closing and opening mechanism. Such construction of the chamber could have an impact on the measuring point. Our aim was to try to move the part with electronic system and the opening and closing mechanism as far as possible from the measuring point to minimise the impact on it. To be cost-effective most of parts were bought as a standard material in stainless stores. Some of them, like the housing for electronics and the stand, were constructed on CNC machines. In Figure 5 the schematic and the final view of our chamber are presented. Total height of the newly designed chamber is 100 cm and the lower part of the moving chamber is around 70 cm above the measuring point.

For moving of the chamber down and up, a servo motor (GS-5515MG 15 kgcm⁻¹) is used. The motor was rebuilt to be able to move either in clockwise or counterclockwise direction continuously. Sensing of the position of chamber is controlled by two magnetic switches which are installed along the path of moving chamber. In addition, a test of the moving part of chamber was done. The electronic system in the chamber was programmed to move the chamber down and up continuously once per minute to test the servo motor performance. The test was run on 25th of February 2011 and motor was found broken on 19th of April 2011. According to this, it could be concluded that the motor was reliably working for 51 days. That means that motor has made 73440 movements of chamber down and up. From the practical point of view the measurements of R_s once per hour could be performed continuously for more than 8 years.

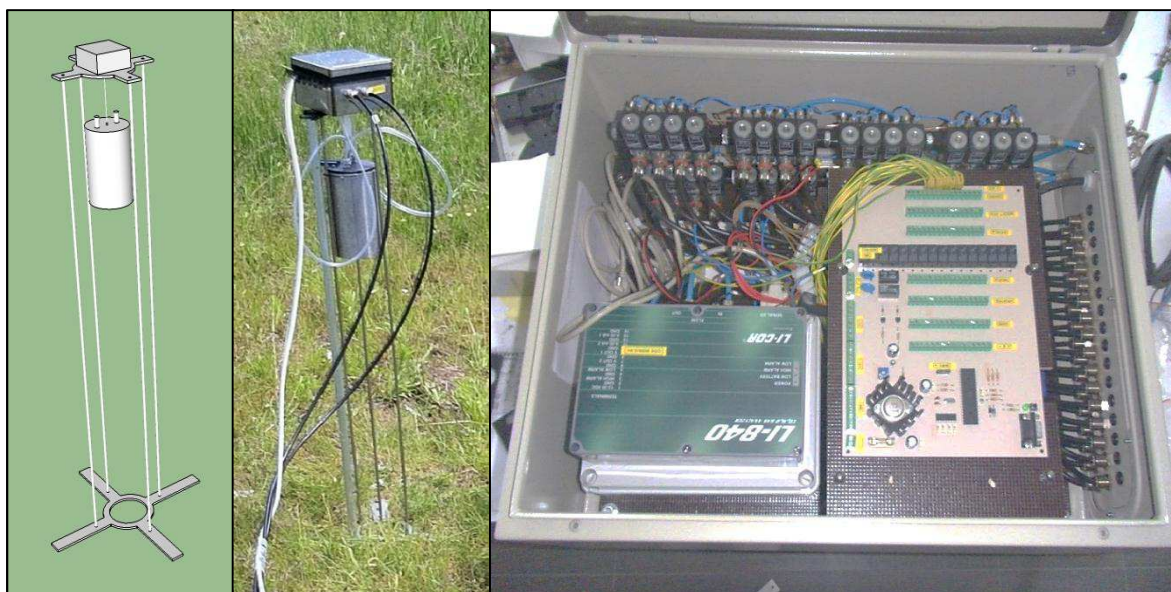


Figure 5: Automatic soil respiration system. Left: Schematic view of automatic chamber design. Middle: Automatic chamber installed on the field. Right: Central data storage electronic with multiplexer containing 2x16 electromagnetic valves.

For the electronic system in the chamber a microcontroller ATmega8 (Atmel Corporation, San Jose, CA) was used. It is a low-power CMOS 8-bit microcontroller based on the AVR enhanced RISC architecture. Peripheral devices and components are connected to the microcontroller.

Each chamber can operate independently of other chambers and does not require a central data storage electronic device. The electronic system in the chamber can be broken down into four constituent parts: the start and stop control part, the measuring part, the chamber control part and the data transmission part. The start and stop control part of the chamber electronic system is responsible for starting the measurement and for waking up the electronic system from power-down mode. For start-up of the system, an interrupt pin of microcontroller with pull up resistor was used. The trigger for starting the measurement is a signal going from 5V towards 0V. The signal can be sent by pushing the button or it could be generated in central data storage device or in the electronic system of the chamber. The measuring cycle lasts 3 minutes and after ending, the electronic system of the chamber sends a signal going from 5V towards 0V to trigger the next chamber if they are connected in series. After the measuring cycle, the chamber enters into power-down mode to lower the power consumption to 5 microamperes.

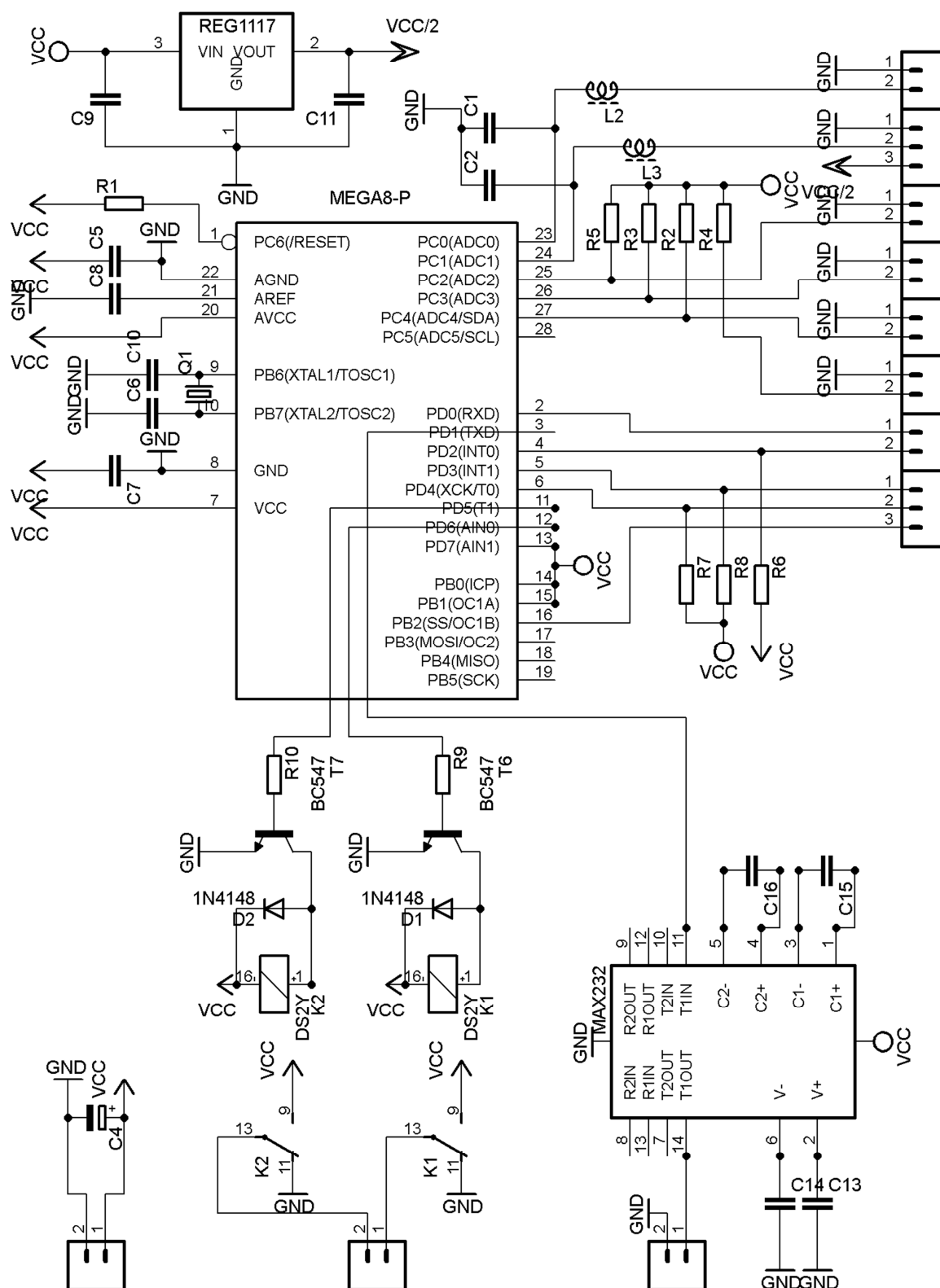


Figure 6: Electrical schematic of chamber electronic circuit board.

When the chamber electronic system wakes up, the measuring part of the circuit performs the measurements. The microcontroller of the chamber electronic system has a built-in 10-bit analog to digital converter (ADC converter). Therefore only a 100 mH inductor and a 100 nF capacitor must be applied to perform an accurate voltage reading. Due to this feature, there is no need to construct a peripheral analog to digital converter and fewer components are needed. The chamber electronic has two single ended channels for measuring voltages between 0 and 2500 mV. One channel is reserved for voltage reading from IRGA and another for any other sensor with output signal from 0 to 2500 mV can be used. Therefore only an accuracy test of voltage readings with chamber electronic was performed. For this purpose we used a laboratory voltage generator (Digimaster, DF1730SB5A) generating voltage in range from 0 to 2500mV. Voltage was measured with chamber electronic and simultaneously with a laboratory Digital Multimeter (M-3890D-USB, Metex Instruments, Seoul, Korea) connected to a PC for logging. Values were logged every second. Linear regression between data from our system and Digital Multimeter was done ($n = 1548$, $R^2 = 0.998$, slope = 1.002, intercept = -0.188). From these results we can see that our system underestimates voltage by approximately 0.2 mV; for equipment that can measure voltage from 0 to 2500 mV this is negligible. From simultaneous measurements accuracy of chamber electronic measurements was calculated and it was $\pm 0.22\%$ for testing range. For measuring temperature usually differential or single-ended voltage measurements and different types of sensors are used. Most frequently used are thermocouples or thermo-sensitive resistors with negative or positive temperature coefficients. There are also several types of integrated circuits which can measure temperature and convert data to a digital signal. For chamber electronic factory calibrated temperature sensors DS18B20 (Maxim Integrated Products, Sunnyvale, CA) with $\pm 0.5^\circ\text{C}$ accuracy in the range between -10°C and $+85^\circ\text{C}$ were used. The sensors use 1-wire communication protocol (1-Wire is a registered trademark of Maxim Integrated Products, Inc). Despite manufacturer guarantee that sensors are calibrated, we performed a test with seven temperature sensors and classical meteorological thermometer (mercury thermometer). As a testing media, water with ice was used and appropriate hand mixing was performed. Temperature ranged from 4 to 17°C and values were logged or manually read every 30 minutes. For each temperature sensor, linear regression with mercury thermometer measurements ($n = 12$) was made. From all parameters of linear regression ($N = 7$), we calculated means and standard deviations ($R^2 = 0.997 \pm 0.001$, slope = 0.975 ± 0.023 , intercept = 0.124 ± 0.377). With these temperature sensors, the temperature is slightly underestimated compared with the mercury thermometer. From simultaneously measurements accuracy of chamber electronic measurements was calculated and it is $\pm 1.1\%$ for testing range. Each chamber has option to connect four temperature sensors and one frequency domain sensor EC-5 (Decagon Devices Inc., Pullman, WA) for measuring soil water content was used. For correct supply voltage of 2.5 V for the sensors, regulator LD1117 (SGS-THOMSON Microelectronics) was used. Sensor output ranges from 250 to 1000 mV at a 2.5 V supply voltage and supposed to be proportional to volumetric soil

water content. IRGA is set up to output each second and ranged from 0 mV to 2500 mV. Single ended channel reserved for IRGA measuring voltage every second.

After the measurements on single-ended channel and channels for temperature, the chamber control part of chamber electronic system starts to control the chamber measurement. The first step is to trigger the multiplexer to switch the right valve if the chambers are connected in series. After this, it takes 30s to vent all the tubes between the IRGA and the chamber. The next step is to move the chamber down to the measuring point, wait for 160 s to finalize the measurement of CO₂ concentration, and move the chamber back up to open position. For moving the chamber up and down two magnetic switches and a motor, connected to two relays for clockwise and counterclockwise movement are used.

The data from chamber electronic system to the central data storage or other media is transmitted via a serial interface (baud rate: 9600, Data bits: 8, Parity: none, Stop bits: 1, Handshaking: none). For this communication an integrated circuit MAX232 with capacitors is used. To establish serial communication with computer it would also be possible to use a serial to USB converter. Hyper Terminal (Windows) or any other free software for reading data from serial ports can be used. Every second chamber electronic system sends a line with comma separated data that includes chamber id, year, month, day, hour, minute, second, CO₂ concentration and five channels of temperature and voltage readings.

For the central data storage device a microcontroller ATmega32 (Atmel Corporation, San Jose, CA) was used. It is a low-power CMOS 8-bit microcontroller based on the AVR enhanced RISC architecture. An interface for SD cards to store data and a multiplexer to switch data transmission relays and valves between chambers is connected to the microcontroller. The whole system was named Ukulele.

The software for microcontrollers (chamber electronic and central data storage) was written in a BASIC-like language (BASCOM-AVR, MCS Electronics, Holland) for Microsoft Windows XP. The program was compiled in microcontroller assembly language and uploaded to the microcontroller using a programmer (PROGGY AVR, AX Elektronika, Slovenia) via AVR Studio 4 software (Atmel Corporation, San Jose, CA).

The electrical schematic of the circuit board was drawn and the circuit board was made at the Laboratory for Electronic Devices at the Slovenian Forestry Institute. The schematic was transferred to the circuit board, which was drilled out on a small CNC machine in the same laboratory.

The developed automatic soil respiration system has closed dynamic chambers. CO₂ concentration in this type of chambers increases during the measurements and the change of CO₂ concentration during time is represented by the slope of the least squares regression

line relating CO₂ concentration and time ($y = ax + b$), where a represents flux gradient $d[CO_2]$. Final Rs flux ($\mu\text{molCO}_2\text{m}^{-2}\text{s}^{-1}$) calculation is done using equation:

$$R_{soil} = \frac{V}{A} \cdot \frac{d[CO_2]}{dt} \cdot \frac{P_0}{R \cdot (T_0 + 273.14)} \quad \dots(22)$$

where V and A represents volume and area of a chamber in m^3 , respectively. P_0 and T_0 are air pressure and temperature at time zero. R is the universal gas constant ($8.314 \text{ Jmol}^{-1}\text{K}^{-1}$).

The system was tested at the grassland site and in the garden of the Slovenian Forestry Institute. The first test was performed in August 2012 at the grassland site together with a preliminary irrigation experiment with Hungarian colleges. On the area of 25 m^2 15 plots were chosen. On each plot one Ukulele soil chamber was installed and 5 plots were equipped with open dynamic (steady-state through-flow) chambers, called Kukulo (Nagy et al., 2011) to compare with our system.

In December 2012 another system was built and set up at the garden of the Slovenian Forestry Institute. Rs was measured at the garden with LI-6400 and corresponding chamber LI-6400-09 in line with the new system on 3rd and 17th of December 2012 and at Grassland site on 18th of December 2012.

The measuring period of Rs from 1st of September 2012 till 30th of November 2012 was used to model Rs as described previously in equations (20) and (21). Monthly sums for the whole period (July 1st 2008 – November 30th 2012) were calculated using the Rs model (T_a and SWC) from Ukulele and the Rs model (T_s and SWC) derived from manual Rs measurements using LI-6400.

Night-time Rs and NEE measurements were also compared to see if ecosystem respiration during night is higher when comparing Rs.

3.4 AUXILARY MEASUREMENTS

Direct measurements of NEE between the ecosystem and the atmosphere according to EC or direct measurements of R_s according to chamber method are possible only in certain environmental conditions and therefore several other measurements are needed. Furthermore, instrumentation for mentioned methods needs a reliable power supply on the field. In the case of inappropriate environmental conditions or malfunction of power supply there will be no data. In these cases, the database can be gap-filled. The procedure for gap-filling eddy covariance and R_s data was already mentioned in chapter 3.2.2 and chapter 3.3, respectively.

For a good quality gap-fill we need reliable environmental parameters which are in relation with the desired gap-filling parameter. For gap-filling eddy covariance data, important environmental parameters are vapour pressure deficit at atmospheric level (VPD), air temperature (T_a) and global radiation (R_g). VPD in this study is always calculated at atmospheric level (equation (23)), although it would sometimes be more appropriate to calculate it at leaf level.

$$VPD = 610.78 \cdot e^{\frac{T_a \cdot 17.2694}{(T_a + 238.3)}} \cdot \left(1 - \frac{Rh}{100}\right) \quad \dots(23)$$

Furthermore, fluxes and other environmental parameters were summarized or averaged based on year, month and vegetation season. Rewetting index was calculated every half hour and the data was then averaged, calculation was performed similar to (Yuste et al., 2003):

$$RI = \alpha + \log \left(\frac{\sqrt{P}}{VPD \cdot t^2} \right) \quad \dots(24)$$

where α is a constant (2.5), P represents amount of precipitation during the last rainfall event (mm), t is time (0.5h) and VPD is mean vapour pressure deficit of the atmosphere.

For reliable gap-fill of eddy-covariance data and for other describing environmental parameters a weather station was installed at each site to measure the following environmental parameters: soil temperature at three depths (2, 10 and 30 cm) using thermocouples (TCAV, Campbell Scientific, Logan, UT USA), soil water content (0-20 cm) using three time domain reflectometers (CS616, Campbell Scientific, Logan, UT USA) inserted vertically, incident radiation (LP02, Campbell Scientific, Logan, UT USA), incident (PPFDi) and reflected (PPFDr) photosynthetic flux density (LI-190, Li-Cor, Lincoln, NE USA), net radiation (NR-LITE, Campbell Scientific, Logan, UT USA), air temperature and humidity (HMP45AC, Vaisala, Helsinki, Finland), soil heat flux (10 cm) using three soil heat flux plates (HFP01SC, Campbell Scientific, Logan, UT USA) and precipitation (Rain gauge, Davis, Hayward, CA USA). All variables were measured at 0.1 Hz and then averaged half-hourly. Meteorological data were passed to a collection centre via wireless connections.

Additionally, for modelling and gap-filling of Rs data, six soil profiles on succession site and three soil profiles on grassland site were prepared. The system for measuring Ts and SWC soil profiles was developed at the Laboratory for electronic devices at the Slovenian Forestry Institute and is described in chapter 3.4.1.

3.4.1 System for measuring Ts and SWC soil profiles

In the study area several Rs measurements using chamber method were done. In natural environments, high spatial variability, especially in soils, is not rare and therefore several repetitions of Rs measurement are needed. The main drivers of Rs are soil temperature (Ts) and soil water content (SWC) (Lloyd and Taylor, 1994). Continuous measurements of these two parameters can be relatively easily performed. In the case of using portable systems for measuring soil respiration, we are limited to sensing temporal variability but in the case of using automated systems we are limited to sensing spatial variability. Both limitations can be minimized with additional measurements of Ts and SWC using appropriate model to gap-fill the data (Lloyd and Taylor, 1994). Spatial and temporal variability of these two parameters could be observed with an appropriate number of Ts and SWC profiles. Several profiles mean that many connections with cables must be made, or alternatively, expensive installation of wireless sensors could be used. Due to these needs in the framework of this study a robust and cost-effective system for measuring and data logging Ts and SWC have been developed, constructed and tested. The system is microcontroller-based with sensors and peripheral components connected to it. All selected electronic components have low power consumption and allow battery-powered operation.

Two frequency domain sensors EC-5 (Decagon Devices Inc., Pullman, WA) for measuring soil water content were used. For correct supply voltage of 2.5V for the sensors, regulator LD1117 (SGS-THOMSON Microelectronics) was used. Sensor output ranges from 250 to 1000 mV at a 2.5 V supply voltage and supposed to be proportional to volumetric soil water content.

The central unit has a built-in 10-bit analog to digital converter (ADC converter). Therefore only a 100 mH inductor and a 100 nF capacitor must be applied to perform an accurate voltage reading. Due to this feature, there is no need to construct a peripheral analog to digital converter and fewer components are needed; consequently the price is lower. The system described in this paper has two single ended channels for measuring voltages between 0 and 2500 mV. Since any other sensors with output signal from 0 to 2500 mV can be used with the presented system, only an accuracy test of voltage readings with our system was performed like was already described in chapter 3.3.1.

For measuring temperature, most data loggers use differential or single-ended voltage measurements and different types of sensors. Most frequently used are thermocouples or thermo-sensitive resistors with negative or positive temperature coefficients. There are also several types of integrated circuits which can measure temperature and convert data to a

digital signal. When several sensors must be used and are connected to the same measurement and data-logging system, usually at least two cables per sensor must be used and several voltage or digital input channels are needed. The system described in this work uses factory calibrated temperature sensors DS18B20. The most important feature of this sensor is that several sensors (up to 100) can be connected in series on the same cable. Each sensor has a unique serial number and therefore the central unit can communicate with a certain sensor and obtain its temperature reading. The cable for short distances can have one wire for data transfer and power supply and another for ground; for long distances, one more wire is needed for power-supply. In any case, the 1-wire protocol requires only one pin for the microcontroller to communicate with several sensors. Reducing the number of cables reduces the risk of damage to cables (by rodents etc.) and the risk of loss of data. For measuring a temperature profile in soil, the sensors can be installed on a specially designed printed circuit with length of 60 cm, according to World Meteorological Organization (WMO) standards to sense temperature at elevations of -50 cm, -30 cm, -20 cm, -10 cm- 5 cm, -2 cm and 5 cm with respect to the soil surface. The circuit is connected to the data-logger via a three-wire cable and placed in a plastic tube with diameter 13 mm and length 65 cm, insulated with foam. This tube for measurement of soil temperature profile is easier to install in soil and reduces the potential damage to temperature sensors. For the placement of the tube for measuring soil temperature profile in rocky soil, a drill with appropriate drilling machine could be used, and in other types of soil an appropriate hand auger could be used. For sensors placed 5 cm above the ground, a special home-made radiation shield was used. For measuring temperature with presented system only 1-wire sensors DS18B20 could be use, or any other temperature sensors with output ranged from 0 to 2500 mV can be connected to single ended channels. Since we used the same 1-wire digital temperature sensors DS18B20 like in automatic soil respiration chamber electronic we assume the same test is reliable.

The Philips Inter-IC communications (I²C) protocol (Philips Semiconductors, The Netherlands) is commonly used for interfacing peripheral devices and microcontrollers. We used this type of communication for data-logging of nine measured parameters and time stamp on an AT24C512 (Atmel Corporation, San Jose, CA) memory module. Measurement frequency in range from 5 to 3600 s can be set and system informs us for how many days the data-logger can store data. (For example: measuring frequency set to 30 minutes, the data-logger can store data for 59 days.) If we do not download the data to an external device (notebook, handheld computer...) and the memory module is full, the microcontroller stops measuring and goes into power-down mode.

The user can communicate with the circuit using terminal software on a notebook or handheld computer. Communication is available via serial interface (baud rate: 56000, Data bits: 8, Parity: none, Stop bits: 1, Handshaking: none). To establish serial communication with computer also serial to USB converter could be used. When connection with the computer is established the microcontroller program starts a user-

interface routine and displays in the terminal program a notice with the instructions on how to set up time and date, the location of data-logger or download the data. One of the advantages of the presented system for measuring and data-logging is that you do not need to install any special software on your computer. Hyper Terminal (Windows) or any other free software for reading data from serial ports can be used.

The microcontroller circuit is powered by a battery pack, consisting of four AA-size, 1.5V alkaline batteries. Since the microcontroller and other devices (except sensors EC-5 for which a voltage regulator is used) can operate at a voltage between 4.5 and 5.5 V, only a diode was used in the supply line to avoid short-circuits and to reduce the voltage from the battery pack. The current drawn is approximately 15 μ A in power save mode and 22 mA during measurement. Each measurement lasts less than 2 seconds and if the measurement frequency is set to 30 minutes, using standard AA alkaline batteries, with a capacity of approximately 2500 mAh, we can expect a battery life of approximately 5.5 years.

For the central unit a microcontroller (ATmega16, Atmel Corporation, San Jose, CA) was used. The ATmega16 is a low-power CMOS 8-bit microcontroller based on the AVR enhanced RISC architecture. The ATmega16 offers several functions that allow the construction of the system with minimum peripheral components, because of which it is cost-effective and robust. To apply a real-time clock, the crystal oscillator with 32.768 kHz frequency must be connected to the microcontroller.

The software for the microcontroller was written in a BASIC-like language (BASCOM-AVR, MCS Electronics, Holland) for Microsoft Windows XP. The program was compiled in microcontroller assembly language and uploaded to the microcontroller using a programmer (PROGGY AVR, AX Elektronika, Slovenia) connected to a desktop computer via AVR Studio 4 software (Atmel Corporation, San Jose, CA).

The system with all its components and the designation of the electrical schematic of the circuit board (figure 7) was built in the Laboratory for Electronic Devices at Slovenian Forestry Institute. The schematic was transferred to the circuit board, which was drilled out on a small CNC machine in the same laboratory. The schematic is shown on figure 8.

Electronic components and connectors were soldered onto each circuit board and sensor cables were prepared. The tubes for temperature profile measurements were prepared according to World Meteorological Organization standards.



Figure 7: (a) Circuit board with sensors DS18B20 and finished measurement stick. (b) Microcontroller circuit board with battery pack. (c) Waterproofed housing with system for measuring and logging soil temperature profile and soil water content. (d) Female DB9 connector for serial communication with the system built outside.

The system for measuring soil profiles was tested at Succession site and measurements started in February 2010. According to the manual for soil water content sensor EC-5, measured mV were transformed to % using the suggested equation for mineral soils with accuracy of $\pm 5\%$. Measurements of soil water content using two time domain reflectometers (CS616, Campbell Scientific, Logan, UT USA) inserted horizontally at 10 cm and soil temperature at the same level using thermocouples (TCAV, Campbell Scientific, Logan, UT USA) were made in a nearby meteorological station. These two devices are in this testing domain called typical devices.

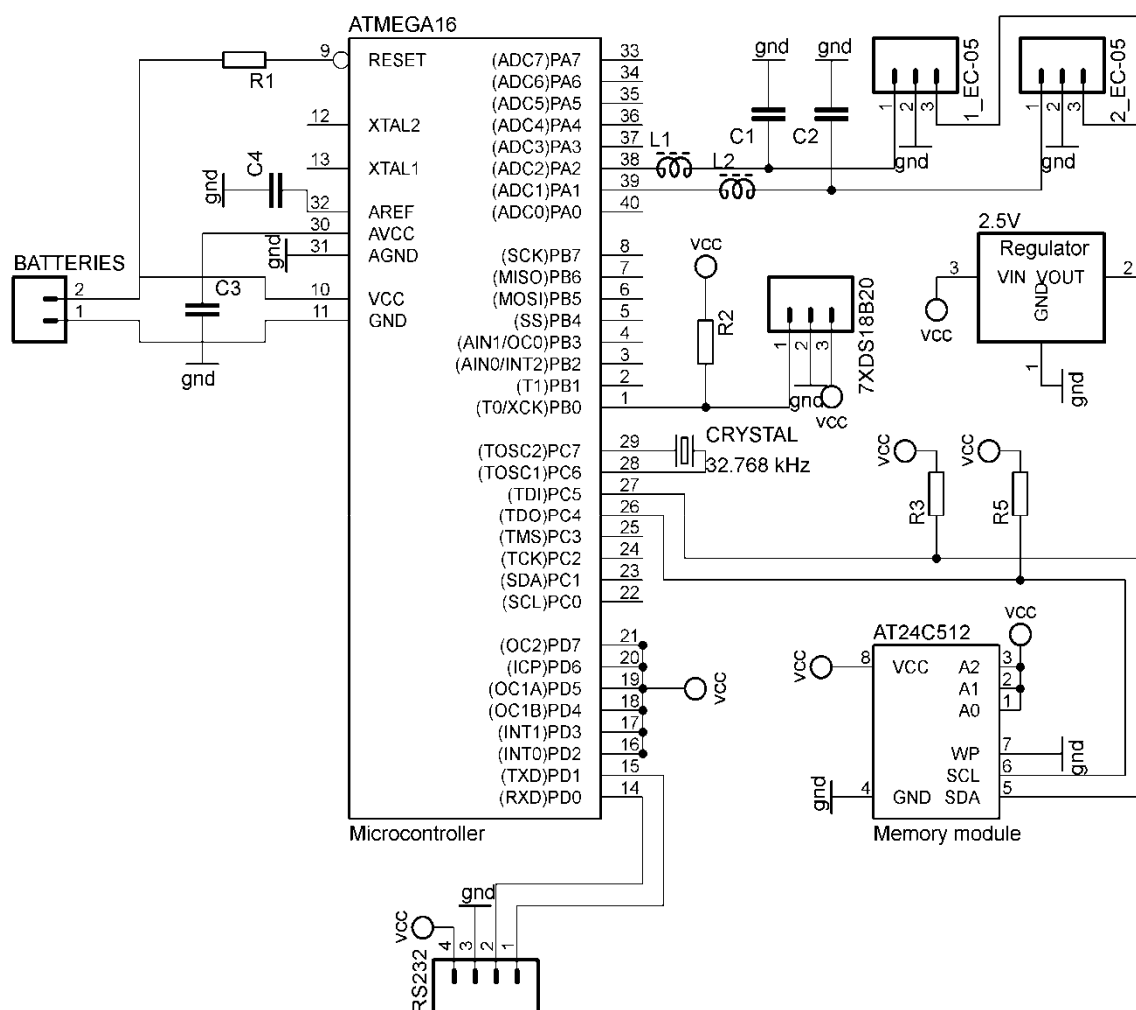


Figure 8: Electrical schematic of circuit board.

The system has a waterproof housing. Three cables for sensors enter the housing through waterproof cable glands. The other side of the box houses a female DB9 connector. The system housing allows a very convenient field installation and data downloading.

Because of rocky soils, tubes for measuring temperature profiles were inserted in holes that were drilled into the soil with a 14 mm diameter drill. The sensors for soil water content were inserted horizontally into a dug soil pit (10 and 30 cm depth). One of installation was done near meteorological station soil profile, to compare new system with typical device.

A notebook was used to download data during periodic visits (usually biweekly). The data were stored and later were checked and appended to the database. In the first few months, small lead-acid rechargeable batteries (6 V, 1.2 Ah) were used. The downside of these batteries is high self-discharge during higher temperatures – because of this, we have some

missing data in April 2010. After replacing the lead-acid batteries with battery packs, consisting of four AA 1.5 V alkaline batteries, we did not have any problems with data loss.

As a support for manual measurements the system for measuring Ta and SWC was installed on Grassland site (3 systems) and on Succession site (6 systems).

4 RESULTS

4.1 SINK ACTIVITY OF INVESTIGATED ECOSYSTEMS

Footprint analyses show that mean distances from where towers monitoring 90% of fluxes are 1530 m and 195 m for Succession site and Grassland site, respectively. More detailed footprints and wind roses for both sites are shown on figure 9.

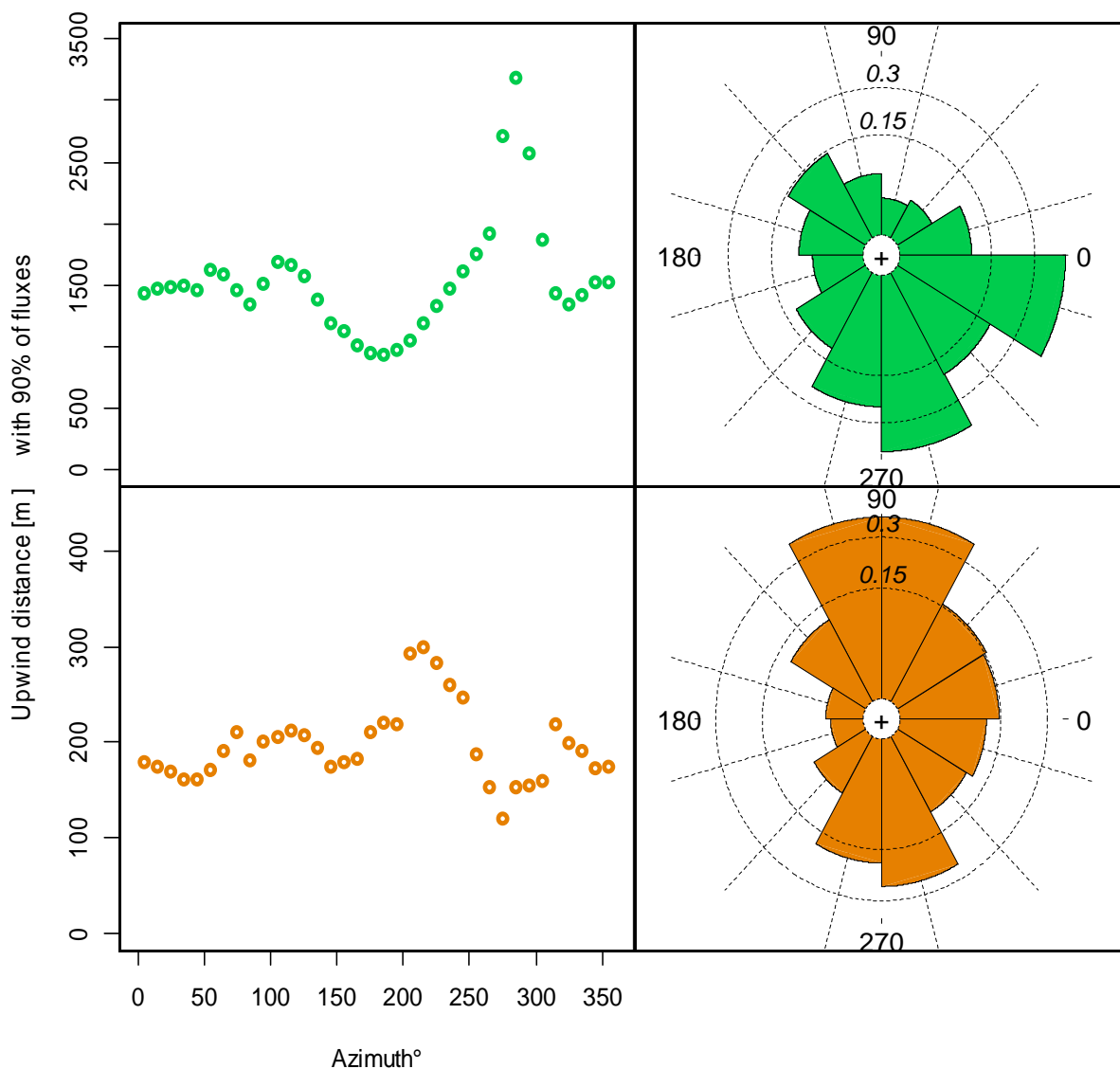


Figure 9: Footprint analyses (using model after Schuepp et al., 1990) and wind roses for Succession site (green color) and for Grassland site (brown color) site according to azimuth.

For the observed period (July 1st 2008 – November 30th 2012) no major differences were measured between Grassland site and Succession site concerning air temperature and precipitation (figure 10).

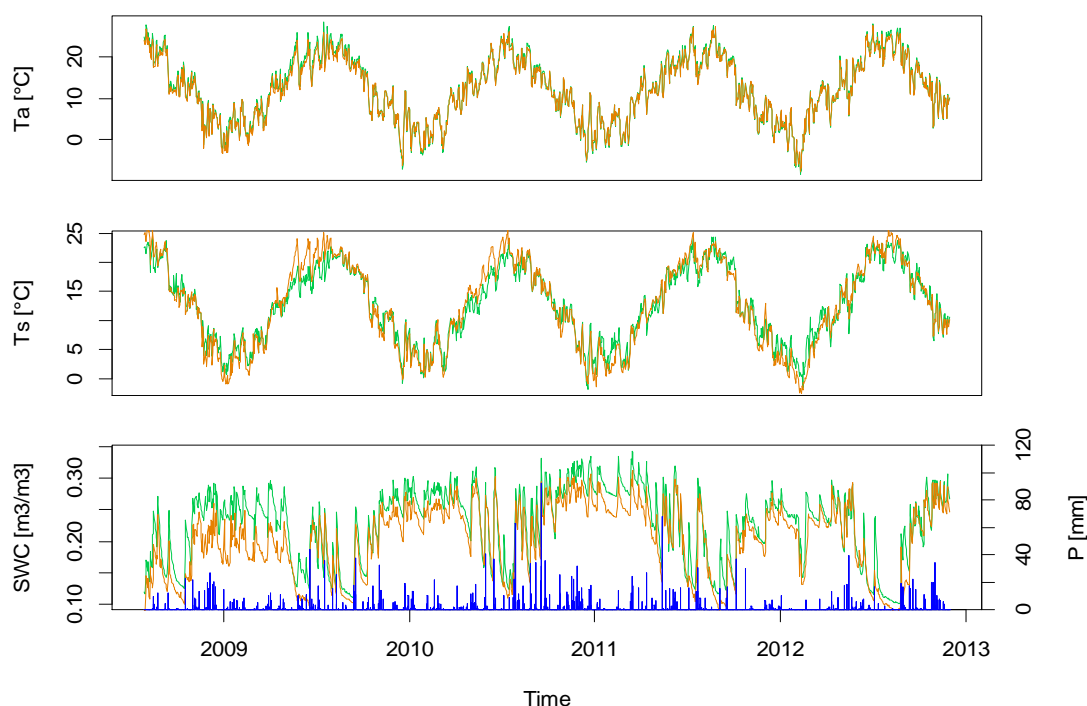


Figure 10: Mean daily Ta, Ts, SWC and P measured at two study sites (Succession site: green line; Grassland site: brown line; precipitation: blue bars.)

Mean air temperature for observed period was 12.3°C and 12.0°C for Succession site and Grassland site, respectively. Soil temperature at the Grassland site was higher in summer and lower in winter than at the Succession site. Mean soil temperature for observed period was 12.6°C and 12.7°C for Succession site and Grassland site, respectively. Mean annual precipitation for both sites was 813 mm. Soil water content was higher at Succession site ($0.23 \text{ m}^3 \text{ m}^{-3}$) than at the Grassland site ($0.20 \text{ m}^3 \text{ m}^{-3}$) on average. Observed period was compared to the normal of region (long term averages 1971-2000). Mean annual temperature at our sites was 1.5°C higher and differences in precipitation were also detected in comparison with climatic normal of the region.

On the Succession site tree phenology observation were also done for the years 2009-2012. On the Grassland site we measured the income and reflected PPFD light and calculate the difference to obtain APAR. In 2009 also detailed herbaceous monitoring was done for both sites (data in table 3). Figure 11 presents the leaf emergence and flowering for different trees species in Succession site and APAR for Grassland site.

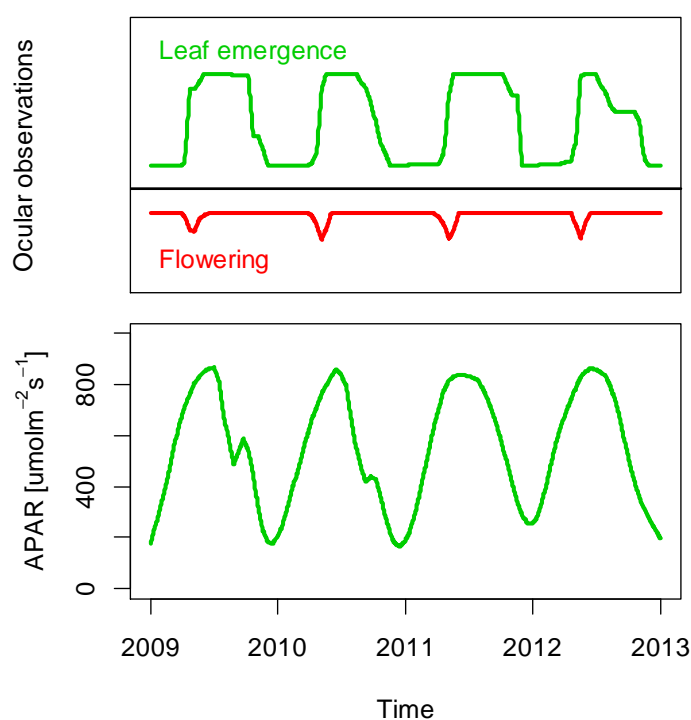


Figure 11: Phenology was observed on both sites. Up: On the Succession site ocular observation of phenology for main tree species every week or biweekly were performed. Down: On the Grassland site continuous measurements of incoming and reflected PPFD were performed (7-days moving window average is presented).

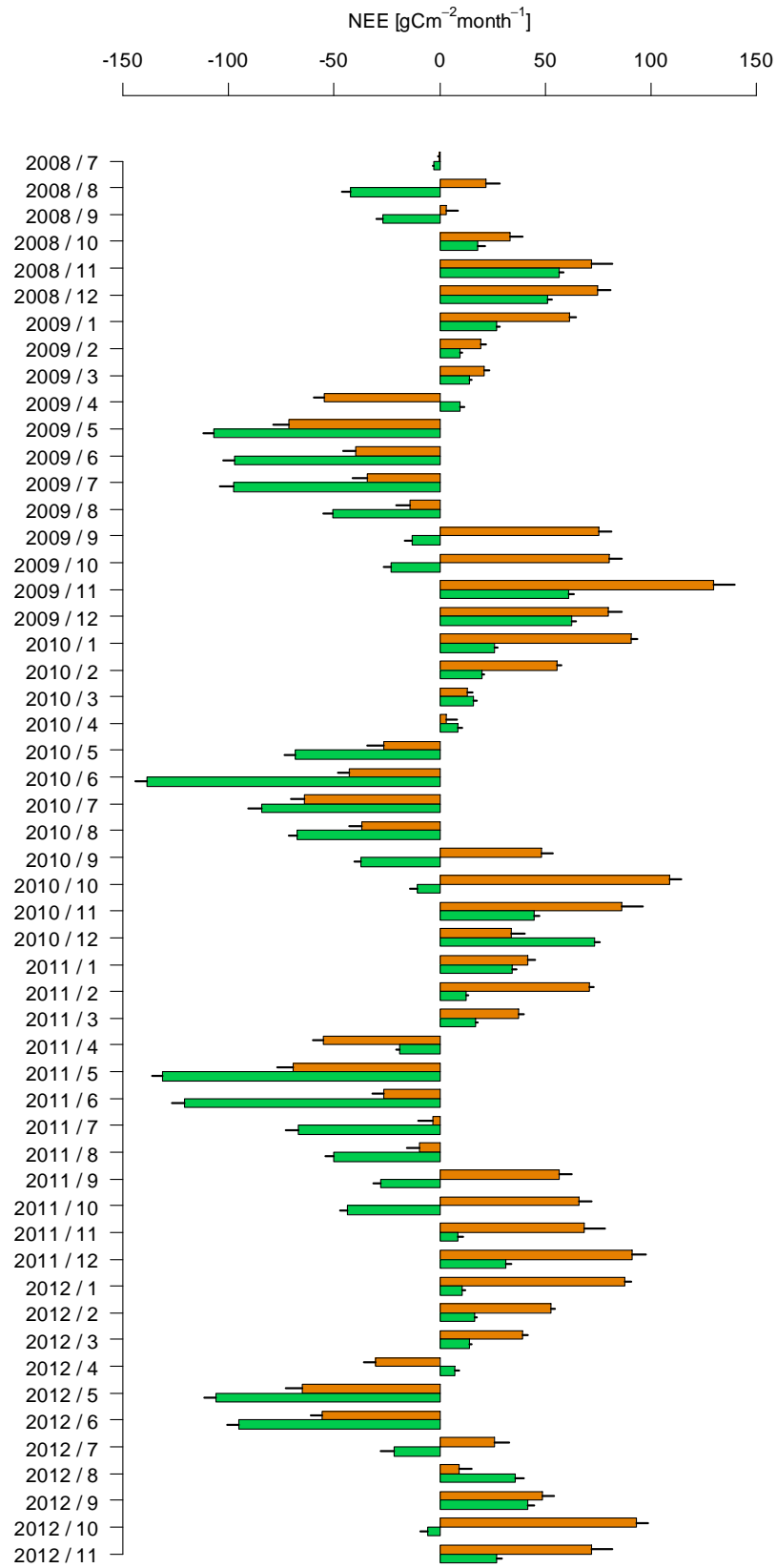
In observed period, Succession site was a net sink of carbon ($NEE = -800 \pm 82 \text{ gCm}^{-2} \text{ period}^{-1}$) while Grassland site was a source of carbon ($NEE = 1273 \pm 147 \text{ gCm}^{-2} \text{ period}^{-1}$). For both land uses figure 12 clearly shows the differences in growing season length and net production rates. The Grassland site had a maximum rate of net C uptake of $-71.2 \pm 7.7 \text{ gC m}^{-2} \text{ month}^{-1}$, while the Succession site had a maximum net uptake of $-138.6 \pm 5.7 \text{ gCm}^{-2} \text{ month}^{-1}$ (figure 12). On the average annual basis Succession site was net sink of carbon ($NEE = -184 \pm 19 \text{ gCm}^{-2} \text{ y}^{-1}$) while Grassland site was a source of carbon ($NEE = 293 \pm 34 \text{ gCm}^{-2} \text{ y}^{-1}$).

Summarized or averaged parameters based on year and vegetation season are presented in table 4. The growing season ranges from April to beginning of October (more detailed phenology analysis could be found on figure 11).

Table 4: Some environmental parameters and NEE averaged or summed by the vegetation and non-vegetation season (from April to beginning of October).

Site	Year	Vegetation season	NEE [$\text{gCm}^{-2} \text{ y}^{-1}$]	S.d. of NEE [$\text{gCm}^{-2} \text{ y}^{-1}$]	P [mm]	Ta [$^{\circ}\text{C}$]	Ts [$^{\circ}\text{C}$]	SWC [$\text{m}^3 \text{m}^{-3}$]	RI
Grassland	2009	No	392.258	14.664	499	8.899	8.417	0.228	2.230
	2009	Yes	-138.525	18.784	230	16.784	20.714	0.169	2.267
	2010	No	388.028	14.838	415	7.742	8.584	0.269	2.150
	2010	Yes	-118.662	18.575	528	14.184	17.949	0.256	2.437
	2011	No	375.624	14.716	324	9.235	9.219	0.250	2.357
	2011	Yes	-106.891	18.356	446	18.220	20.609	0.196	2.399
	2012	No	343.927	11.618	258	9.564	8.706	0.244	2.665
	2012	Yes	-67.652	18.528	344	18.402	19.796	0.178	1.880
Succession	2009	No	150.783	5.865	285	7.622	8.655	0.263	2.381
	2009	Yes	-356.449	12.971	362	16.745	18.017	0.208	2.207
	2010	No	170.032	5.874	434	6.091	7.783	0.302	2.403
	2010	Yes	-387.265	13.040	687	14.721	15.621	0.260	2.194
	2011	No	60.714	5.902	235	8.920	9.162	0.281	2.416
	2011	Yes	-416.094	12.988	382	16.155	17.767	0.231	2.491
	2012	No	62.027	4.742	180	8.825	9.835	0.275	2.463
	2012	Yes	-137.945	13.042	317	15.290	16.361	0.204	2.325

Figure 12: Monthly NEE with estimated standard deviation. Succession: green bars, grassland: brown bars.



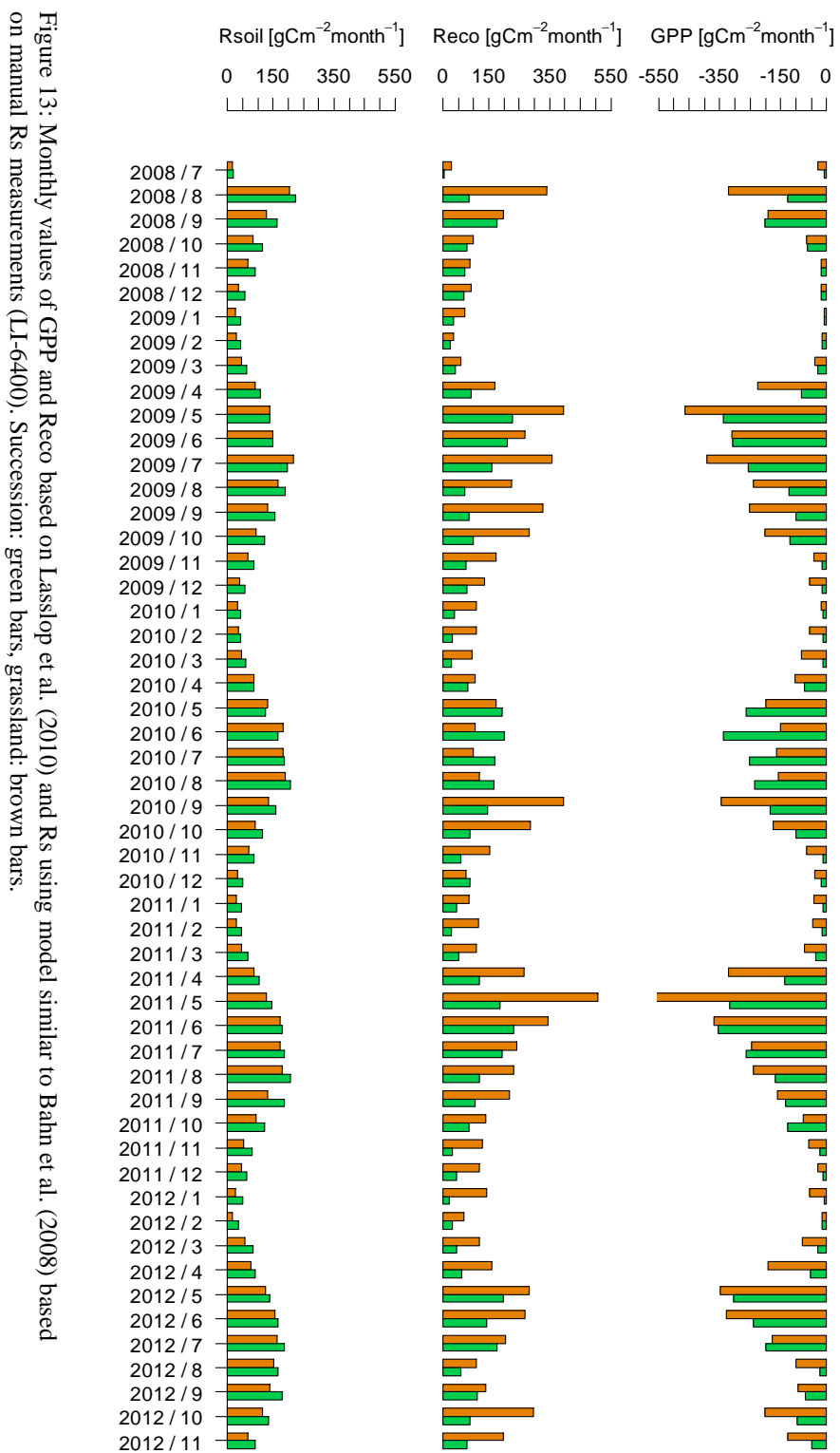


Figure 13: Monthly values of GPP and Reco based on Lasslop et al. (2010) and Rs using model similar to Bahn et al. (2008) based on manual Rs measurements (LI-6400). Succession: green bars, grassland: brown bars.

Summarized modelled monthly Reco and Rs were compared. At higher mean monthly air temperatures higher Rs was observed comparing with Reco.

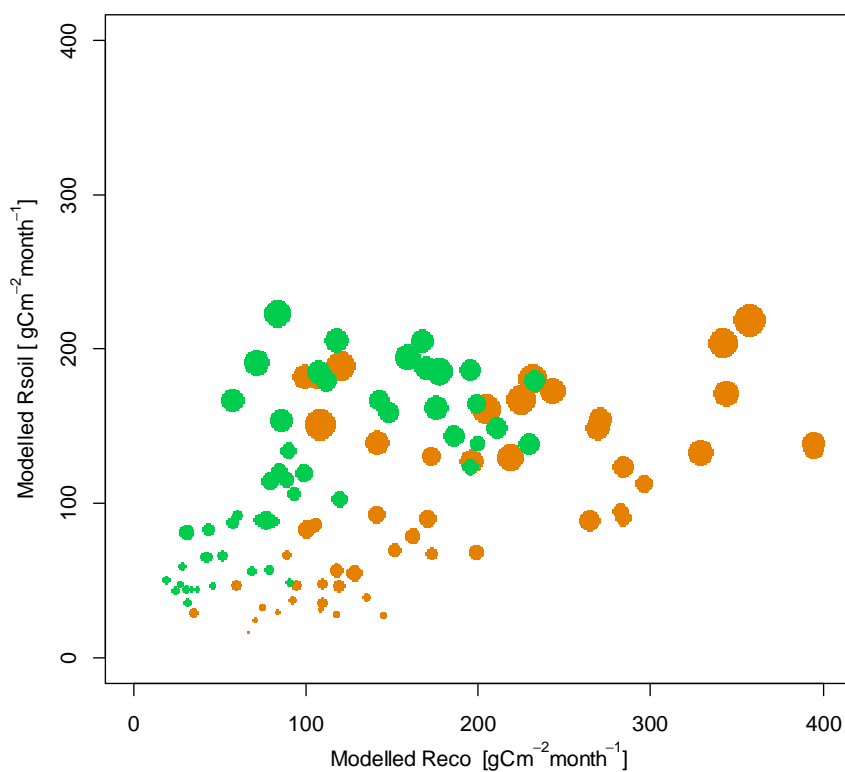


Figure 14: Relationship between modeled monthly Rs (Bahn et al., 2008), modeled monthly Reco (Lasslop et al., 2010) and Ta. Larger points present higher Ta which varies from 0.5°C to 28°C. Green points: Succession site, brown points: Grassland site.

4.2 DATA QUALITY AND EDDY COVARIANCE MEASUREMENTS

Concerning the eddy covariance data for the observed period (July 1st 2008 – November 30th 2012), 59.7% and 33.7% of expected data have not been discarded for Succession site and Grassland site, respectively. More detailed differentiation of data gaps and valid data are presented in table 5.

Table 5: Percentage of missing, hard and soft flagged eddy covariance data presented as data gaps. Hard flags: rainy or foggy conditions, or when condensation occurs on the instrument optical lens. Soft flags: stationarity test and friction velocity filtering. Gap-filled data with quality indicators present how data gaps were filled (A - Rg, Ta and VPD data are available in temporal window smaller than 14 days or Rg is available in temporal window smaller than 7 days, B - Rg, Ta and VPD data are available in temporal window greater than 14 days and smaller than 28 days. C - only flux is available at different temporal window sizes start at 7 days (for details see chapter 3.2.2)).

Year	Site	Missing data (1)	Hard flags (2)	Soft flags (3)	Data gaps (1+2+3)	Gap-filled data			Valid data
						A	B	C	
2008	Succession	14.8	9.2	18.2	42.2	99.6	0.3	0.1	57.8
2009		8.1	8.6	18.5	35.2	100.0	0.0	0.0	64.8
2010		8.8	13.0	17.8	39.6	99.9	0.0	0.0	60.4
2011		2.6	21.5	17.6	41.7	100.0	0.0	0.0	58.3
2012		11.6	17.4	13.8	42.8	99.1	0.8	0.1	57.2
2008	Grassland	23.1	26.4	8.9	58.4	99.3	0.6	0.1	41.6
2009		26.9	27.1	12.2	66.2	82.0	15.1	2.9	33.8
2010		31.5	23.3	18.5	73.3	97.8	2.1	0.1	26.7
2011		7.1	38.6	22.3	68.0	99.9	0.1	0.0	32.0
2012		8.7	31.2	25.8	65.7	99.9	0.1	0.1	34.3

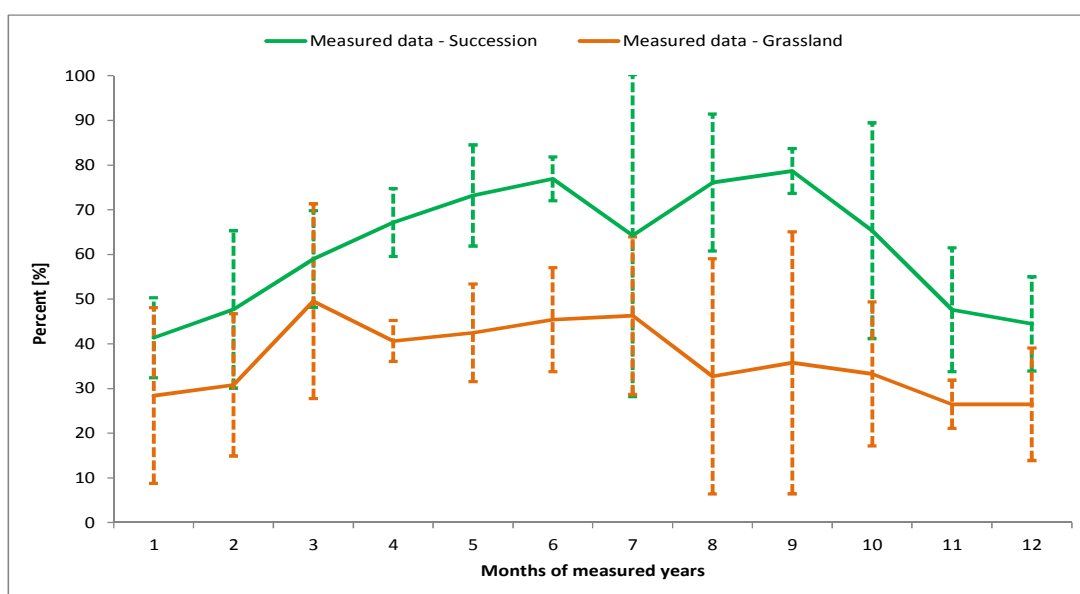


Figure 15: Percent of valid data during measuring campaign (January 1st 2009 – November 30th 2012) averaged by months (Succession site: green line; Grassland site: brown line)

A good agreement between energy fluxes measured at the eddy station and energy balance, calculated at the weather stations using net radiation and soil heat fluxes, was found for both sites (figure 16).

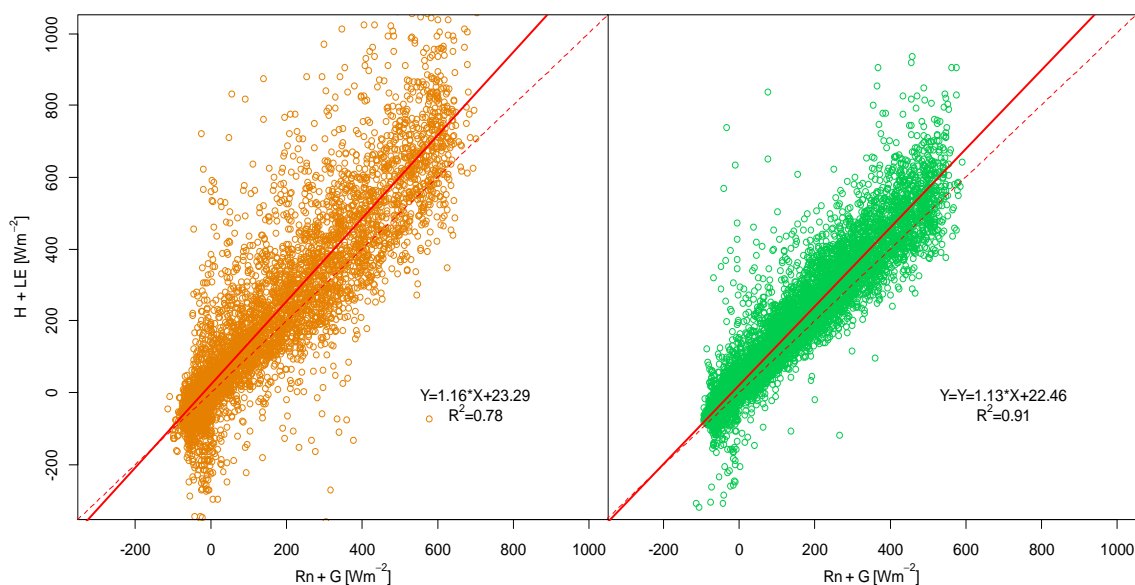


Figure 16: Energy balance closure for Succession site (green points) and Grassland site (brown points) site. The relation between consumed ($LE + H$) and available ($Rn + G$) energy. LE and H determined from eddy covariance, Rn and G measured half-hourly on meteorological station with net radiometer (NR-LITE, Campbell Scientific, Logan, UT USA) and soil heat flux plates at 10 cm depth (HFP01SC, Campbell Scientific, Logan, UT USA).

4.3 INSTRUMENT SELF-HEATING CORRECTION

After Burba correction was applied on our datasets cumulative NEE fluxes changed (figure 21). For observation period Succession site shifted from sink ($-800 \text{ gCm}^{-2}\text{period}^{-1}$) to weak sink ($-122 \text{ gCm}^{-2}\text{period}^{-1}$) of carbon, while the Grassland site remained a source (1273 and $1980 \text{ gCm}^{-2}\text{period}^{-1}$ without and with Burba correction, respectively).

In the frame of our work also investigation on instrument self-heating correction was done. Data for detailed investigation on OP IRGA self-heating effect presented in this study were measured between 22nd of January 2011 and 3rd of April 2012. At the research area in this period the lowest temperature could be expected (usually in January or February) and also warming up at March could be observed. Mean T_a for observed period was 4.8°C with minimum mean daily value of -9.8°C and maximum mean daily value of 15.8°C .

From previous studies it is evident that main impact on instrument self-heating effect is from T_a and W_s (Grelle and Burba, 2007; Burba et al., 2008).

Table 6: Linear models derived from measurements of OP-IRGA body temperatures, mock temperatures and T_a between 22nd of January 2011 and 3rd of April 2012.

Modelled parameter	Offset	Parameter for T_a	R^2
T bottom	1.477	1.006	0.989
T top	0.275	1.008	0.991
T spar	-0.076	1.026	0.996
T mock	-0.309	1.057	0.981

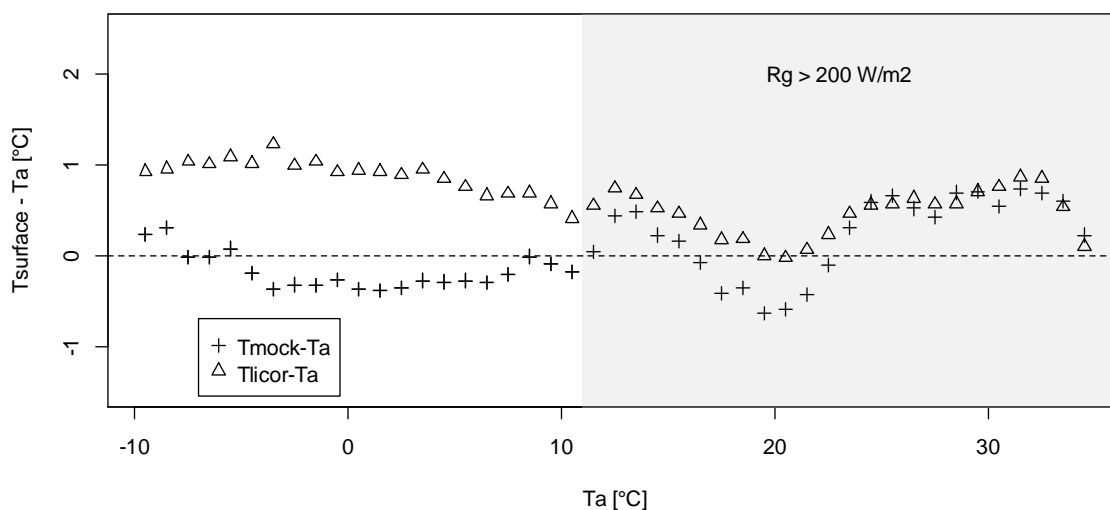


Figure 17: Temperature difference between T_{mock} , T_{licor} and T_a . Values are averaged by T_a classes with step of 1°C . Gray zone represents values where R_g might influence the surface temperature (T_{surface}).

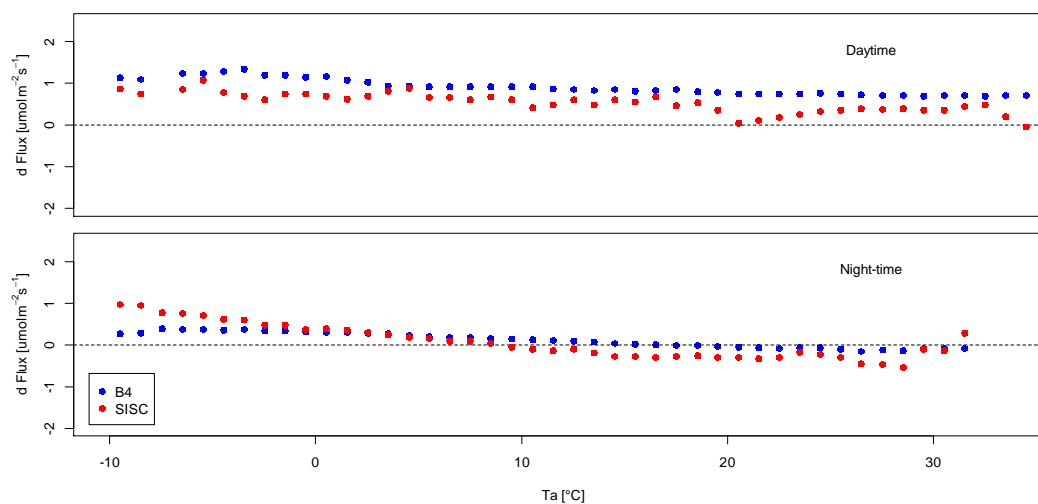


Figure 18: Flux corrected by B4 and SISC plotted vs. air temperature for daytime (up panel) and night-time (down panel). Air temperature and corrected fluxes were averaged by temperature classes with step of 1°C .

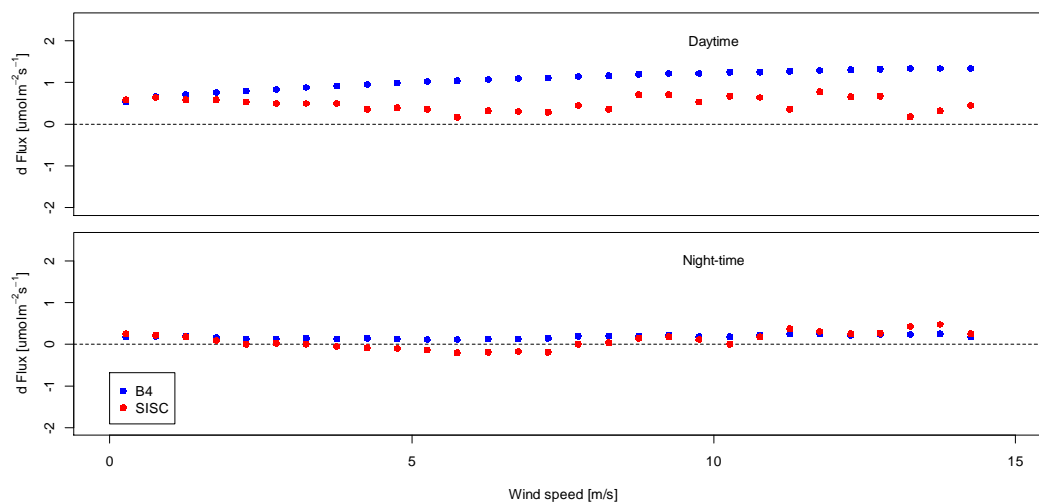


Figure 19: Flux corrected by B4 and SISC plotted vs. wind speed for daytime (up panel) and night-time (down panel). Wind speed and corrected fluxes were averaged by wind speed classes with step of 0.5 ms^{-1} .

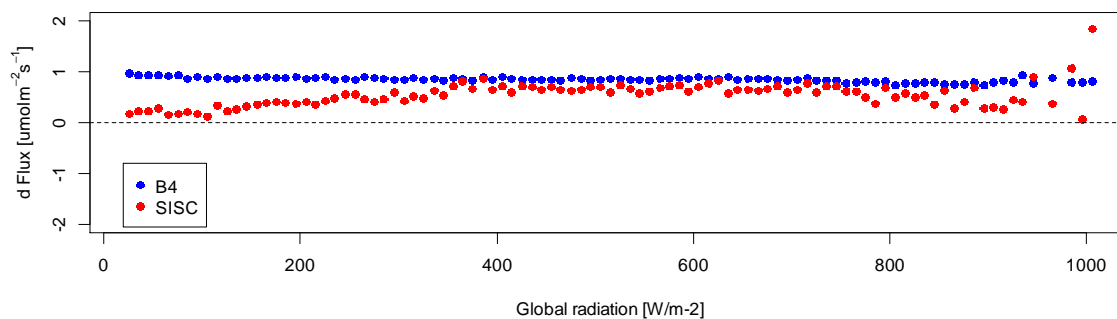


Figure 20: Flux corrected by B4 and SISC plotted vs. global radiation. Global radiation and corrected fluxes were averaged by global radiation classes with step of 10 Wm^{-2} .

NEE for observed period without applying self-heating correction (only WPL) was $-800 \text{ gCm}^{-2}\text{period}^{-1}$ and $1273 \text{ gCm}^{-2}\text{period}^{-1}$ for Succession site and Grassland site, respectively. After applying B4 correction NEE shifted to $1980 \text{ gCm}^{-2}\text{period}^{-1}$ for Grassland site and $-122 \text{ gCm}^{-2}\text{period}^{-1}$ for Succession site. Applying SISC correction NEE changed to $-522 \text{ gCm}^{-2}\text{period}^{-1}$ and $1574 \text{ gCm}^{-2}\text{period}^{-1}$ for Succession site and Grassland site respectively.

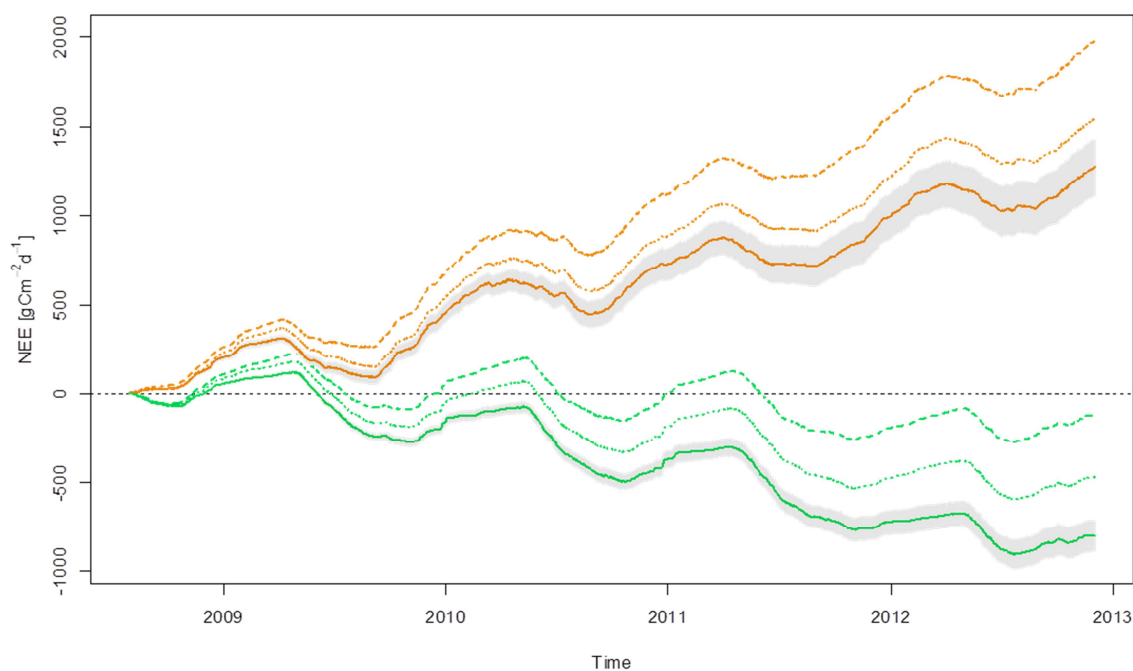


Figure 21: Cumulative fluxes of NEE: B4 correction applied (dashed line), SISC correction applied (dotted line) and NEE without self-heating correction (solid line) with uncertainty band. Brown lines: Grassland site; green lines: Succession site.

Figures 22 and 23 represents two scenarios of applied instrument self-heating correction: hot and cold period. It is clearly shown the differences between B4 and SISC correction, especially in cold period where non-natural behaviour of B4 correction is evident.

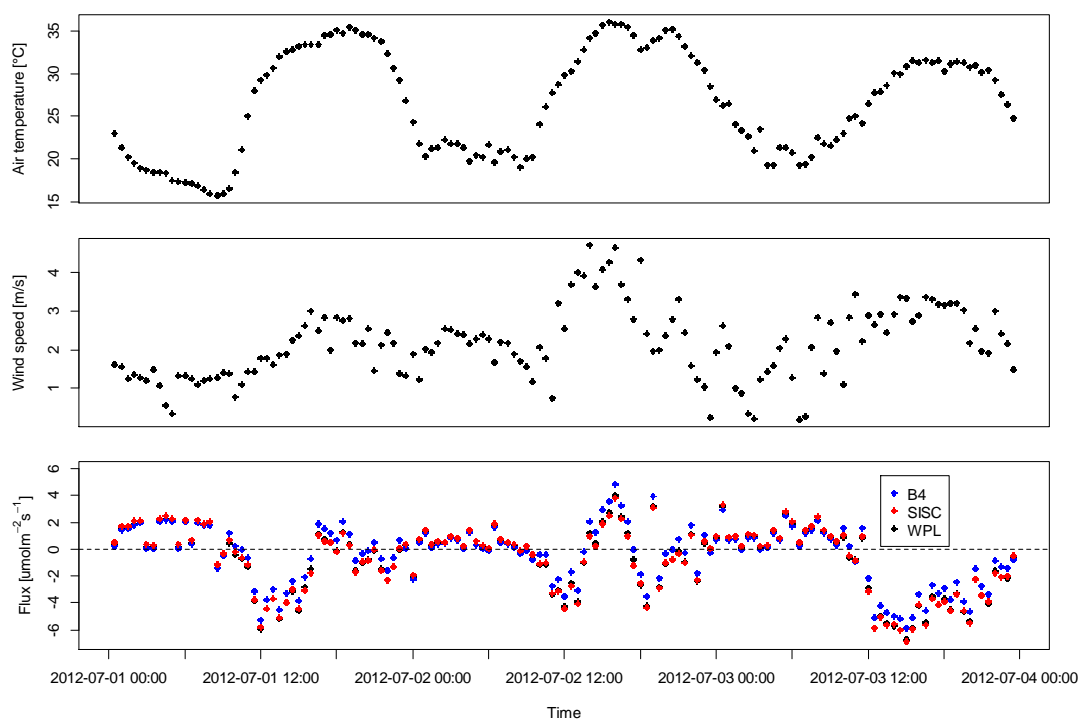


Figure 22: Half-hourly Ta and Ws data. Flux data are presented without self-heating correction, with B4 correction and SISC correction. Data are presented for six warm days in July 2012.

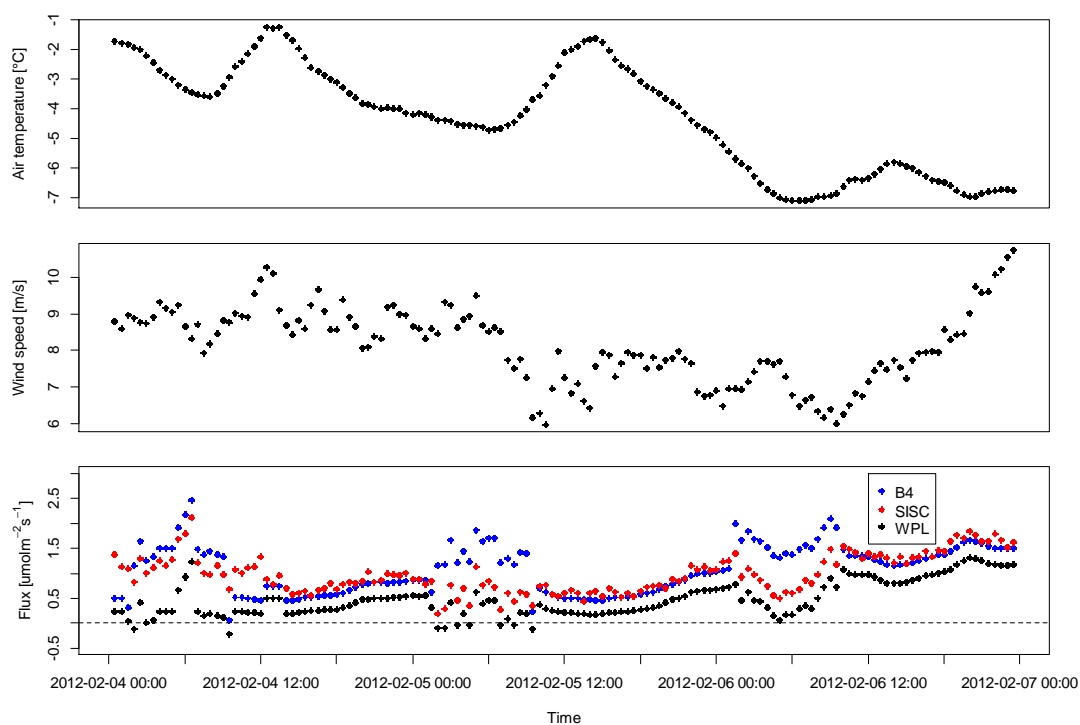


Figure 23: Half-hourly Ta and Ws data. Flux data are presented without self-heating correction, with B4 correction and SISC correction. Data are presented for six cold days in February 2012.

4.4 SOIL RESPIRATION

Some tests of chamber electronics in relation with temperature and voltage readings were done in Laboratory for electronic devices and were described in chapter 3.3.1.

On figure 24 is presented the comparison between open dynamic and close dynamic chamber technique using Kukulo and Ukulele chambers.

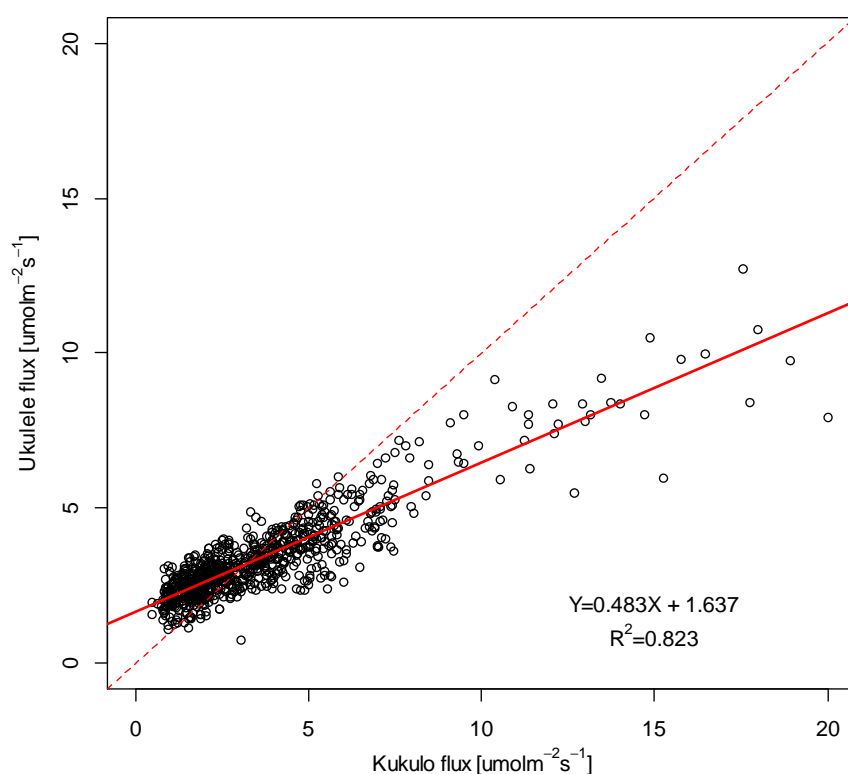


Figure 24: Half-hourly R_s fluxes measured with new designed closed dynamic automatic chamber system (Ukulele) plotted vs. open dynamic automatic chamber system (Kukulo).

Comparison of Ukulele and LI-6400 flux in December 2012 is presented in figure 25. Unfortunately, non-vegetation period and quite low temperatures impact on low fluxes and therefore only flux rates between 0.5 and 1.5 $\mu\text{molCm}^{-2}\text{s}^{-1}$ could be compared.

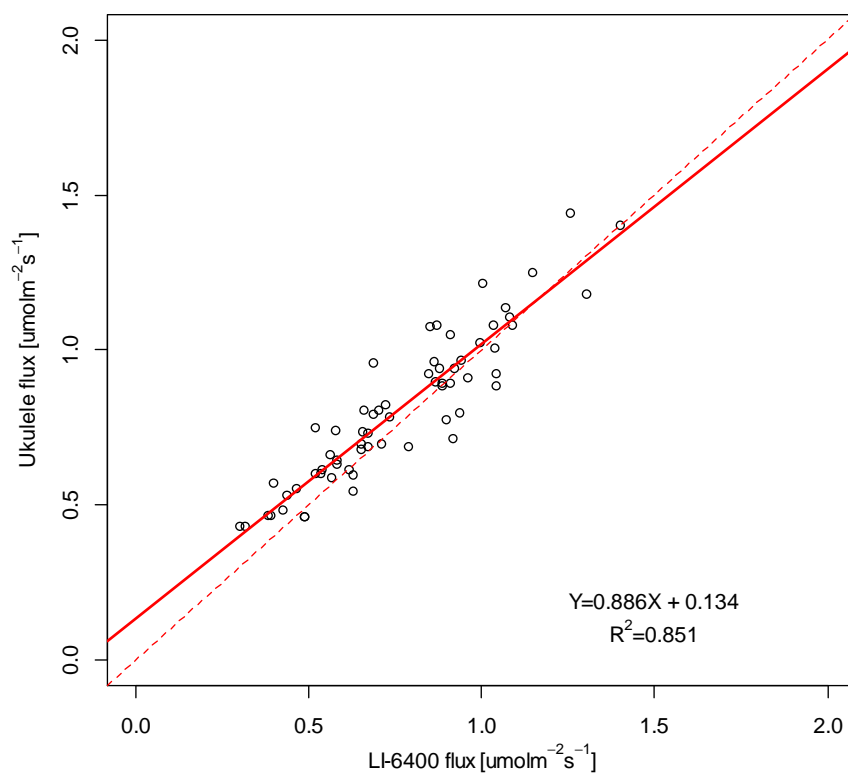


Figure 25: Hourly R_s fluxes measured with new designed closed dynamic automatic chamber system (Ukulele) plotted vs. closed dynamic manual chamber system (LI-6400 with chamber LI-6400-9).

Modeled monthly sums using equation (21) derived from Ukulele measurements and manual LI-6400 measurements and extrapolated to the whole period (July 1th 2008 – November 30th 2012).

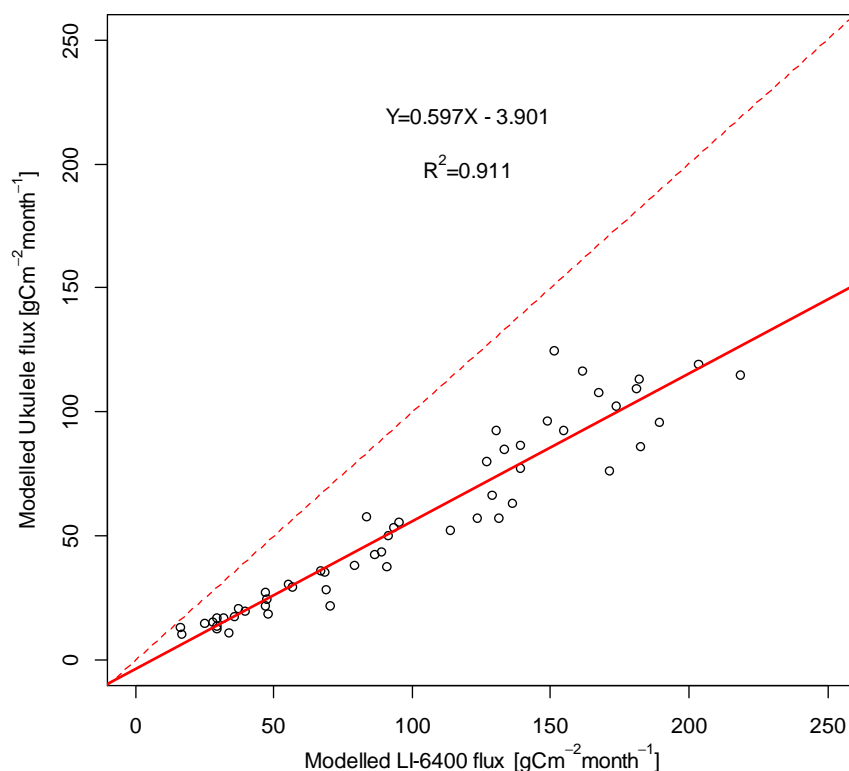


Figure 26: Modeled monthly sums of half-hourly R_s fluxes based on measurements with new designed closed dynamic automatic chamber system (Ukulele) plotted vs. R_s fluxes based on measurements with closed dynamic manual chamber system (LI-6400 with chamber LI-6400-9). For model (similar to Bahn et al., 2008) data measured from 1st of September 2012 till 30th of November 2012 and biweekly from July 2008 to November 2010 for automatic and manual system, respectively.

Night time fluxes measured by EC (ecosystem respiration) and night fluxes measured by Ukulele period from 1st of September 2012 till 30th of November 2012 (observed period) are shown in figure 26.

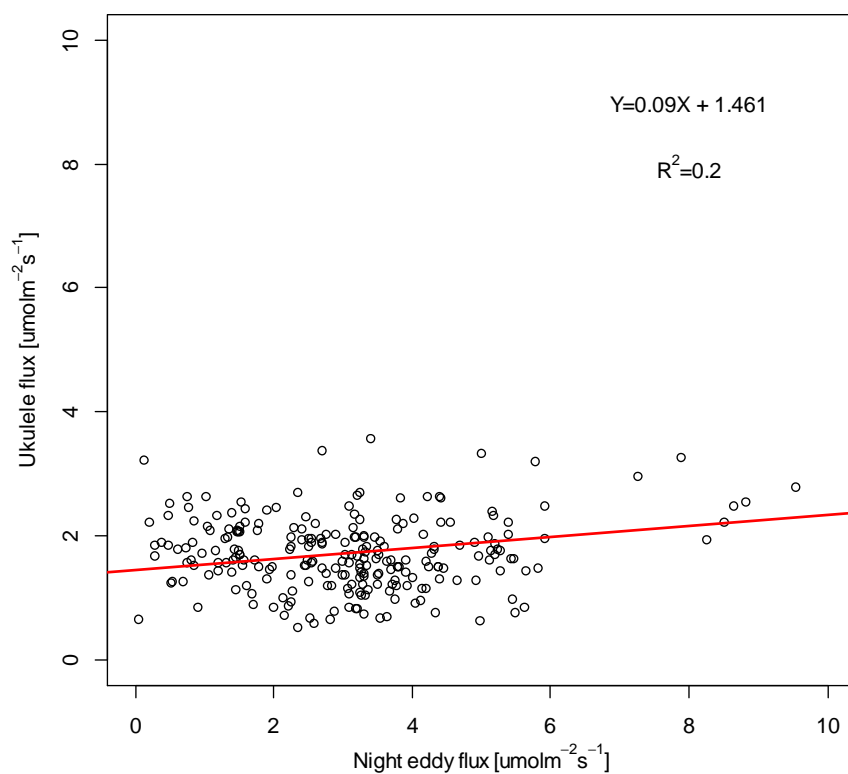


Figure 27: Half-hourly Rs fluxes (night-time) measured with new designed closed dynamic automatic chamber system (Ukulele) plotted vs. night-time ecosystem fluxes measured by Eddy covariance method. Data measured from 1st of September 2012 till 30th of November 2012.

Concerning the chamber measurements at 15 plots on 25 m² area in observed period from 1st of September 2012 till 30th of November 2012 air temperatures at 2 cm above the soil surface varied from 0.3°C to 45.2°C with mean at 9.1°C and soil temperatures at 5 cm below the soil surface varied from 2.5°C to 36.8°C with mean at 14.8°C. Furthermore was assumed that there is no autocorrelation between plots. As far we know from other observations on Grassland site temperature is quite homogeneous parameter. Therefore temperature measurements in soil respiration campaign were performed only at two automated soil respiration chambers. Soil water content was measured at each measuring point of automated soil respiration chamber, due to the fact that this parameter can highly vary. SWC sensors EC-05 were inserted vertically to measuring SWC from 0-5 cm. In observed period values of SWC varies from 11.5% to 30.2% with mean at 22.1%.

Mean value of Rs for observation period was 22.867 gCm⁻²period⁻¹. Maximum standard deviation was 0.204 gCm⁻²period⁻¹ (CV: 0.9%) and minimum standard deviation was 0.025 gCm⁻²period⁻¹ (CV: 0.1%) for 2 or 14 measuring points, respectively. Unfortunately manual periodic measurements were not performed at the same time with automatic system, but we can use data from the same periods of years 2008, 2009, 2010. Values of manual periodic measurements cannot be reported in g of carbon per period, while measurements were performed manually from 9.00 to 11.00 hours on 21 selected measuring points marked with collars (332 measurements). We found large variation in manual measurements with mean at 2.6 μmolCm⁻²s⁻¹ and standard deviation at 1.8 μmolCm⁻²s⁻¹ (69%), but also the variation of automatic measurements for observation period (between 9:00 and 11:00) was quite large with mean 1.8 μmolCm⁻²s⁻¹ and standard deviation at 0.8 μmolCm⁻²s⁻¹ (44%).

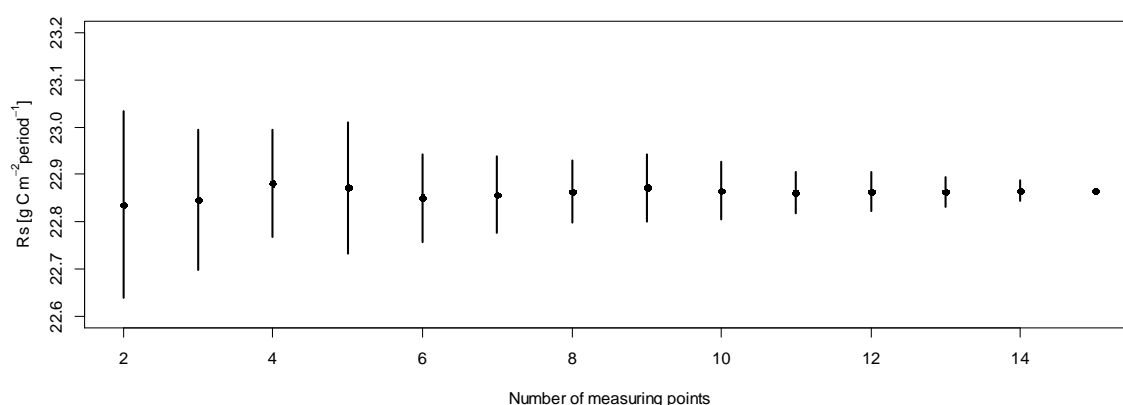


Figure 28: Soil respiration with standard deviation estimation for period from 1st of September 2012 till 30th of November 2012 measured with Ukulele system plotted vs. number of measuring points. Standard deviation was calculated from 100 datasets generated randomly choosing between 2 to 14 measuring points.

It was already mentioned that soil temperature is the main driver of Rs. With increasing the main driver for certain process also the variability in process increase. Figure 29 clearly

shows how number of measuring points can minimize variability of Rs at higher soil temperature.

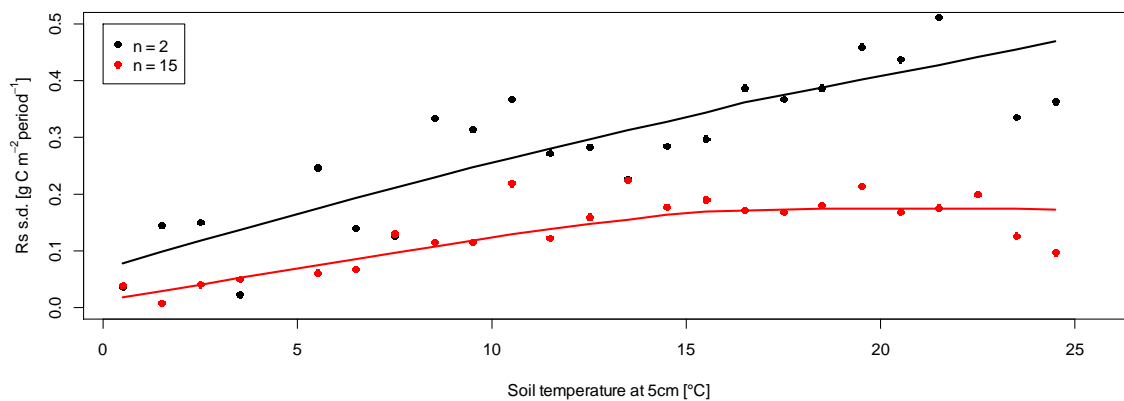


Figure 29: Standard deviation of soil respiration for 2 and 15 measurements points plotted vs. soil temperature. Standard deviation of soil respiration was averaged by temperature classes with step of 1°C. Solid lines are trend lines of presented points.

Before using developed system for measuring Ts and SWC profiles it was tested against typical devices. Later on 3 systems on Grassland site and 6 systems on Succession site as a support to Rs measurements were installed.

Ts was compared with typical device and linear regression was fit between them ($R^2 = 0.9976$, slope = 0.9912, intercept = 0.2744).

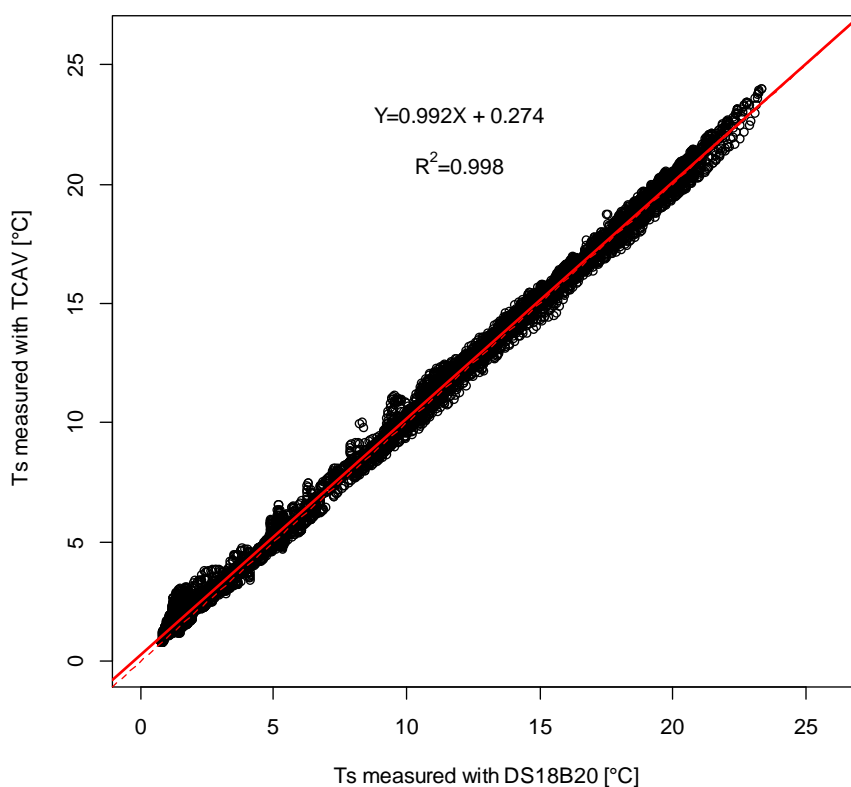


Figure 30: Ts at 10 cm depth measured with new system for measuring soil profiles plotted vs. thermocouples (TCAV, Campbell Scientific, Logan, UT USA) connected to CR3000 data logger.

Soil water content was compared with a typical device and a linear regression was fit between them ($R^2 = 0.9614$, slope = 0.8315, intercept = 0.0338).

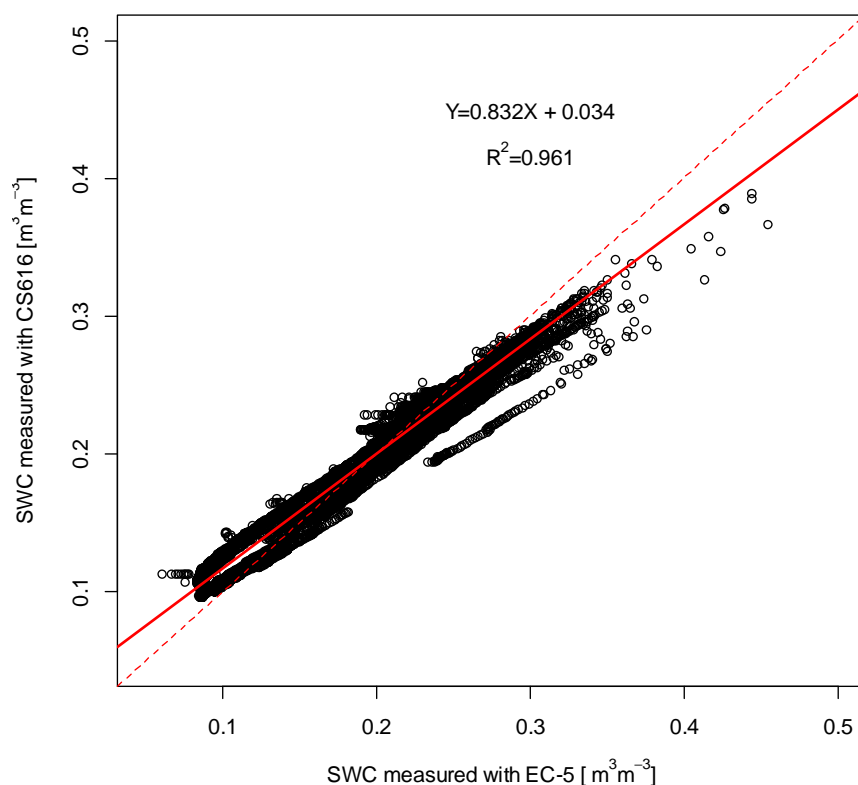


Figure 31: SWC at 10 cm depth measured with new system for measuring soil profiles plotted vs. time domain reflectometer (CS616, Campbell Scientific, Logan, UT USA) connected to CR3000 data logger.

From these results we can see that our system systematically underestimates temperature for approximately 0.27 °C and overestimate soil water content, especially at higher values of this parameter (figure 31). Differences in soil water content measurements are also present because construction of EC-5 sensor differs from CS616 sensor.

In table 7 are presented models for R_s based on T_s and SWC. If all 15 measuring points are together included in analysis parameters for Loyd and Taylor: $a = 1.34$, $b = 352.39$ (0.49) and for model similar to Bahn: $a = 1.20$, $b = 332.15$, $c = -16.58$, $d = -0.56$. Models can explain 49% and 50% using equation (20) and equation (21), respectively. Parameters for both models are significant ($P < 0.001$).

Parameters of models (after equation (21)) for R_s derived from manual measurements using LI-6400 are shown in table 8. Models are separated for Grassland site and for Succession site (divided for forest patch and gaps). R_s for Succession site was calculated based on area cover of each treatment, 0.45 and 0.55 for forest patches and for gaps, respectively. Only model parameter after equation (21) is presented in table 8.

Table 7: Models for R_s based on T_s and SWC derived for each Ukulele chamber.

Model after equation (20)																
Chamber	1	2	3	4	5	6	7	8	9	10	11	12	13	14	15	
Model parameters	a	0.92	0.91	1.08	1.20	1.36	1.22	1.30	1.56	0.95	1.29	1.09	1.04	1.45	0.99	1.53
	b	329.19	292.99	321.51	284.09	317.06	295.50	281.72	287.87	346.79	325.40	397.72	335.26	270.52	316.11	265.88
Model significance	R^2	0.60	0.27	0.58	0.48	0.37	0.33	0.39	0.47	0.55	0.49	0.66	0.44	0.52	0.51	0.56
	a	<0.001	<0.001	<0.001	<0.001	<0.001	<0.001	<0.001	<0.001	<0.001	<0.001	<0.001	<0.001	<0.001	<0.001	<0.001
	b	<0.001	<0.001	<0.001	<0.001	<0.001	<0.001	<0.001	<0.001	<0.001	<0.001	<0.001	<0.001	<0.001	<0.001	<0.001
Model after equation (21)																
Chamber	1	2	3	4	5	6	7	8	9	10	11	12	13	14	15	
Model parameters	a	1.05	1.77	1.61	1.18	1.37	1.21	1.25	1.50	0.96	1.49	1.08	1.00	1.43	1.40	1.49
	b	287.25	46.23	181.35	324.23	351.07	337.11	354.32	337.39	343.22	270.02	406.96	388.81	298.91	175.64	320.09
	c	-26.17	-10.28	-9.07	1.64	0.70	1.21	3.60	-0.67	-29.79	-32.39	15.75	2.95	1.94	-19.78	2.18
	d	-0.92	-0.65	-0.43	0.32	0.19	0.21	0.35	0.29	-1.11	-1.22	1.05	0.41	0.36	-1.01	0.39
Model significance	R^2	0.65	0.40	0.76	0.50	0.37	0.34	0.43	0.50	0.55	0.56	0.66	0.46	0.54	0.63	0.60
	a	<0.001	<0.001	<0.001	<0.001	<0.001	<0.001	<0.001	<0.001	<0.001	<0.001	<0.001	<0.001	<0.001	<0.001	<0.001
	b	<0.001	0.185	<0.001	<0.001	<0.001	<0.001	<0.001	<0.001	<0.001	<0.001	<0.001	<0.001	<0.001	<0.001	<0.001
	c	<0.001	<0.001	<0.001	0.105	0.716	0.46	<0.001	0.017	0.028	<0.001	0.386	0.028	0.198	<0.001	0.005
	d	<0.001	<0.001	<0.001	0.006	0.288	0.146	<0.001	0.018	0.038	<0.001	0.318	0.004	0.025	<0.001	<0.001

Table 8: Parameters of models (similar to Bahn et al., 2008) for soil respiration derived from manual measurements using LI-6400. Models are separated for Grassland site, forest patches and gaps at Succession site.

LI-6400		Grassland site	Succession site	
			gaps	forest patches
Model parameters	a	2.35	2.94	2.78
	b	354.24	326.69	351.02
	c	1.21	0.52	2.24
	d	0.16	0.11	0.27
Model significance	R ²	0.57	0.58	0.58
	a	<0.001	<0.001	<0.001
	b	<0.001	<0.001	<0.001
	c	<0.001	<0.001	<0.001
	d	<0.001	<0.001	<0.001

5 DISCUSSION AND CONCLUSIONS

Sink activity of investigated ecosystems (H1). The location of both eddy covariance towers and their footprint (figures 4 and 9) correspond to the aim of monitoring fluxes on overgrown abandoned pasture and on extensive pasture. The environmental conditions in the observed period (July 1st 2008 – November 30th 2012) were also found to be very similar for both investigated ecosystems (Figure 10). Eddy covariance measurements in observed period revealed sink activity at the succession site and relatively high release of CO₂ from the grassland site. However, sink activity during vegetation periods (Figure 12) corresponds to phenological observation at both sites (Figure 11). The latter observation does not coincide with the generalized view that European grassland ecosystems predominantly act as sink for atmospheric CO₂ (Soussana et al., 2007, Gilmanov et al., 2007). On the other hand, the shifts from sink to source are frequently reported for grasslands when environmental conditions limit productivity (e.g. Nagy et al., 2007). In ecosystems which are often affected by drought periods (due to low precipitation rates or shallow soils), the annual productivity and consequently the NEE are primarily controlled by precipitation levels and distribution. This was observed also in our ecosystems: during the vegetation periods with low rewetting index the measured weekly sink activity was also found to be low (Table 4).

During the study period, there were two short drought periods with strongest effects in late May 2009 and 2011 which affected the two investigated ecosystem differently (Figures 10 and 12).

At the Grassland site, late May is generally the period of most intensive growth of herbaceous layer and peak flowering time for many herbaceous species. Consequently, the shortage of water resulted in retarded growth and in reduction or complete absence of flowering in many herbaceous species. Due to the phenology of the most abundant species in the area (negligible summer and autumn re-growth), this effect on productivity could not be mitigated later in the season. A tight coupling of productivity (and NEE) to timing of precipitation has been previously reported by Xu and Baldocchi, (2004) for Mediterranean annual grassland in California and by Frank and Karn, (2005) for the mixed-grass prairie of the Northern Great Plains.

The succession site appears, in contrast to pasture, less susceptible to drought episodes, which might be the consequence of larger rooting depth (Jackson et al., 1996; Potts et al., 2006): the deeper the soil where the shrubs and trees are invading, the higher the soil water content due to lower levels of evaporation caused by tree/shrub shading which affects soil temperature (Figure 10).

In 2012 the drought period was observed in August and it resulted in both ecosystems becoming a source of CO₂, but it again affected the succession site later. After precipitation, the grassland site remained a source of CO₂, while the succession site

became a sink (Figure 12). Another possible explanation for this is related to different strategies of grasses and woody plants to cope with water stress (intensive vs. extensive water users according to Rodriguez-Iturbe et al. (2001)). The conservative use of water by woody plants (stomata close during the highest daily temperatures and during radiation in summer) has been showing in different water limited ecosystems (Laio et al., 2001; Wan and Sosebee, 1991).

Our measurements had clearly revealed differences in the annual courses of NEE for the two studied sites. The succession site showed one month time lag before becoming a net C sink in spring and continued to accumulate carbon for another two months in autumn in comparison to the grassland site. Since both sites are similar in terms of herbaceous layer (82% of common species), phenological development of its main species and peak biomass (244 ± 60 g of dry mass m^{-2} at the grassland site vs. 227 ± 80 gm^{-2} at the succession site, 2009 data), it is possible to conclude that the shifts of C balance are mainly governed by the activity of the forest patches. In the period when the herbaceous layer of the succession site sequesters carbon with similar intensity as the grassland site (based on peak biomass per hectare) it is to be expected that the respiration of forest patches compensates this sink, making the forest succession ecosystem close to carbon neutral. These conclusions can be supported by phenological observations (Figure 11) which show that the negative NEE values coincide with bud bursting and early leaf development. Interestingly, Frank and Karn (2005) reported the contrary: in their study the shrub prairie acted as a sink early in growing season compared with the grass prairie which is probably governed by different ecology of the invading shrubs.

In regard to the unexpectedly high CO_2 emissions after rain events for both sites, but especially for the grassland site, recent works have highlighted the role of geochemical rock weathering (dissolution and precipitation) processes in the total surface-atmosphere CO_2 exchange (Emmerich, 2003; Kowalski et al., 2008; Serrano-Ortiz et al., 2009; Serrano-Ortiz et al., 2010). Furthermore, CO_2 degassing from subterraneous systems can significantly contribute to NEE of karst ecosystems as shown by Were et al. (2010). Preliminary radar surveys have in fact shown the presence of caverns at the pasture but, unfortunately, we were not able to perform such a survey at the succession site. It can be concluded that high concentrations of CO_2 , built up from inorganic C sources and soil microbial activity during the previous dry and warm period (interpulse), are physically displaced as percolating water fills soil pore spaces and caverns (Huxman et al., 2004).

Flux partitioning was performed based on biological processes (Lasslop et al., 2010) and did not use biogeochemical modelling that would couple existing models for biological and geochemical processes (Serrano-Ortiz et al., 2009). Additionally, a model for R_s was used according to equation (21), which is also based on biological processes. Flux partitioning of NEE to GPP and Reco reflects the biological processes (Figure 13), but extracting R_s from Reco shows some discrepancies, especially during higher air temperatures (Figure

14). It was already reported that the LI-6400 also gave higher values of R_s in comparison to Reco derived from EC for non-calcareous terrain (Liang et al., 2004). Here biogeochemical modelling would be needed, but additional measurements should be performed and this is out of the scope of our work.

Based on the eddy covariance measurements it can be concluded that overgrown area increased sink activity compared to the extensive grassland in observed period (July 1st 2008 – November 30th 2012). Carbon balance is changed if abandoned grasslands are overgrown with tree species and become a carbon sink.

Data quality and eddy covariance measurements (H2). Initial areas for micrometeorology investigation, also with EC, were carefully selected and presented as ideal sites i.e. level terrain with smooth homogeneous surface and good fetch (McMillen, 1988). With increasing awareness of environmental problems the measurements started above non-ideal or problematic terrain and EC is nowadays widely used. Eddy covariance datasets usually have gaps due to instrument malfunctioning or electrical power failures; bad data are recorded due to low turbulence, inappropriate environmental conditions, wind not coming from the footprint of interest etc. A quality check of the dataset is important so that the results do not contain bias or errors.

The heterogeneity of our investigated ecosystems contributed to the quality of eddy covariance data. On average in observed period (July 1st 2008 – November 30th 2012) 59.7% of data were valid for succession site, which for example is very similar to 8 years of measurements above mid latitude forest (Barford et al., 2001) where 58.8% of data were valid. For grassland site 33.7% of data were valid in observed period, which is similar as in research of scrublands in Mediterranean areas (Serrano-Ortiz et al., 2009) where 42.4% of 4-year dataset were valid. The measurements on meadow (Haslwanter et al., 2009) also showed similar result with 32.4% of valid data. The percentages of valid data for both ecosystems are very low during the non-vegetation period (Figure 15). This could be problematic for the investigations of karstic ecosystems, since it was already reported (Were et al., 2010; Serrano-Ortiz et al., 2010; Kowalski et al., 2008) that in non-vegetation period NEE could be strongly influenced by subterranean CO₂ degassing from soil pores and cavities. Standard procedures usually account only for biogenic processes (Lasslop et al., 2010), since gap-filling of data in order to estimate the NEE exchange in certain period, could lead to errors for the non-vegetation period.

Detailed breakdown of non-valid data (Table 5) into missing data, hard flagged data and soft flagged data shows some difference against other reports available in literature. The missing data were caused mainly by brief failures in power supply, except for a great portion of missing data on grassland site at the end of year 2009 and at the beginning of year 2010, which was caused by a problem with sonic anemometer which was damaged by lightning. Data that was discarded because of precipitation or suspected condensation on the lens of OP IRGA were called hard flagged data and data discarded because of stationarity lower than 60% and u^* being lower than u^* threshold were called soft flagged data. The differences in comparison with other research could be established especially at the grassland site. However, for both sites soft flagged data present around 17% of datasets, which is lower in comparison to other research (Haslwanter et al., 2009; Serrano-Ortiz et al., 2009) and indicates good turbulence conditions among the investigated ecosystems. The percentage of hard flagged data for succession site, very similar to other research (Haslwanter et al., 2009; Xu and Baldocchi, 2004), was 13.9% of the dataset, while the percentage of hard flagged data for grassland site is considerably higher (29.3%). Detailed calculation has shown that a lot of data were hard flagged because of the

condensation on the OP IRGA lens. This problem can be solved with the increase of measuring height or with the use of CP IRGA. The increase of measuring height would result in a considerably larger footprint (Figures 4 and 9) which could be affected by fluxes from specific karstic structures found near the eddy covariance tower.

Quality check and detailed calculation of missing, hard flagged and soft flagged data is one of the ways to validate flux data measured by EC. Another possibility is to validate measurements through energy balance closure. The degree of energy balance closure provides an objective check of EC. When systematic energy imbalances occur, they may reveal bias in NEE measurements (Twine et al., 2000). Key components of energy balance are: net radiation (measured with net radiometer or other radiation sensors), soil heat flux (measured with heat flux plates or calculated from soil temperature profiles), and latent and sensible heat flux (measured with EC). Minor components (heat stored in the canopy, soil water etc. and energy spent on photosynthesis by the plant) could improve the energy balance closure (Burba and Anderson, 2010) but they are rarely included. Energy balance closures for our investigated ecosystems overestimate energy fluxes measured with eddy covariance. This is rarely reported (Twine et al., 2000; Wilson et al., 2002), but could be explained by high spatial heterogeneity of our ecosystems (i.e. tree patches and white, highly reflective stones) which could have caused an underestimation of net radiation for the whole footprint. High heterogeneity of the soil also affects the soil heat flux measurements and a single measuring point is not suitable for heterogenic ecosystems.

It can be concluded that some features of karst ecosystems, such as the heterogeneity of the terrain and environmental conditions, have affected the eddy covariance measurements and the quality of measurements. At the succession site the eddy covariance instrumentation was set up at the height of 15 m although the height of vegetation does not exceed 7 m. This was done in order to enlarge the footprint and minimize the impact of patchy tree vegetation. In the expected footprint area there were no special karstic structures were found, e.g. cave entrances etc. At the grassland site the eddy covariance instrumentation was set up at the height of only 2 m to exclude the influence of sinkholes and nearby small cave entrances. This has affected the measurements which gave a lot of hard flagged data due to the condensation on the OP IRGA lens. It can be concluded that different approaches, in terms of eddy covariance instrumentation height, were used in these investigated ecosystems. Research in calcareous ecosystems could be difficult in comparison to research in other terrestrial ecosystems because of possible contribution of inorganic CO₂ (Kowalski et al., 2008; Serrano-Ortiz et al., 2010). Additional measurements of CO₂ isotopic composition must be made (Plestenjak et al., 2012) or other equipment for continuous monitoring of isotopic composition (Bowling et al., 2003) instead of IRGA must be used.

Instrument self-heating correction (H3). Parameters (W_s and T_a) which influence the air heating in OP IRGA measuring cell were tested in this study. Similar relationships between IRGA body temperature and mentioned parameters were discovered by other research groups (e.g. Burba et al., 2008). Minimum differences occur when T_a is around 20°C (Figure 17), while the most problematic conditions are during night or conditions with low W_s or when R_g exceeds 400 Wm^{-2} (Figures 18, 19 and 20). But these differences could vary with different methods of installation of instruments and IRGA inclination. Using OP IRGA for measuring and calculating fluxes from gas densities will always introduce some errors into our calculation, also because other parameters such as position of the IRGA body, distance between sonic anemometer and IRGA, and effect of solar radiation influence the real air temperature in the OP IRGA measuring cell. When using mentioned instruments it seems that is necessary to perform high frequency measurements of air temperature with fine-wire thermometers in measuring cell (Grelle and Burba, 2007; Burba et al., 2008). This method is the best solution for self-heating effect when using OP instruments. One of the problems with fine-wire installation in field experiments is great possibility that fine-wire thermometers will break in rainy or windy weather conditions. In the presented study slow responding, but robust, temperature sensors were used to estimate the differences between the body temperatures of mock IRGA and real OP IRGA (installation suggested by Burba et al., 2008). The advantage of the presented approach is suitability for long-term and continuous operation. The observed period was chosen to show how B4 and SISC methods impact the NEE. 6-day cold and 6-day warm periods were chosen (Figures 22 and 23) to show how both self-heating corrections impact the WPL corrected fluxes. It can be observed that in the period when the air temperatures were above 10°C during night, SISC and B4 method produce very similar flux values. When the air temperature falls below 0°C during the day, the SISC method produced higher flux values in comparison to B4 method. Furthermore, during low temperature 6-day period some artificial introduced fluxes could be observed with the B4 method (Figure 23). For detailed overview in which weather conditions do the B4 and SISC method differ from WPL corrected fluxes see Figures 18, 19 and 20.

Grelle and Burba, (2007) suggested fine-wire correction (PRT) based on temperature measurements in OP IRGA measurement cell. Results for PRT correction show the same trend as SISC correction (Grelle and Burba, 2007). Cumulative fluxes with applied B4 method have the highest values and fluxes corrected with WPL correction have in both studies the lowest values, while values of cumulative fluxes with applied PRT correction and SISC method are in between for both ecosystems (Figure 21). In both approaches the real temperature of OP IRGA is measured, but with the different sensor types and different frequency. As already mentioned, one of potential drawbacks of fine-wire installation is the fragility, but on the other hand it is much better for fast response measurements. Measurement with robust but slow responding sensors allows us to perform measurements continuously with the same installation. It is obvious that besides air temperature and W_s

the OP IRGA inclination and the whole setup together with sonic anemometer (where usually T_{sonic} is measured at high frequency) have an influence on self-heating effect. Since there are many different setup combinations it seems that is not possible to derive one self-heating correction for all sites around the world (e.g. Reverter et al., 2010) and self-heating correction must be determined for each site specifically. Thus it seems to be important that every time OP IRGA is used also the temperature sensors for monitoring the IRGA body temperature are installed. With the installation of new instrumentation produced by Li-Cor (Burba et al., 2012) self-heating effect is minimized, but unfortunately there is a lot of older instrumentation being used around the world where self-heating correction must be applied.

It can be concluded that the application of the B4 method (Burba et al., 2008) for the correction of fluxes due to self-heating effect is not appropriate for our investigated ecosystem, because it produces unreasonable results. Our measurements have shown that there is a need for self-heating correction for our ecosystems and therefore it is more appropriate to use site specific self-heating correction based and developed on the measurements suggested by Burba et al. (2008).

Soil respiration (H4). Different measuring principles of Rs have resulted in different values of Rs, which are strongly dependent on soil types, especially when using the soil CO₂ gradient approach (Liang et al., 2004; Nagy et al., 2011). It was already proven that Rs values measured with open dynamic chamber are higher in comparison to values measured with closed dynamic chamber (Liang et al., 2004) and the same was observed in our study (Figure 24). It must be taken into account that the comparison of Ukulele and Kukulo systems was performed over very short period of time and therefore with very limited environmental parameters, such as Ts and SWC. However, the correlation between the techniques used in Kukulo and Ukulele system was good ($R^2 = 0.82$, $n = 864$). The results from the comparison between Ukulele and LI-6400 in December 2012 (Figure 25) have shown the same trend as reported in other studies (Liang et al., 2004). The correlation between LI-6400 and Ukulele was good ($R^2 = 0.85$, $n = 63$), but these results are based on a very short time and low Ts. Therefore, the comparison between modelled Rs derived from LI-6400 and Ukulele measurements according to equation (21) were also done (Figure 26). LI-6400 model again produces higher values of monthly Rs compared with Ukulele model, but the correlation was good ($R^2 = 0.91$, $n = 53$). In this comparison it must also be taken into account that the measurement period was short (from 1st of September 2012 till 30th of November 2012). In Figure 27 a comparison between night-time eddy covariance fluxes (Reco) and night-time Ukulele flux is made. Reco is greater than soil flux and this is an expected relationship. In other research (Nagy et al., 2011) similar relationships between Rs and ecosystem respiration were found. The correlation in this comparison is not very high, but again: the short measurement period with Ukulele system must be taken into account.

For the same observed period a test was performed to show how a number of measuring points can impact the measurements of soil respiration. The time window (45 minutes) in which all of the chambers measured soil respiration was called a cycle. During each cycle we had 15 soil respiration measurements distributed on 25 m². 100 datasets were generated choosing from 2 to 14 measuring points randomly. All datasets were then merged, according to the number of measuring points, and mean and standard deviation were calculated (Figure 28). Mean values for Rs were quite constant at 22.867 gCm⁻²period⁻¹. Maximum standard deviation was 0.204 gCm⁻²period⁻¹ (CV: 0.9%) and minimum standard deviation was 0.025 gCm⁻²period⁻¹ (CV: 0.1%) for 2 or 14 measuring points, respectively. Unfortunately, manual periodic measurements were not performed at the same time as automatic measurements with the system, but we can use data from the same periods of years 2008, 2009, 2010. The values of manual periodic measurements cannot be reported in g of carbon per period, because measurements were performed manually between 9.00 to 11.00 hours on 21 selected measuring points marked with collars (332 measurements). We found a large variation in manual measurements with mean at 2.6 μmolCm⁻²s⁻¹ and standard deviation at 1.8 μmolCm⁻²s⁻¹ (CV: 69%), but also the variation in automatic measurements for the observation period (between 9:00 and 11:00) was quite large with

mean $1.8 \mu\text{molCm}^{-2}\text{s}^{-1}$ and standard deviation of $0.8 \mu\text{molCm}^{-2}\text{s}^{-1}$ (CV: 44%). The values for CV around 40% are commonly observed (Kutsch et al., 2010). However, with LI-6400 we monitored an area 4 times larger than the area monitored with the automated system. A big percentage of uncertainty result for LI-6400 belongs to spatial heterogeneity, while the spatial variability in measurements with automated chambers is not expressed as much. Manual chambers (LI-6400) are well suited for covering spatial variability and automated chambers offer an important opportunity to study the temporal variation of Rs. Best results can probably be obtained by combining continuous monitoring of Rs with automated chambers and spatial measurements with manual chambers (Kutsch et al., 2010).

Flux partitioning of Rs into heterotrophic and autotrophic flux component was not performed during field measurements. For this, it would be essential to know more about biological processes, but in our investigated ecosystem this was not possible due to very stony soils and roots being often found in tiny soil pockets between stones or rocks. Separation of organic and inorganic component of Rs seemed to be more essential on calcareous terrain. This could be executed as suggested in several studies (Plestenjak et al., 2012; Inglima et al., 2009; Kuzyakov, 2006) or done with an appropriate equipment for continuous measurement of isotopic composition connected to an appropriate chamber system.

It can be concluded that knowledge of temporal variability can be greatly improved with an automatic system. Corresponding measurements of soil temperature and moisture together with manual Rs measurements on a larger area could improve the knowledge about spatial variability of Rs.

6 SUMMARY

6.1 SUMMARY

Micrometeorology is a part of meteorology dealing with atmospheric phenomena and processes limited to the atmospheric boundary layer, which is defined as the layer of a fluid in which heat, momentum and mass exchanges take place between the surface and the fluid. With the expansion of electronic and instrument development micrometeorological methods have become more widely used and available for ecological studies. The suspects for global changes related to climate encouraged ecologist to investigate greenhouse gasses more thoroughly. The increasing atmospheric concentration of carbon dioxide (CO₂) during the last 400 years was caused by anthropogenic emissions. Ecosystems can, over extended periods of time, have a carbon gain, i.e. they act as carbon sink, or release carbon, i.e. they act as carbon source. Monitoring of the carbon cycle and determining whether a given ecosystem is a sink or a source of carbon (sink activity) is important in terms of knowledge of the sink capacity of a single ecosystem and consequently the question of mitigating the climate change effects. This balance can be studied by applying different approaches. For direct estimate of the net ecosystem carbon exchange (NEE) between the ecosystems and the atmosphere the Eddy covariance (EC) method (Desjardins, 1974) has been commonly used. In an ecosystem decomposition and respiratory activity of the heterotrophic and autotrophic organisms could be combined under a common component of ecosystem respiration (Reco). Soil respiration (Rs) represents, especially in the winter, a major part of Reco. Rs is an important component of the carbon cycle, which is driven by photo-assimilate supply (Bahn et al., 2009) and is strongly influenced by soil temperature and humidity (Almagro et al., 2009).

Despite intensive research, carbon cycle is still underinvestigated and not fully understood for many ecosystems, especially the ones which are of minor direct importance in terms of food and wood production. In this study we used the Eddy covariance method for the karst ecosystem. Furthermore, we used portable and automatic soil respiration systems for measuring Rs and as supporting measurements the soil temperature and soil water content profiles were established. In the framework of this study we want answers to the following objectives:

Based on micro-meteorological measurements we expect an increased sink activity in the current overgrown area in comparison to the extensively used grasslands. Carbon balance should change, and ecosystem is a larger carbon sink if the succession site with woody species began as abandoned pastures and meadows.

We expect that some features of karst ecosystems, such as relief, the heterogeneity of the terrain and wind conditions could influence the use of Eddy covariance method and can significantly affect the quality of measurements. Since vegetation also influences the measurements, we anticipate that different approaches should be used for NEE measurements on the extensive pasture and on overgrown area.

The data of eddy covariance measurements has to be corrected for the heat loss of electronics used for measurement (Burba et al., 2008) when the ambient temperatures are low. We have assumed that in our case this correction would not be necessary due to the temperature range of the ecosystem.

We expect that R_s measurements, with an improved automatic system and corresponding measurements of soil temperature and moisture, could be improved by a larger number of cuvettes that would improve the information about the temporal and spatial variability of soil CO_2 flux. The automatic system for measuring soil respiration with several cuvettes and associated soil temperature and moisture measurements greatly improves the knowledge of temporal and spatial variability of R_s .

The measurements of net exchange of gases between the ecosystem and the atmosphere using EC are made above the ecosystem in the surface layer where turbulence is more or less constant. The advantage of EC is that, with appropriate position of sensors above the canopy, gas (e.g. CO_2 , O_3 , NO_x , CH_4 ...), heat and water exchange can be measured for any ecosystem, regardless of its heterogeneity. The method requires input of data on wind speeds from all three directions (x, y, z), the concentration of a gas being monitored (for example CO_2) and recording of air temperature at a frequency of at least 10 Hz. Data processing takes place under established and recognized methodologies that are proposed by many researchers (Aubinet et al., 2000; Webb et al., 1980; Foken and Wichura, 1996; Reichstein et al., 2005; Papale et al., 2006; Richardson and Hollinger, 2007; Lasslop et al., 2010) and after successful processing of data half-hourly NEE values are obtained. Before the installation of the flux tower in the field, main objectives of experiment must be carried out. If our aim is to use EC, we need to know the main feature of this method, i.e. that EC works well over homogenous and flat terrain. Using the tower fluxes from the wind direction will be recorded and therefore it is useful to know the prevailing wind direction for our site. The general rule of thumb is that the measurement height must be 100 times lower than the desired fetch of our flux tower, but the height of the tower according to another rule of thumb should ideally be twice the canopy height. Datasets of NEE with applied corrections usually contain numerous gaps due to various reasons. The dataset must therefore be gap-filled (Reichstein et al., 2005; Serrano-Ortiz et al., 2009). Furthermore, uncertainty analysis (Richardson and Hollinger, 2007; Wohlfahrt et al., 2008; Haslwanter et al., 2009) must be done to reach a valuable NEE estimation and flux partitioning must be performed (Lasslop et al., 2010; Gilmanov et al., 2010; Unger et al., 2009; Reichstein et al., 2005) to divide NEE into components of interest for the investigated ecosystem.

Further investigations show that differences between OP and CP instruments are caused by surface heating of the OP instrument due to electronics and that such heat should be accounted for in the density correction (Grelle and Burba, 2007). Burba et al. (2008) have suggested a self-heating correction technique which can be applied to previously calculated

fluxes based on data from OP. At present, the Burba correction is generally used only for cold sites but without objective criteria as to where and when must be applied. Applying Burba correction to annual net ecosystem exchange (NEE) data measured with OP systems for several ecosystems has pushed annual NEE values towards carbon loss everywhere, with greater magnitude at colder sites (Reverter et al., 2011).

There are numerous studies on NEE, gross primary production (GPP) and respiration (Reco) of different natural ecosystems based on EC but in some conditions (e.g., low canopy vegetation) also the chamber method could be used. Most commonly the chamber method is used for measuring R_s which represents the second largest carbon flux between the ecosystems and the atmosphere (Raich and Schlesinger, (1992). The measurements taken in closed dynamic chambers allow us to get the R_s value for shorter periods, e.g. hours. Some researchers have made their own automatic systems for R_s measurements, tested them and used them in their research. The chambers of all these systems have to be installed on the measuring area and should allow to be closed before the measurement and reopened after the measurement. They must be designed in a way that minimizes long-term impact on the measuring point. In addition, besides R_s measurements, it is necessary, especially in the more heterogeneous ecosystem, to perform measurements of soil moisture and soil temperature. These two parameters can in some cases explain 80% of the time variability of R_s (Tang et al., 2006).

The study was conducted at the Podgorski Kras plateau (400-430 m a.s.l.) in the sub-Mediterranean region of Slovenia (SW Slovenia). Within the study area two study sites were chosen on the basis of current and historic land use. The spatial distance of the sites is 1 km. The grassland site has been used in the last decades more or less constantly as a low intensity pasture. On the succession site small trees and shrubs cover 40% of the area. The average height of the tree layer, which is mostly represented by *Quercus pubescens*, is 7 m and the volume of woody biomass above ground is $96 \text{ m}^3 \text{ ha}^{-1}$. At both sites, in July 2008, an open-path eddy covariance system consisting of an open path infrared gas (CO_2 and H_2O) analyzer (LI-7500, Li-Cor, Lincoln, NE USA) and sonic anemometer (Succession site: CSAT3, Campbell Scientific, Logan, UT USA. Grassland: USA-1, Metek GmbH, Elmshorn, Germany) was installed at the height of 15 m height at the succession site and at the height of 2 m at the grassland site. Since EC is a well-recognized method, programs to process one-hour processing files are readily available. One of the freely available programs is EdiRe Data Software (University of Edinburgh, 1999). EdiRe program was set up with basic information about the measured ecosystem before starting. In the program it was also necessary to include all the corrections that must be applied to data. Various methods can be found for gap-filling meteorological and eddy covariance data. Most researchers have used their own procedures to gap-fill datasets, but there are some procedures that are used more often. One of these is the procedure of Falge et al. (2001), which was upgraded with covariation of fluxes with meteorological variables and with the temporal auto-correlation of the fluxes by Reichstein et al. (2005). Self-heating correction

was applied to our data sets according to method 4 in Burba et al. (2008) (B4). In addition, we investigated further into site-specific instrument self-heating correction (SISC). A more thorough investigation of OP IRGA self-heating was performed only at the succession site between 22nd of January 2011 and 3rd of April 2012. There are several techniques available to break-down NEE into GPP and Reco. Light-response curves like suggested by Lasslop et al. (2010) for daytime data including temperature sensitivity of respiration and VPD limitation of GPP were applied for our dataset.

Rs measurements were conducted periodically throughout 14 days with a portable meter LI-6400 and the chamber LI-6400-09 (Li-Cor Inc., Lincoln, NE) between July 2008 and November 2010. The measurements were carried out with the help of staff of the Department of Agronomy, Biotechnical Faculty. Portable soil respiration systems do not allow a deeper insight into temporal variability of soil respiration. For this, automated systems for measuring soil respiration are needed. At the Laboratory for Electronic Devices, which was established in 2009 at the Slovenian Forestry Institute, an automatic chamber with an improved mechanism for opening and closing was developed. An automatic soil respiration system includes automatic chamber(s) with electronics, a central data storage device and infrared gas analyzer LI-840. The developed automatic soil respiration system has chambers with closed dynamic characteristic. The system was tested at the grassland site and in the garden of the Slovenian Forestry Institute. Additionally, for modelling and gap-filling of Rs data, six soil profiles at succession site and tree soil profiles at Grassland site were prepared. The system for measurement of soil temperature and soil water content profiles was also developed at the Laboratory for electronic devices in Slovenian Forestry Institute.

Footprint analyses of EC show that mean distances from where towers are monitoring 90% of fluxes are 1530 m and 195 m for the succession site and the grassland site, respectively. During the observed period (July 1st 2008 – November 30th 2012) no major differences were measured between the grassland site and the succession site concerning air temperature and precipitation. At the succession site tree phenology observations were also performed for the years 2009-2012. At the grassland site we have measured the incoming and reflected PPFD light and calculated the difference to obtain APAR. In the observed period, the succession site was a net sink of carbon ($NEE = -800 \pm 82 \text{ gCm}^{-2}\text{period}^{-1}$) while the grassland site was a source of carbon ($NEE = 1273 \pm 147 \text{ gCm}^{-2}\text{period}^{-1}$). For both land uses Figure 12 clearly shows the differences in growing season length and net production rates. The grassland site had a maximum rate of net C uptake of $-71.2 \pm 7.7 \text{ gCm}^{-2}\text{month}^{-1}$, while the succession site had a maximum net uptake of $-138.6 \pm 5.7 \text{ gCm}^{-2}\text{month}^{-1}$ (Figure 12). On the average annual basis, the succession site was a net sink of carbon ($NEE = -184 \pm 19 \text{ gCm}^{-2}\text{y}^{-1}$) while the grassland site was a source of carbon ($NEE = 293 \pm 34 \text{ gCm}^{-2}\text{y}^{-1}$). Based on the eddy covariance measurements it can be concluded that overgrown area increased sink activity in comparison to the extensive grassland during the observed period

(July 1st 2008 – November 30th 2012). The carbon balance has changed if abandoned grassland was overgrown with tree species and it has turned into a carbon sink.

With regard to EC data quality for the observed period (July 1st 2008 – November 30th 2012), 59.7% and 33.7% of expected data have not been discarded for the succession site and for the grassland site, respectively. The energy fluxes measured at the eddy station and energy balance calculated at the weather stations using net radiation and soil heat fluxes were found to coincide well for both sites. It can be concluded that some features of karst ecosystems, such as the heterogeneity of the terrain and environmental conditions, have affected the eddy covariance measurements and the quality of measurements. At the succession site the eddy covariance measuring equipment was set up at the height of 15 m although the height of vegetation does not exceed 7 m. This was done in order to enlarge the footprint and to minimize the impact of patchy tree vegetation. At the expected footprint area no special karstic structures were found, such as cave entrances etc. At the grassland site eddy covariance measuring equipment was set up at the height of only 2 m to exclude sinkholes and a nearby small cave entrance. This has affected the measurements which gave a lot of hard flagged data due to the condensation on the OP IRGA lens. It can be concluded that different approaches, in terms of eddy covariance instrumentation height, were used in these investigated ecosystems. Research in calcareous ecosystems in comparison to research in other terrestrial ecosystems could be difficult because of possible contribution of inorganic CO₂ (Kowalski et al., 2008; Serrano-Ortiz et al., 2010). Additional measurements of CO₂ isotopic composition must be done (Plestenjak et al., 2012) or other equipment for continuous monitoring of isotopic composition (Bowling et al., 2003) instead of IRGA must be used.

After Burba correction was applied to our datasets, the cumulative NEE fluxes changed. For the observation period the succession site shifted from being a sink ($-800 \text{ gCm}^{-2}\text{period}^{-1}$) to being a weak sink ($-122 \text{ gCm}^{-2}\text{period}^{-1}$) of carbon, while the grassland site remained a source of carbon (1273 and $1980 \text{ gCm}^{-2}\text{period}^{-1}$ without and with Burba correction, respectively). After the application of SISC correction, NEE changed to $-522 \text{ gCm}^{-2}\text{period}^{-1}$ and $1574 \text{ gCm}^{-2}\text{period}^{-1}$ for the succession site and for the grassland site, respectively. It can be concluded that the application of B4 method (Burba et al., 2008) to correct fluxes due to self-heating effect is not appropriate for our investigated ecosystem, because it produces unreasonable results (Figure 23). Our measurements have shown the need for self-heating correction for our ecosystems and it is therefore more appropriate to use site-specific self-heating correction that is based and developed on the measurements suggested by Burba et al. (2008).

The Rs measurements with the automatic system during the observed period between 1st September 2012 and 30th of November 2012 have suggested a mean value of Rs for the observation period of $22.867 \text{ gCm}^{-2}\text{period}^{-1}$. Maximum standard deviation was $0.204 \text{ gCm}^{-2}\text{period}^{-1}$ (CV: 0.9%) and minimum standard deviation was $0.025 \text{ gCm}^{-2}\text{period}^{-1}$ (CV:

0.1%) for 2 and for 14 measuring points, respectively. Unfortunately, manual periodic measurements were not performed at the same time as measurements with the automatic system, but we can use the data from the same periods of years 2008, 2009, 2010. The values of manual periodic measurements cannot be reported in g of carbon per period, because the measurements were performed manually between 9.00 and 11.00 hours on 21 selected measuring points marked with collars (332 measurements). We have found large variations in manual measurements with mean at $2.6 \mu\text{molCm}^{-2}\text{s}^{-1}$ and standard deviation at $1.8 \mu\text{molCm}^{-2}\text{s}^{-1}$ (CV: 69%), but also the variation of automatic measurements for observation period (between 9:00 and 11:00) was quite large with mean $1.8 \mu\text{molCm}^{-2}\text{s}^{-1}$ and standard deviation at $0.8 \mu\text{molCm}^{-2}\text{s}^{-1}$ (CV: 44%). The values for CV around 40% are commonly observed (Kutsch et al., 2010). It can be concluded that knowledge of temporal variability can be greatly improved with the use of an automatic system. The corresponding measurements of soil temperature and moisture together with manual R_s measurements on the larger area could improve the knowledge about spatial variability of R_s .

6.2 POVZETEK

V zadnjem obdobju se zaradi povečevanja atmosferske koncentracije ogljikovega dioksida (CO_2) intenzivno proučuje dinamika kroženja ogljika za različne terestične ekosisteme. Ekosistemi so lahko glede na njihove lastnosti in stanje v katerem se nahajajo potencialni vir oz. ponor toplogrednih plinov v biosferi, med katere štejemo tudi CO_2 . Pri raziskavah kroženja ogljika v kopenskih ekosistemih se v ta namen poslužujemo različnih pristopov. Za direktno oceno neto izmenjave ogljika (NEE) med ekosistemom in atmosfero se najpogosteje uporablja metoda Eddy covariance, ki so jo uspešno uporabili v najrazličnejših vrstah ekosistemov. Prva uporaba omenjene metode sega v 70-a leta prejšnjega stoletja (Desjardins, 1974; Baldocchi et al., 1988). Število raziskav z uporabo te metode se je vsako leto povečevalo.

Spremljanje ogljikovega cikla in ugotavljanje ponora oziroma vira za nek ekosistem je pomembno predvsem z vidika poznavanja ponorne sposobnosti posameznega ekosistema in posledično z vprašanjem blaženja podnebnih sprememb. Z metodo Eddy covariance dobimo vpogled v izmenjavo ogljika za celoten ekosistem (NEE), ne pa tudi v posamezne segmente ogljikovega cikla. Ob predpostavki, da iz ekosistema ni drugih odtokov ogljika ali posebnih posegov v smislu odvzema biomase ali drugih večjih motenj, lahko privzamemo, da je NEE enak neto primarni produkciji ekosistema (NEP). Skoraj edini primarni producenti so avtotrofne rastline (GPP) in tako predstavljajo veliko večino produkcije biomase v ekosistemu. V ekosistemu tečejo tudi procesi razgradnje in v njem se gibljejo tudi heterotrofni organizmi, ki dihaajo; vse to lahko združimo pod skupno komponento dihanje ekosistema (Reco). NEP je torej razlika med GPP in Reco. V komponenti dihanja celotnega ekosistema (Reco), še posebno v zimskem času, večji del predstavlja dihanje tal (R_s). V tleh se nahajajo korenine avtotrofnih organizmov, mikroorganizmi, vretenčarji, nevretenčarji in glive. Dihanje tal je torej pomembna komponenta ogljikovega cikla.

Kljub intenzivnosti raziskav so nekateri tipi ekosistemov glede izmenjave ogljika slabo raziskani. Tu gre običajno za nizkoproduktivne ekosisteme, ki z gospodarskega vidika niso zanimivi ali pa so to ekosistemi z veliko heterogenostjo, kar močno oteži raziskavo. Kraški ekosistemi zaradi obeh razlogov sodijo med manj raziskane ekosisteme. Če začnemo pri heterogenosti terena, relief z vrtačami lahko oteži mikrometeorološke meritve. Prav tako se velika heterogenost pojavlja v tleh, ki so v kraškem ekosistemu lahko globoka od nekaj centimetrov do nekaj metrov v talnih žepih, kar močno omejuje uporabo nekaterih konvencionalnih metod pri meritvah. Nekater študije, s področja kroženja ogljika izvedene na kraških ekosistemih, opozarjajo na pomemben prispevek geogenega toka CO_2 iz tal (Emmerich, 2003; Kowalski et al., 2008; Inglis et al., 2009; Serrano-Ortiz et al., 2009; Serrano-Ortiz et al., 2010), kar vodi do še kompleksnejše in zahtevnejše raziskave.

Meritve neto izmenjave plinov med ekosistemom in atmosfero z metodo Eddy covariance potekajo nad ekosistemom, v plasti kjer zračni tokovi niso več pod vplivom vegetacije.

Dobra lastnost metode je, da lahko ob primerni višini stolpa izmerimo izmenjavo plina (npr. CO₂, O₃, NO_x, CH₄...) za kateri koli ekosistem ne glede na heterogenost. Metoda potrebuje vhodne podatke o hitrostih vetra v vseh treh smereh (x, y, z) in podatke o koncentraciji spremljanega plina, npr. CO₂, ter temperaturi posnete s frekvenco vsaj 10 Hz. Obdelava surovih podatkov poteka po ustaljenih in priznanih metodologijah, ki so jih predlagali številni raziskovalci (Aubinet et al., 2000; Webb et al., 1980; Foken and Wichura, 1996; Reichstein et al., 2005; Papale et al., 2006; Richardson and Hollinger, 2007; Lasslop et al., 2010) in po uspešni obdelavi teh surovih podatkov dobimo polurne vrednosti NEE.

Gilmanov et al. (2010) poročajo o ponornih aktivnostih, izmerjenih z metodo Eddy covariance, na ekstenzivnih in intenzivnih traviščih. V analizo so vzeli 316 ploskev iz celega sveta in v 80% so na vseh ploskvah izmerili ponor ogljika. Ekstenzivna travišča so v povprečju vezala 0.7 MgCha⁻¹leto⁻¹, intenzivna pa 1.8 MgCha⁻¹leto⁻¹. Za primerjavo naj navedemo ponorno sposobnost 80 let starega bukovega sestoja na Danskem, izmerjeno z isto metodo, ki znaša v povprečju 1.79 MgCha⁻¹leto⁻¹ (Pilegaard et al., 2001). Teklemariam et al. (2009) navajajo za 100 let star mešani gozd bora, javorja in trepetlike podobno ponorno sposobnost in sicer 1.4 MgCha⁻¹leto⁻¹. Meritve z metodo Eddy covariance na zaraščajočih se površinah kažejo na to, da so ti ekosistemi lahko močnejši ponor ogljika od zgoraj naštetih. Tako so Vaccari et al. (2012) na otoku Pianosa na opuščeni, zaraščajoči kmetijskih površinah izmerili ponor ogljika in sicer 2.6 MgCha⁻¹leto⁻¹. Pri teh navedbah gre seveda za NEE in torej ne vemo ničesar o razdelitvi tokov ogljika na posamezne komponente ogljikovega cikla. Kot smo že omenili je osnovna delitev NEE na GPP in Reco, pri čemer velik del Reco predstavlja Rs.

Osnovni problem meritev v naravnih ekosistemih je heterogenost in ta je lahko še posebej izražena prav v tleh, kjer se dogajajo tudi procesi dihanja tal. Za boljše izmero določenega talnega parametra nam tako ne zadostuje več meritev v eni točki, ampak je potrebno meritve vzporedno izvajati na več točkah, torej prostorsko. Take zahteve podražijo samo izvedbo meritev, omogočijo pa nam boljši vpogled v časovno in prostorsko dinamiko spremljanih parametrov. Tako izvedene meritve prinašajo številne prednosti, predvsem to, da lahko dobimo vrednosti Rs za krajša časovna obdobja, npr. ure. Za lastne potrebe so nekateri raziskovalci sami izdelali avtomatske sisteme za meritve Rs, jih testirali in nato uporabili v svojih raziskavah. Najpomembnejši del takih sistemov so avtomatske komore, ki so postavljene na merilno mesto in morajo omogočati zapiranje pred meritvijo in ponovno odpiranje po meritvi. Izvedene morajo biti tako, da dolgoročno čim manj vplivajo na merilno mesto. Večina raziskovalcev uporablja sistem, kjer se odpira le pokrov komore, njen obod pa ostane na merilnem mestu (npr.: McGinn et al., 1998; Edwards and Riggs, 2003; Delle Vedove et al., 2007). Kljub široki uporabi komor za meritve Rs, ni izdelanega standarda o dimenzijah in tipu komor za izvedbo teh meritev. Pumpanen et al. (2004) so tako preizkusili 20 različnih izvedb komor za meritve Rs in jih primerjali s kalibracijskimi vrednostmi znanega toka CO₂ od 0.32 do 10.01 μmolCO₂m⁻²s⁻¹. Ugotovili so, da v

povprečju vse komore dosegajo dobre rezultate in od kalibracijskih vrednosti ne odstopajo za več kot 4%. Poleg meritev R_s je potrebno, še posebej v bolj heterogenih ekosistemih, izvajati meritve talne vlage in temperature. Ta dva parametra lahko v nekaterih primerih pojasnita tudi 80% časovne variabilnosti R_{soil} (Tang et al., 2006). Za izvedbo meritev talne vlage imamo na voljo različne izvedbe senzorjev, za meritve talne temperature pa se najpogosteje uporabljajo termočleni. Meritvam talnih procesov je potrebno dati še poseben poudarek na kraških ekosistemih, kjer lahko k toku ogljika iz kraškega ekosistema v atmosfero pomembno prispeva tudi geogeni CO_2 .

V okviru doktorske disertacije smo poskušali ogovoriti na naslednje hipoteze:

Na podlagi izvedenih mikrometeoroloških meritev pričakujemo povečanje ponora za obravnavano zaraščajočo se površino v primerjavi z ekstenzivnim pašnikom. Bilanca ogljika se torej spremeni, če se pašniki opuščajo in se travišča zaraščajo z lesnatimi vrstami.

Predvidevamo, da so nekatere lastnosti kraških ekosistemov, kot so relief, heterogenost terena, veterne razmere odločilne za uspešno uporabo metode Eddy covariance in lahko pomembno vplivajo na kvaliteto meritev. Ker na uspešnost meritev odločilno vpliva tudi vegetacija, predvidevamo, da bo potrebno pri meritvah na ekstenzivno rabljenem pašniku in na zaraščajoči površini uporabiti drugačne pristope.

Pri obdelavi podatkov Eddy covariance meritev se uporablja korekcija meritev NEE, ki upošteva toplotne izgube merilne elektronike (Burba et al., 2008). Predvidevamo, da v našem primeru zaradi temperaturnega režima ekosistema korekcija ni potrebna.

Predvidevamo, da meritve R_s lahko izboljšamo z avtomatskim sistemom za meritve dihanja tal in pripadajočimi meritvami temperature tal (T_s) in vsebnosti vode v tleh (SWC), ter večjim številom merilnih mest. Avtomatski sistem za meritve R_s z večjim številom merilnih komor, lahko znatno prispeva k poznavanju časovne in prostorske variabilnosti R_s .

Na področju Podgorskega krasa smo vzpostavili mikrometeorološke meritve po metodi Eddy covariance, na opuščeni, zaraščajoči se površini in na ekstenzivnem pašniku. Meteorološke parametre smo prenašali v zbirni center preko brezžične povezave, podatke za obdelavo po metodi Eddy covariance pa smo enkrat na dva tedna pretočili na prenosni računalnik. Sam preračun polurnih vrednosti NEE poteka v več korakih. Prvi korak je priprava podatkov, kjer binarne podatke ustrezno transformiramo v datoteke, ki vsebujejo enourne nize vhodnih podatkov. Ker je metoda Eddy covariance priznana metoda, so na voljo programi za obdelavo enournih datotek. Eden izmed prosto dostopnih programov je EdiRe Data software (University of Edinburgh, 1999), razvit na univerzi v Edinburghu. Program EdiRe je bilo potrebno pred pričetkom obdelav primerno nastaviti in podati osnovne podatke o merjenem ekosistemu. Prav tako je bilo potrebno v obdelavo vključiti

vse korekcije, ki jih metoda zahteva (Aubinet et al., 2000; Webb et al., 1980; Foken and Wichura, 1996). Po uspešni obdelavi dobimo polurne vrednosti NEE in podatke o energijski bilanci. Te podatke je bilo potrebno nato s primernim statističnim orodjem združiti z meteorološkimi podatki. Zaradi neprimernih vremenski okoliščin, kot so padavine ali kondenzat na merilnih inštrumentih, ali zaradi izpada električnega napajanja, pa so se v NEE podatkih pojavile večje ali manjše vrzeli, izpadi podatkov. Naloga drugega koraka v obdelavi je bila, zapolniti manjkajoče vrednosti (ang. Gap-filling). Za dopolnjevanje NEE je bilo opisanih kar nekaj postopkov in z nekaj dopolnili smo se pri dopolnjevanju naših podatkov posluževali predloge iz prispevka Reichstein et al. (2005). Tretji korak pri obdelavi je analiza negotovosti (Papale et al., 2006; Richardson and Hollinger, 2007), četrti pa razdelitev polurnih tokov NEE na GPP in Reco (Lasslop et al., 2010). Izmerjene podatke smo torej obdelali po ustaljenih metodologijah. Za obe ploskvi (zaraščajočo površino in ekstenzivni pašnik) smo pripravili analizo kvalitete podatkov in analize med seboj primerjali. Poleg uveljavljenih korekcij so Burba et al. (2008) objavili prispevek, v katerem predlagajo korekcijo izmerjenih tokov zaradi segrevanja merilnega inštrumenta. Le-to naj bi bila posledica toplotnih izgub merilne elektronike, natančneje odprtega infrardečega plinskega analizatorja LI-7500. Ker smo tudi v naši raziskavi na Podgorskem krasu uporabljali omenjeni merilni inštrument, smo predlagano korekcijo uporabili. Ker je korekcija predlagana predvsem za hladnejše ekosisteme predvidevamo, da v naših razmerah ni smiselna, saj so se temperature na proučevanem območju gibale od -10 do 35°C. Podrobneje smo preučili vpliv segrevanja merilnega inštrumenta LI-7500. Kot predlaga Burba et al. (2008) v opisu metode 4 (B4) smo merili temperaturo zraka v neposredni bližini inštrumenta in temperaturo inštrumenta.

Poleg meritev tokov NEE, so v okviru raziskav na Podgorskem krasu potekale meritve R_s in sicer periodično na 14 dni s prenosnim merilnikom LI-6400 in ustrezno komoro. Meritve so izvajali sodelavci oddelka za agronomijo Biotehniške Fakultete. Ob meritvah smo kontinuirano merili tudi temperaturo in vlago tal. Na osnovi izmerjene vrednosti R_s in pripadajoče T_s in SWC smo osnovali model, s katerim smo napovedali polurne vrednosti R_s . Za bolj kvalitetno oceno R_s , smo potrebovali enega od obstoječih avtomatskih sistemov za meritve dihanja tal. Slaba lastnost obstoječih sistemov je vpliv mehanskih delov avtomatskih komor na merilno mesto. Ovratniki, ki so vstavljeni okoli merilnega mesta in pomagajo pri stabilnosti komore, lahko vplivajo na sprememo T_s in SWC merilnega mesta. V Laboratorju za elektronske naprave Gozdarskega inštituta Slovenije, smo razvili sistem avtomatskih komor z izboljšanim mehanizmom odpiranja in zapiranja. Sistem vsebuje tako krmilno elektroniko in hranilnik podatkov, kot tudi merilec koncentracije CO_2 LI-840 proizvajalca Li-Cor.

Prav tako smo v Laboratorju za elektronske naprave Gozdarskega inštituta Slovenije razvili sistem za meritve in shranjevanje podatkov o talnih temperaturnih profilih in o talni vlagi. Osnovni gradnik hranilnika je mikrokontroler z nekaj periferije, ki upravlja senzorje in skrbi za minimalno porabo električne energije. V mirovanju tako celoten sistem porabi pod

15 uA toka pri napetosti od 4.5-6 V, kar ustreza samopraznjenju baterijskega vložka. Hranilnik je namenjen snemanju dveh senzorjev za talno vlago, ki imata izhod od 0 do 2500 mV in sedmih temperaturnih senzorjev. V našem primeru smo uporabili senzorje talne vlage EC-05 proizvajalca Decagon Devices. Za meritve temperature smo uporabili temperaturne senzorje proizvajalca Dalass. Temperaturni senzorji uporabljajo 1-žični protokol komunikacije in so tovarniško kalibrirani. Omenjeni protokol omogoča priključitev več senzorjev na isti tripolni vodnik; vsak senzor ima namreč svoj naslov in hranilnik ob meritvah od vsakega posebej zahteva podatek o izmerjeni temperaturi, s čimer se zmanjša število vodnikov. S to izboljšavo se močno zmanjša možnost poškodb posameznega vodnika in s tem izguba podatkov. Senzorje smo namestili, na za to posebej izdelano tiskano vezje dolžine 60 cm, po WMO standardih (-50 cm, -30 cm, -20 cm, -10 cm, - 5 cm, -2 cm in 5 cm), vezje povezali s hranilnikom in ga vstavili v plastično cev premera 13 mm in dolžine 65 cm. Tako izdelana palica za meritve talnega temperaturnega profila olajša montažo na terenu in zmanjša možnosti poškodb temperaturnih senzorjev.

Analize dosega meritev (ang. footprint analyzes) po metodi Eddy covariance kažejo, da tokovi CO₂ v 90% prihajajo v povprečju iz razdalje 1530 m za ploskev zaraščanje in 195 m za ploskev pašnik od merilnega mesta. V opazovanem obdobju (1.7.2008 - 30.11.2012) ni bilo večjih razlik med ploskvama glede temperature zraka in padavin. Na zaraščajoči površini je bila v obdobju 2009-2012 spremljana tudi fenologija drevesnih vrst, na pašniku pa je bila fenološka aktivnost spremljana s pomočjo meritve APAR. V opazovanem obdobju je bila zaraščajoča površina neto ponor ogljika ($NEE = -800 \pm 82 \text{ gCm}^{-2}\text{obdobje}^{-1}$), medtem ko je bila ploskev pašnik vir ogljika ($NEE = 1273 \pm 147 \text{ gCm}^{-2}\text{obdobje}^{-1}$). Za obe rabi zemljišč slika 12 jasno kaže razlike v dolžini rastne sezone in NEE. Ploskev pašnik je imela največjo ponorno moč $-71.2 \pm 7.7 \text{ gCm}^{-2}\text{mesec}^{-1}$, medtem ko je bila na ploskvi zaraščanje le ta $-138.6 \pm 5.7 \text{ gCm}^{-2}\text{mesec}^{-1}$ (slika 12). Ploskev zaraščanje deluje kot ponor ogljika ($NEE = -184 \pm 19 \text{ gCm}^{-2}\text{leto}^{-1}$), medtem ko ploskev pašnik deluje kot njegov vir ($NEE = 293 \pm 34 \text{ gCm}^{-2}\text{leto}^{-1}$). Na osnovi meritev z metodo Eddy covariance lahko zaključimo, da zaraščanje opuščanih ekstenzivnih kraških pašnikov spremeni ponorno aktivnost za ogljik iz vira v njegov ponor. Kvaliteta podatkov izmerjenih po metodi Eddy covariance kaže na to, da je bilo v preučevanem obdobju od 1.7.2008 do 30.11.2012 izločenih 40.3% podatkov na ploskvi zaraščanje in 66.3% podatkov na ploskvi pašnik. Meritve kažejo na dobro ujemanje med energijskimi tokovi izmerjenimi po metodi Eddy covariance in energijskimi tokovi izmerjenimi na meteorološki postaji. Lahko zaključimo, da nekatere posebnosti kraških ekosistemov, kot sta heterogenost terena in vremenske razmere, vplivajo na kvaliteto izmerjenih podatkov po metodi Eddy covariance. Na ploskvi zaraščanje smo merilno opremo za izvedbo omenjene metode, kljub višini vegetacije samo 7 m, postavili na višino 15 m. To je bilo storjeno, da smo povečali doseg merilnega mesta in s tem zmanjšali vpliv gozdne vegetacije, ki se pojavlja v manjših zaplatah. V pričakovanem dosegu merilnega mesta ni bilo najdenih posebnih kraških struktur, kot npr. jame itd. Na ploskvi pašnik je bila merilna oprema za spremljanje tokov

CO₂ po metodi Eddy covariance nameščena na višino samo 2 m in sicer zato, da bi iz pričakovanega dosega merilnega mesta izločili bližnje vrtače in vhod v manjšo jamo. Kar nekaj podatkov je bilo zaradi nizko nameščene merilne opreme izločenih, saj je obstajal sum o kondenzatu na optiki odprtega infrardečega analizatorja. Lahko zaključimo, da je potreben drugačen pristop pri izvedbi eddy covariance meritev, na ploskvi pašnik v primerjavi s ploskvijo zaraščanje. Raziskovanje kroženja ogljika v ekosistemi s karbonatno matično podlago je med drugim lahko oteženo tudi zaradi prispevka geogenega CO₂ (Kowalski et al., 2008; Serrano-Ortiz et al., 2010), ki zahteva dodatne meritve, kot na primer izotopsko sestavo CO₂ (Plestenjak et al., 2012). Možna je tudi uporaba druge merilne opreme za neprekinjeno spremljanje izotopske sestave CO₂ (Bowling et al., 2003) namesto uporabljenega infrardečega analizatorja. Po aplikaciji B4 korekcije zaradi samogretja merilnega inštrumenta LI-7500 so se vrednosti NEE za preučevana ekosistema spremenile. Ploskev zaraščanje je postala šibak ponor ogljika ($-122 \text{ gCm}^{-2}\text{obdobje}^{-1}$), ponorna aktivnost na ploskvi pašnik pa je ostala pozitivna ($1980 \text{ gCm}^{-2}\text{obdobje}^{-1}$). Po aplikaciji SISC korekcije je ploskev zaraščanje ostala ponor ogljika ($-522 \text{ gCm}^{-2}\text{obdobje}^{-1}$), ponorna aktivnost na ploskvi pašnik pa je prav tako ostala pozitivna ($1574 \text{ gCm}^{-2}\text{obdobje}^{-1}$). Na podlagi meritev in izračunov lahko zaključimo, da aplikacija B4 v naših ekosistemi ni upravičena, saj daje nerazumne rezultate tudi pri detajlnem pregledu polurnih vrednosti NEE (sliki 22 in 23). Naše meritve kažejo na to, da je potrebno za vsak preučevan ekosistem razviti svojo korekcijo zaradi samogretja merilnega inštrumenta, leta pa je lahko izvedena po metodi predlagani v prispevku Burba et al. (2008).

Rezultat meritev dihanja tal v preučevanem obdobju od 1.9.2012 do 30.11.2012 z avtomatskim merilnim sistemom je srednja vrednost Rs pri $22.867 \text{ gCm}^{-2}\text{obdobje}^{-1}$ z največjim $0.204 \text{ gCm}^{-2}\text{obdobje}^{-1}$ (CV: 0.9%) in najmanjšim $0.025 \text{ gCm}^{-2}\text{obdobje}^{-1}$ (CV: 0.1%) standardnim odklonom za 2 oziroma 14 merilnih mest. Na žalost ročne meritve Rs niso bile izvajane skozi celotno preučevano obdobje, lahko pa za primerjavo obdobji uporabimo meritve iz let 2008, 2009 in 2010. Vrednosti pridobljene iz avtomatskega sistema ne moremo direktno primerjati z vrednostmi iz ročnega sistema, saj so bile slednje merjene le med 9:00 in 11:00 uro. Rezultat povprečnega toka CO₂ iz ročnih meritev za omenjeno preučevano obdobje znaša $2.6 \mu\text{molCm}^{-2}\text{s}^{-1}$ s standardnim odklonom $1.8 \mu\text{molCm}^{-2}\text{s}^{-1}$ (CV: 69%). Za enako časovno okno smo z avtomatskim merilnim sistemom izmerili povprečno vrednost $1.8 \mu\text{molCm}^{-2}\text{s}^{-1}$ s standardnim odklonom $0.8 \mu\text{molCm}^{-2}\text{s}^{-1}$ (CV: 44%). O vrednostih CV okoli 40% poročajo že Kutsch et al. (2010). Vrednosti pridobljene iz avtomatskega sistema seveda ne moremo direktno primerjati z vrednostmi iz ročnega sistema (322 meritev), saj so bile slednje merjene le med 9:00 in 11:00 uro. Na podlagi naših meritev lahko zaključimo, da z uporabo avtomatskega sistema za meritve dihanja tal dobimo boljši vpogled v časovno dinamiko Rs. Pripadajoče meritve Ts in SWC skupaj z ročnimi meritvami dihanja tal na večjih površinah, pa nam dajo boljši vpogled v prostorsko variabilnost Rs.

7 REFERENCES

- Alberti G., Delle Vedove G., Zuliani M., Peressotti A., Castaldi S., Zerbi G. 2010. Changes in CO₂ emissions after crop conversion from continuous maize to alfalfa. *Agriculture Ecosystems & Environment*, 136, 1-2: 139-147
- Alberti G., Peressotti A., Piuissi P., Zerbi G. 2008. Forest ecosystem carbon accumulation during a secondary succession in the Eastern Prealps of Italy. *Forestry*, 81, 1: 1-11
- Almagro M., Lopez J., Querejeta J. I., Martinez-Mena M. 2009. Temperature dependence of soil CO₂ efflux is strongly modulated by seasonal patterns of moisture availability in a Mediterranean ecosystem. *Soil Biology & Biochemistry*, 41, 3: 594-605
- Arya S. P. 1988. *Introduction to Micrometeorology*. San Diego, California, Academic Press: 307 p.
- Atkin O. K., Edwards E. J., Loveys B. R. 2000. Response of root respiration to changes in temperature and its relevance to global warming. *New Phytologist*, 147, 1: 141-154
- Aubinet M., Grelle A., Ibrom A., Rannik U., Moncrieff J., Foken T., Kowalski A. S., Martin P. H., Berbigier P., Bernhofer C., Clement R., Elbers J., Granier A., Grunwald T., Morgenstern K., Pilegaard K., Rebmann C., Snijders W., Valentini R., Vesala T. 2000. Estimates of the annual net carbon and water exchange of forests: The EUROFLUX methodology. *Advances in Ecological Research*, 30, 30: 113-175
- Bahn M., Rodeghiero M., Anderson-Dunn M., Dore S., Gimeno C., Drosler M., Williams M., Ammann C., Berninger F., Flechard C., Jones S., Balzarolo M., Kumar S., Newesely C., Priwitzer T., Raschi A., Siegwolf R., Susiluoto S., Tenhunen J., Wohlfahrt G., Cernusca A. 2008. Soil Respiration in European Grasslands in Relation to Climate and Assimilate Supply. *Ecosystems*, 11, 8: 1352-1367
- Bahn M., Schmitt M., Siegwolf R., Richter A., Bruggemann N. 2009. Does photosynthesis affect grassland soil-respired CO₂ and its carbon isotope composition on a diurnal timescale? *New Phytologist*, 182, 2: 451-460
- Baldocchi D. D. 2003. Assessing the eddy covariance technique for evaluating carbon dioxide exchange rates of ecosystems: past, present and future. *Global Change Biology*, 9, 4: 479-492

- Baldocchi D. D., Hicks B. B., Meyers T. P. 1988. Measuring biosphere-atmosphere exchanges of biologically related gases with micrometeorological methods. *Ecology*, 69, 5: 1331-1340
- Barford C. C., Wofsy S. C., Goulden M. L., Munger J. W., Pyle E. H., Urbanski S. P., Huttyra L., Saleska S. R., Fitzjarrald D., Moore K. 2001. Factors controlling long- and short-term sequestration of atmospheric CO₂ in a mid-latitude forest. *Science*, 294, 5547: 1688-1691
- Barr A. G., Morgenstern K., Black T. A., McCaughey J. H., Nesic Z. 2006. Surface energy balance closure by the eddy-covariance method above three boreal forest stands and implications for the measurement of the CO₂ flux. *Agricultural and Forest Meteorology*, 140, 1-4: 322-337
- Beziat P., Ceschia E., Dedieu G. 2009. Carbon balance of a three crop succession over two cropland sites in South West France. *Agricultural and Forest Meteorology*, 149, 10: 1628-1645
- Bowling D. R., Sargent S. D., Tanner B. D., Ehleringer J. R. 2003. Tunable diode laser absorption spectroscopy for stable isotope studies of ecosystem-atmosphere CO₂ exchange. *Agricultural and Forest Meteorology*, 118, 1-2: 1-19
- Burba G., Schmidt A., Scott R. L., Nakai T., Kathilankal J., Fratini G., Hanson C., Law B., McDermitt D. K., Eckles R., Furtaw M., Velgersdyk M. 2012. Calculating CO₂ and H₂O eddy covariance fluxes from an enclosed gas analyzer using an instantaneous mixing ratio. *Global Change Biology*, 18, 1: 385-399
- Burba G. G., Anderson D. 2010. A Brief Practical Guide to Eddy Covariance Flux Measurements: Principles and Workflow Examples for Scientific and Industrial Applications. LI-COR Biosciences: 212 p.
- Burba G. G., McDermitt D. K., Grelle A., Anderson D. J., Xu L. K. 2008. Addressing the influence of instrument surface heat exchange on the measurements of CO(2) flux from open-path gas analyzers. *Global Change Biology*, 14, 8: 1854-1876
- Campbell J. E., Lobell D. B., Genova R. C., Field C. B. 2008. The global potential of bioenergy on abandoned agriculture lands. *Environmental Science & Technology*, 42, 15: 5791-5794

- Ciais P., Reichstein M., Viovy N., Granier A., Ogee J., Allard V., Aubinet M., Buchmann N., Bernhofer C., Carrara A., Chevallier F., De Noblet N., Friend A. D., Friedlingstein P., Grunwald T., Heinesch B., Keronen P., Knohl A., Krinner G., Loustau D., Manca G., Matteucci G., Miglietta F., Ourcival J. M., Papale D., Pilegaard K., Rambal S., Seufert G., Soussana J. F., Sanz M. J., Schulze E. D., Vesala T., Valentini R. 2005. Europe-wide reduction in primary productivity caused by the heat and drought in 2003. *Nature*, 437, 7058: 529-533
- Clement R. J., Burba G. G., Grelle A., Anderson D. J., Moncrieff J. B. 2009. Improved trace gas flux estimation through IRGA sampling optimization. *Agricultural and Forest Meteorology*, 149, 3-4: 623-638
- Delle Vedove G., Alberti G., Zuliani M., Peressotti A. 2007. Automated Monitoring of Soil Respiration: an Improved Automatic Chamber System. *Italian Journal of Agronomy*, 4: 377-382
- Desjardins R. L. 1974. Technique to measure CO_2 exchange under field conditions. *International Journal of Biometeorology*, 18, 1: 76-83
- Edwards N. T., Riggs J. S. 2003. Automated monitoring of soil respiration: A moving chamber design. *Soil Science Society of America Journal*, 67, 4: 1266-1271
- Emmerich W. E. 2003. Carbon dioxide fluxes in a semiarid environment with high carbonate soils. *Agricultural and Forest Meteorology*, 116, 1-2: 91-102
- Falcucci A., Maiorano L., Boitani L. 2007. Changes in land-use/land-cover patterns in Italy and their implications for biodiversity conservation. *Landscape Ecology*, 22, 4: 617-631
- Falge E., Baldocchi D., Olson R., Anthoni P., Aubinet M., Bernhofer C., Burba G., Ceulemans R., Clement R., Dolman H., Granier A., Gross P., Grünwald T., Hollinger D., Jensen N.-O., Katul G., Keronen P., Kowalski A., Lai C. T., Law B. E., Meyers T., Moncrieff J., Moors E., Munger J. W., Pilegaard K., Rannik Ü., Rebmann C., Suyker A., Tenhunen J., Tu K., Verma S., Vesala T., Wilson K., Wofsy S. 2001. Gap filling strategies for defensible annual sums of net ecosystem exchange. *Agricultural and Forest Meteorology*, 107, 1: 43-69
- Flanagan L. B., Wever L. A., Carlson P. J. 2002. Seasonal and interannual variation in carbon dioxide exchange and carbon balance in a northern temperate grassland. *Global Change Biology*, 8, 7: 599-615

- Foken T., Wichura B. 1996. Tools for quality assessment of surface-based flux measurements. *Agricultural and Forest Meteorology*, 78, 1-2: 83-105
- Ford D., Williams P. 1989. *Karst Geomorphology and Hydrology*. London., Unwin Hyman: 601 p.
- Frank A. B., Karn J. E. 2005. Shrub effects on carbon dioxide and water vapor fluxes over grasslands. *Rangeland Ecology & Management*, 58, 1: 20-26
- Gilmanov T. G., Aires L., Barcza Z., Baron V. S., Belelli L., Beringer J., Billesbach D., Bonal D., Bradford J., Ceschia E., Cook D., Corradi C., Frank A., Gianelle D., Gimeno C., Gruenwald T., Guo H. Q., Hanan N., Haszpra L., Heilman J., Jacobs A., Jones M. B., Johnson D. A., Kiely G., Li S. G., Magliulo V., Moors E., Nagy Z., Nasyrov M., Owensby C., Pinter K., Pio C., Reichstein M., Sanz M. J., Scott R., Soussana J. F., Stoy P. C., Svejcar T., Tuba Z., Zhou G. S. 2010. Productivity, Respiration, and Light-Response Parameters of World Grassland and Agroecosystems Derived From Flux-Tower Measurements. *Rangeland Ecology & Management*, 63, 1: 16-39
- Gilmanov T. G., Soussana J. E., Aires L., Allard V., Ammann C., Balzarolo M., Barcza Z., Bernhofer C., Campbell C. L., Cernusca A., Cescatti A., Clifton-Brown J., Dirks B. O. M., Dore S., Eugster W., Fuhrer J., Gimeno C., Gruenwald T., Haszpra L., Hensen A., Ibrom A., Jacobs A. F. G., Jones M. B., Lanigan G., Laurila T., Lohila A., Manca G., Marcolla B., Nagy Z., Pilegaard K., Pinter K., Pio C., Raschi A., Rogiers N., Sanz M. J., Stefani P., Sutton M., Tuba Z., Valentini R., Williams M. L., Wohlfahrt G. 2007. Partitioning European grassland net ecosystem CO₂ exchange into gross primary productivity and ecosystem respiration using light response function analysis. *Agriculture Ecosystems & Environment*, 121, 1-2: 93-120
- Goldewijk K. K. 2001. Estimating global land use change over the past 300 years: The HYDE Database. *Global Biogeochemical Cycles*, 15, 2: 417-433
- Grayston S. J., Vaughan D., Jones D. 1997. Rhizosphere carbon flow in trees, in comparison with annual plants: The importance of root exudation and its impact on microbial activity and nutrient availability. *Applied Soil Ecology*, 5, 1: 29-56
- Grelle A., Burba G. 2007. Fine-wire thermometer to correct CO₂ fluxes by open-path analyzers for artificial density fluctuations. *Agricultural and Forest Meteorology*, 147, 1-2: 48-57

- Haslwanter A., Hammerle A., Wohlfahrt G. 2009. Open-path vs. closed-path eddy covariance measurements of the net ecosystem carbon dioxide and water vapour exchange: A long-term perspective. *Agricultural and Forest Meteorology*, 149, 2: 291-302
- Hirata R., Hirano T., Saigusa N., Fujinuma Y., Inukai K., Kitamori Y., Takahashi Y., Yamamoto S. 2007. Seasonal and interannual variations in carbon dioxide exchange of a temperate larch forest. *Agricultural and Forest Meteorology*, 147, 3-4: 110-124
- Houghton R. A. 1999. The annual net flux of carbon to the atmosphere from changes in land use 1850-1990. *Tellus Series B-Chemical and Physical Meteorology*, 51, 2: 298-313
- Hurt G. C., Frolking S., Fearon M. G., Moore B., Shevliakova E., Malyshev S., Pacala S. W., Houghton R. A. 2006. The underpinnings of land-use history: three centuries of global gridded land-use transitions, wood-harvest activity, and resulting secondary lands. *Global Change Biology*, 12, 7: 1208-1229
- Huxman T. E., Snyder K. A., Tissue D., Leffler A. J., Ogle K., Pockman W. T., Sandquist D. R., Potts D. L., Schwinning S. 2004. Precipitation pulses and carbon fluxes in semiarid and arid ecosystems. *Oecologia*, 141, 2: 254-268
- Inglisma I., Alberti G., Bertolini T., Vaccari F. P., Gioli B., Miglietta F., Cotrufo M. F., Peressotti A. 2009. Precipitation pulses enhance respiration of Mediterranean ecosystems: the balance between organic and inorganic components of increased soil CO₂ efflux. *Global Change Biology*, 15, 5: 1289-1301
- Climate change 2001: the scientific basis: contribution of Working Group I to the Third Assessment report of the Intergovernmental Panel on Climate Change. 2001. Houghton J. T. Ding Y. Griggs D. J. Noguer M. van der Linden P. J. Dai X. Maskell K. Johnson C. A. (eds.). Cambridge, Cambridge University Press: 881 p.
- Jackson R. B., Banner J. L., Jobbagy E. G., Pockman W. T., Wall D. H. 2002. Ecosystem carbon loss with woody plant invasion of grasslands. *Nature*, 418, 6898: 623-626
- Jackson R. B., Canadell J., Ehleringer J. R., Mooney H. A., Sala O. E., Schulze E. D. 1996. A global analysis of root distributions for terrestrial biomes. *Oecologia*, 108, 3: 389-411

- Kaligarić M., Culiberg M., Kramberger B. 2006. Recent vegetation history of the North Adriatic grasslands: Expansion and decay of an anthropogenic habitat. *Folia Geobotanica*, 41, 3: 241-258
- Kowalski A. S., Serrano-Ortiz P., Janssens I. A., Sanchez-Moraic S., Cuezva S., Domingo F., Were A., Alados-Arboledas L. 2008. Can flux tower research neglect geochemical CO₂ exchange? *Agricultural and Forest Meteorology*, 148, 6-7: 1045-1054
- Kurc S. A., Small E. E. 2007. Soil moisture variations and ecosystem-scale fluxes of water and carbon in semiarid grassland and shrubland. *Water Resources Research*, 43, 6: W06416
- Kutsch W. L., Bahn M., Heinemeyer A. 2010. *Soil Carbon Dynamics. An Integrated Methodology*. New York, Cambridge University Press: 298 p.
- Kuzyakov Y. 2006. Sources of CO₂ efflux from soil and review of partitioning methods. *Soil Biology & Biochemistry*, 38, 3: 425-448
- Laio F., Porporato A., Fernandez-Illescas C. P., Rodriguez-Iturbe I. 2001. Plants in water-controlled ecosystems: active role in hydrologic processes and response to water stress - IV. Discussion of real cases. *Advances in Water Resources*, 24, 7: 745-762
- Lambers H., Stulen I., vanderWerf A. 1996. Carbon use in root respiration as affected by elevated atmospheric O₂. *Plant and Soil*, 187, 2: 251-263
- Lasslop G., Reichstein M., Papale D., Richardson A. D., Arneth A., Barr A., Stoy P., Wohlfahrt G. 2010. Separation of net ecosystem exchange into assimilation and respiration using a light response curve approach: critical issues and global evaluation. *Global Change Biology*, 16, 1: 187-208
- Liang N. S., Nakadai T., Hirano T., Qu L. Y., Koike T., Fujinuma Y., Inoue G. 2004. In situ comparison of four approaches to estimating soil CO₂ efflux in a northern larch (*Larix kaempferi* Sarg.) forest. *Agricultural and Forest Meteorology*, 123, 1-2: 97-117
- Lloyd J., Taylor J. A. 1994. On the temperature-dependence of soil respiration. *Functional Ecology*, 8, 3: 315-323

- Ma S. Y., Baldocchi D. D., Xu L. K., Hehn T. 2007. Inter-annual variability in carbon dioxide exchange of an oak/grass savanna and open grassland in California. *Agricultural and Forest Meteorology*, 147, 3-4: 157-171
- MacDonald D., Crabtree J. R., Wiesinger G., Dax T., Stamou N., Fleury P., Lazpita J. G., Gibon A. 2000. Agricultural abandonment in mountain areas of Europe: Environmental consequences and policy response. *Journal of Environmental Management*, 59, 1: 47-69
- Matese A., Alberti G., Gioli B., Toscano P., Vaccari F. P., Zaldei A. 2008. Compact(-)Eddy: A compact, low consumption remotely controlled eddy covariance logging system. *Computers and Electronics in Agriculture*, 64, 2: 343-346
- McGinn S. M., Akinremi O. O., McLean H. D. J., Ellert B. 1998. An automated chamber system for measuring soil respiration. *Canadian Journal of Soil Science*, 78, 4: 573-579
- McKinley D. C., Blair J. M. 2008. Woody plant encroachment by *Juniperus virginiana* in a mesic native grassland promotes rapid carbon and nitrogen accrual. *Ecosystems*, 11, 3: 454-468
- McLauchlan K. K., Hobbie S. E., Post W. M. 2006. Conversion from agriculture to grassland builds soil organic matter on decadal timescales. *Ecological Applications*, 16, 1: 143-153
- McMillen R. T. 1988. An eddy-correlation technique with extended applicability to non-simple terrain. *Boundary-Layer Meteorology*, 43, 3: 231-245
- Mottet A., Ladet S., Coque N., Gibon A. 2006. Agricultural land-use change and its drivers in mountain landscapes: A case study in the Pyrenees. *Agriculture Ecosystems & Environment*, 114, 2-4: 296-310
- Nagy Z., Pinter K., Czobel S., Balogh J., Horvath L., Foti S., Barcza Z., Weidinger T., Csintalan Z., Dinh N. Q., Grosz B., Tuba Z. 2007. The carbon budget of semi-arid grassland in a wet and a dry year in Hungary. *Agriculture Ecosystems & Environment*, 121, 1-2: 21-29
- Nagy Z., Pinter K., Pavelka M., Darenova E., Balogh J. 2011. Carbon fluxes of surfaces vs. ecosystems: advantages of measuring eddy covariance and soil respiration simultaneously in dry grassland ecosystems. *Biogeosciences*, 8, 9: 2523-2534

- Nobel P. S. 2009. *Physicochemical and Environmental Plant Physiology*. Los Angeles, California, University of California, Department of Ecology and Evolutionary Biology: 582 p.
- Ocheltree T. W., Loescher H. W. 2007. Design of the AmeriFlux portable eddy covariance system and uncertainty analysis of carbon measurements. *Journal of Atmospheric and Oceanic Technology*, 24, 8: 1389-1406
- Papale D., Reichstein M., Aubinet M., Canfora E., Bernhofer C., Kutsch W., Longdoz B., Rambal S., Valentini R., Vesala T., Yakir D. 2006. Towards a standardized processing of Net Ecosystem Exchange measured with eddy covariance technique: algorithms and uncertainty estimation. *Biogeosciences*, 3, 4: 571-583
- Pereira J. S., Mateus J. A., Aires L. M., Pita G., Pio C., David J. S., Andrade V., Banza J., David T. S., Paco T. A., Rodrigues A. 2007. Net ecosystem carbon exchange in three contrasting Mediterranean ecosystems - the effect of drought. *Biogeosciences*, 4, 5: 791-802
- Pilegaard K., Hummelshøj P., Jensen N. O., Chen Z. 2001. Two years of continuous CO₂ eddy-flux measurements over a Danish beech forest. *Agricultural and Forest Meteorology*, 107, 1: 29-41
- Pinto-Correia T. 1993. Land abandonment: changes in the land use patterns around Mediterranean basin. *Ciheam—Options Mediterraneennes*, 1: 97-112
- Pleničar M., Polšak A., Šikić D. 1973. Osnovna geološka karta SFRJ 1:100.000, Tolmač za list Trst = Geological map of Yugoslavia 1:100,000, Commentary to the map section Trieste. Beograd, Savezni geološki zavod: 109 p.
- Plestenjak G., Eler K., Vodnik D., Ferlan M., Čater M., Kanduč T., Simončič P., Ogrinc N. 2012. Sources of soil CO₂ in calcareous grassland with woody plant encroachment. *Journal of Soils and Sediments*, 12, 9: 1327-1338
- Post W. M., Kwon K. C. 2000. Soil carbon sequestration and land-use change: processes and potential. *Global Change Biology*, 6, 3: 317-327
- Potts D. L., Huxman T. E., Cable J. M., English N. B., Ignace D. D., Eilts J. A., Mason M. J., Weltzin J. F., Williams D. G. 2006. Antecedent moisture and seasonal precipitation influence the response of canopy-scale carbon and water exchange to rainfall pulses in a semi-arid grassland. *New Phytologist*, 170, 4: 849-860

- Pumpanen J., Kolari P., Ilvesniemi H., Minkinen K., Vesala T., Niinistö S., Lohila A., Larmola T., Morero M., Pihlatie M., Janssens I., Yuste J. C., Grünzweig J. M., Reth S., Subke J.-A., Savage K., Kutsch W., Østreng G., Ziegler W., Anthoni P., Lindroth A., Hari P. 2004. Comparison of different chamber techniques for measuring soil CO₂ efflux. *Agricultural and Forest Meteorology*, 123, 3–4: 159-176
- Raich J. W., Potter C. S., Bhagawati D. 2002. Interannual variability in global soil respiration, 1980-94. *Global Change Biology*, 8, 8: 800-812
- Raich J. W., Schlesinger W. H. 1992. The global Carbon-dioxide flux in soil respiration and its relationship to vegetation and climate. *Tellus Series B-Chemical and Physical Meteorology*, 44, 81-99
- Rambal S., Joffre R., Ourcival J. M., Cavender-Bares J., Rocheteau A. 2004. The growth respiration component in eddy CO₂ flux from a *Quercus ilex* mediterranean forest. *Global Change Biology*, 10, 9: 1460-1469
- Rambal S., Ourcival J. M., Joffre R., Mouillot F., Nouvellon Y., Reichstein M., Rocheteau A. 2003. Drought controls over conductance and assimilation of a Mediterranean evergreen ecosystem: scaling from leaf to canopy. *Global Change Biology*, 9, 12: 1813-1824
- Reichstein M., Falge E., Baldocchi D., Papale D., Aubinet M., Berbigier P., Bernhofer C., Buchmann N., Gilmanov T., Granier A., Grunwald T., Havrankova K., Ilvesniemi H., Janous D., Knohl A., Laurila T., Lohila A., Loustau D., Matteucci G., Meyers T., Miglietta F., Ourcival J. M., Pumpanen J., Rambal S., Rotenberg E., Sanz M., Tenhunen J., Seufert G., Vaccari F., Vesala T., Yakir D., Valentini R. 2005. On the separation of net ecosystem exchange into assimilation and ecosystem respiration: review and improved algorithm. *Global Change Biology*, 11, 9: 1424-1439
- Reichstein M., Tenhunen J. D., Rouspard O., Ourcival J. M., Rambal S., Dore S., Valentini R. 2002a. Ecosystem respiration in two Mediterranean evergreen Holm Oak forests: drought effects and decomposition dynamics. *Functional Ecology*, 16, 1: 27-39
- Reichstein M., Tenhunen J. D., Rouspard O., Ourcival J. M., Rambal S., Miglietta F., Peressotti A., Pecchiari M., Tirone G., Valentini R. 2002b. Severe drought effects on ecosystem CO₂ and H₂O fluxes at three Mediterranean evergreen sites: revision of current hypotheses? *Global Change Biology*, 8, 10: 999-1017

- Reverter B. R., Carrara A., Fernandez A., Gimeno C., Sanz M. J., Serrano-Ortiz P., Sanchez-Canete E. P., Were A., Domingo F., Resco V., Burba G. G., Kowalski A. S. 2011. Adjustment of annual NEE and ET for the open-path IRGA self-heating correction: Magnitude and approximation over a range of climate. *Agricultural and Forest Meteorology*, 151, 12: 1856-1861
- Reverter B. R., Sanchez-Canete E. P., Resco V., Serrano-Ortiz P., Oyonarte C., Kowalski A. S. 2010. Analyzing the major drivers of NEE in a Mediterranean alpine shrubland. *Biogeosciences*, 7, 9: 2601-2611
- Richardson A. D., Hollinger D. Y. 2007. A method to estimate the additional uncertainty in gap-filled NEE resulting from long gaps in the CO₂ flux record. *Agricultural and Forest Meteorology*, 147, 3-4: 199-208
- Richardson A. D., Hollinger D. Y., Burba G. G., Davis K. J., Flanagan L. B., Katul G. G., Munger J. W., Ricciuto D. M., Stoy P. C., Suyker A. E., Verma S. B., Wofsy S. C. 2006. A multi-site analysis of random error in tower-based measurements of carbon and energy fluxes. *Agricultural and Forest Meteorology*, 136, 1-2: 1-18
- Rodriguez-Iturbe I., Porporato A., Laio F., Ridolfi L. 2001. Intensive or extensive use of soil moisture: plant strategies to cope with stochastic water availability. *Geophysical Research Letters*, 28, 23: 4495-4497
- Rounsevell M. D. A., Annetts J. E., Audsley E., Mayr T., Reginster I. 2003. Modelling the spatial distribution of agricultural land use at the regional scale. *Agriculture Ecosystems & Environment*, 95, 2-3: 465-479
- Rounsevell M. D. A., Reginster I., Araujo M. B., Carter T. R., Dendoncker N., Ewert F., House J. I., Kankaanpaa S., Leemans R., Metzger M. J., Schmit C., Smith P., Tuck G. 2006. A coherent set of future land use change scenarios for Europe. *Agriculture Ecosystems & Environment*, 114, 1: 57-68
- Schlesinger W. H. 2000. Carbon sequestration in soils: some cautions amidst optimism. *Agriculture Ecosystems & Environment*, 82, 1-3: 121-127
- Schuepp P. H., Leclerc M. Y., Macpherson J. I., Desjardins R. L. 1990. Footprint prediction of scalar fluxes from analytical solutions of the diffusion equation. *Boundary-Layer Meteorology*, 50, 1-4: 353-373

- Schulze E. D., Beck E., Müller-Hohenstein K. 2002. *Plant Ecology*. Heidelberg, Spektrum Akademischer Verlag: 450 p.
- Scott R. L., Huxman T. E., Williams D. G., Goodrich D. C. 2006. Ecohydrological impacts of woody-plant encroachment: seasonal patterns of water and carbon dioxide exchange within a semiarid riparian environment. *Global Change Biology*, 12, 2: 311-324
- Serrano-Ortiz P., Domingo F., Cazorla A., Were A., Cuezva S., Villagarcia L., Alados-Arboledas L., Kowalski A. S. 2009. Interannual CO₂ exchange of a sparse Mediterranean shrubland on a carbonaceous substrate. *Journal of Geophysical Research-Biogeosciences*: 114
- Serrano-Ortiz P., Kowalski A. S., Domingo F., Rey A., Pegoraro E., Villagarcia L., Alados-Arboledas L. 2007. Variations in daytime net carbon and water exchange in a montane shrubland ecosystem in southeast Spain. *Photosynthetica*, 45, 1: 30-35
- Serrano-Ortiz P., Roland M., Sanchez-Moral S., Janssens I. A., Domingo F., Godderis Y., Kowalski A. S. 2010. Hidden, abiotic CO₂ flows and gaseous reservoirs in the terrestrial carbon cycle: Review and perspectives. *Agricultural and Forest Meteorology*, 150, 3: 321-329
- Soussana J. F., Allard V., Pilegaard K., Ambus P., Amman C., Campbell C., Ceschia E., Clifton-Brown J., Czobel S., Domingues R., Flechard C., Fuhrer J., Hensen A., Horvath L., Jones M., Kasper G., Martin C., Nagy Z., Neftel A., Raschi A., Baronti S., Rees R. M., Skiba U., Stefani P., Manca G., Sutton M., Tubaf Z., Valentini R. 2007. Full accounting of the greenhouse gas (CO₂, N₂O, CH₄) budget of nine European grassland sites. *Agriculture Ecosystems & Environment*, 121, 1-2: 121-134
- Tang X. L., Zhou G. Y., Liu S. G., Zhang D. Q., Liu S. Z., Li J., Zhou C. Y. 2006. Dependence of soil respiration on soil temperature and soil moisture in successional forests in southern China. *Journal of Integrative Plant Biology*, 48, 6: 654-663
- Teklemariam T., Staebler R. M., Barr A. G. 2009. Eight years of carbon dioxide exchange above a mixed forest at Borden, Ontario. *Agricultural and Forest Meteorology*, 149, 11: 2040-2053
- Twine T. E., Kustas W. P., Norman J. M., Cook D. R., Houser P. R., Meyers T. P., Prueger J. H., Starks P. J., Wesely M. L. 2000. Correcting eddy-covariance flux

- underestimates over a grassland. *Agricultural and Forest Meteorology*, 103, 3: 279-300
- Unger S., Maguas C., Pereira J. S., Aires L. M., David T. S., Werner C. 2009. Partitioning carbon fluxes in a Mediterranean oak forest to disentangle changes in ecosystem sink strength during drought. *Agricultural and Forest Meteorology*, 149, 6-7: 949-961
- Vaccari F. P., Lugato E., Gioli B., D'Acqui L., Genesio L., Toscano P., Matese A., Miglietta F. 2012. Land use change and soil organic carbon dynamics in Mediterranean agro-ecosystems: The case study of Pianosa Island. *Geoderma*, 175, 29-36
- Valentini R., Matteucci G., Dolman A. J., Schulze E. D., Rebmann C., Moors E. J., Granier A., Gross P., Jensen N. O., Pilegaard K., Lindroth A., Grelle A., Bernhofer C., Grunwald T., Aubinet M., Ceulemans R., Kowalski A. S., Vesala T., Rannik U., Berbigier P., Loustau D., Guomundsson J., Thorgeirsson H., Ibrom A., Morgenstern K., Clement R., Moncrieff J., Montagnani L., Minerbi S., Jarvis P. G. 2000. Respiration as the main determinant of carbon balance in European forests. *Nature*, 404, 6780: 861-865
- Wan C. G., Sosebee R. E. 1991. Water relations and transpiration of honey mesquite on 2 sites in west Texas. *Journal of Range Management*, 44, 2: 156-160
- Webb E. K., Pearman G. I., Leuning R. 1980. Correction of flux measurements for density effects due to heat and water-vapor transfer. *Quarterly Journal of the Royal Meteorological Society*, 106, 447: 85-100
- Were A., Serrano-Ortiz P., de Jong C. M., Villagarcia L., Domingo F., Kowalski A. S. 2010. Ventilation of subterranean CO₂ and Eddy covariance incongruities over carbonate ecosystems. *Biogeosciences*, 7, 3: 859-867
- Wilson K., Goldstein A., Falge E., Aubinet M., Baldocchi D., Berbigier P., Bernhofer C., Ceulemans R., Dolman H., Field C., Grelle A., Ibrom A., Law B. E., Kowalski A., Meyers T., Moncrieff J., Monson R., Oechel W., Tenhunen J., Valentini R., Verma S. 2002. Energy balance closure at FLUXNET sites. *Agricultural and Forest Meteorology*, 113, 1-4: 223-243
- Wohlfahrt G., Fenstermaker L. F., Arnone J. A. 2008. Large annual net ecosystem CO₂ uptake of a Mojave Desert ecosystem. *Global Change Biology*, 14, 7: 1475-1487

- Wu J. B., Guan D. X., Yuan F. H., Yang H., Wang A. Z., Jin C. J. 2012. Evolution of atmospheric carbon dioxide concentration at different temporal scales recorded in a tall forest. *Atmospheric Environment*, 61, 9-14
- Xu L. K., Baldocchi D. D. 2004. Seasonal variation in carbon dioxide exchange over a Mediterranean annual grassland in California. *Agricultural and Forest Meteorology*, 123, 1-2: 79-96
- Yuste J. C., Janssens I. A., Carrara A., Meiresonne L., Ceulemans R. 2003. Interactive effects of temperature and precipitation on soil respiration in a temperate maritime pine forest. *Tree Physiology*, 23, 18: 1263-1270

ZAHVALA

Hvala mentorju prof. dr. Francu Batiču in somentorju dr. Primožu Simončiču, ki sta mi omogočila študij in mi pomagala iz marsikatero, največkrat, birokratske zagate. Prav tako se jima zahvaljujem za ekspeditiven pregled doktorske naloge in podani oceni. Hvala prof. dr. Juriju Diaciju in prof. dr. Alessandru Peressottiju, ki sta kot predsednik in član komisije, pregledala doktorsko nalogo in podala oceni.

Zahvalo namenjam tudi Agenciji Republike Slovenije za raziskovalno dejavnost, ki je financirala raziskave v okviru projektov J4-1009 in V4-0536 in program usposabljanja mladega raziskovalca v okviru raziskovalnega programa P4-0085 (Aplikativna botanika, genetika in ekologija na Biotehniški fakulteti Univerze v Ljubljani).

Zahvaljujem se Univerzi v Vidmu, posebej prof. dr. Alessandru Peressottiju za posojilo opreme na ploskvi Pašnik. Prav tako se zahvaljujem prof. dr. Alessandru Peressottiju in dr. Giorgio Albertiju za vse razlage in začetne tečaje o Eddy covariance metodi.

Posebna zahvala gre vodstvu Gozdarskega Inštituta Slovenije med leti 2008 in 2013, še posebej dr. Mirku Medvedu, dr. Tomislavu Levaniču in vodji oddelka za Gozdno ekologijo in lovstvo dr. Primožu Simončiču za sredstva in podporo pri postavitvi Laboratorija za elektronske naprave na Gozdarskem Inštitutu Slovenije.

Posebno zahvalo namenjam prof. dr. Dominiku Vodniku in dr. Klemenu Elerju za prijetno delo, ki smo ga skupaj opravili na raziskovalnih ploskvah.

Hvala Iztoku Sinjurju, Milanu Kobalu, Gregorju Plestenjaku, Andreju Vončini, Gabrijelu Leskovcu in Marjanci Jamnik za pomoč pri terenskem delu.

Še posebna zahvala gre Vidi, za razumevanje ob številnih odsotnostih od doma, ter vsem domačim in družini za vso podporo.